Trichome patterning in *Arabidopsis thaliana*: Mechanism and the role of TTG1 depletion/trapping

Inaugural-Dissertation

zur

Erlangung des Doktorgrades

der Mathematisch-Naturwissenschaftlichen Fakultät

der Universität zu Köln

vorgelegt von

Rachappa Siddalingappa Balkunde

aus Kurabkhelgi, Indien

2011

Berichterstatter:	Prof. Dr. Martin Hülskamp
Berichterstatter:	Prof. Dr. Siegfried Roth
Prüfungsvorsitzender:	Prof. Dr. Angelika A. Noegel
Tag der mündlichen Prüfung:	22. 10. 2010

Contents

Acknowledgment **V**

Zusammenfassung **VII**

Abstract **IX**

Publication **XI**

List of Figures **XIV**

List of Tables **XV**

List of Abbreviations **XIX**

1 Introduction **1**
1.1 Pattern formation in biological system-Role of intercellular communication 1
1.2 Models of biological pattern formation 3
1.3 Epidermal pattern formation in *Arabidopsis thaliana* 5
1.4 Trichome patterning in *Arabidopsis thaliana* 6
1.4.1 Positive regulators or activators 6
1.4.2 Negative regulators or inhibitors 9
1.5 Expression, interaction and transcriptional regulation of trichome regulators 10
1.6 The role of TTG1 in trichome patterning: new findings 13
1.7 Aim of the research 14

2 Results **15**
2.1 Analysis of TTG1:YFP depletion in *gl3* mutant 15
2.2 Effect of trichome patterning related bHLH proteins on the subcellular distribution of TTG1:YFP 16
2.2.1 GL3 is the main modulator of TTG1 intracellular localization 17
2.2.2 Additive effect of GL3 homologues on the subcellular localization of TTG1:YFP 19
2.2.3 TTG1:YFP subcellular localization analysis in the roots of *gl3* and *gl3 egl3* mutants 20
2.3 Influence of GL3 on the nuclear trapping/ transport of TTG1 22

2.3.1 Mapping mutual interaction domains in TTG1 and GL3 23
2.3.2 Nuclear Transportation Trap (NTT) assay to test if TTG1 has any functional NLS 25
2.3.3 *In planta* analysis of the GL3 and TTG1 interaction specificity for TTG1 nuclear trapping 27
2.4 GL3 counteracts TTG1 mobility between the tissue layers 32
2.5 Analysis of TTG1 transport rates in different epidermal cell types using the photoconvertible marker KikGR1 35
2.5.1 Standardization of TTG1:KikGR1 photoconvertion condition . 35
2.5.2 Analysis of TTG1:KikGR1(red) transport rate in different epidermal cell types 36
2.6 Analysis of mobility of the nuclear targeted TTG1:YFP 41
2.7 Genetic analysis of the *ttg1* alleles 44
2.8 Effect of altering nuclear TTG1 concentration on trichome patterning and morphogenesis 50
2.8.1 Analysis of overexpression of CFP:GL3, CFP:GL3△78 and CFP:GL3△NLS in *ttg1*pTTG1::TTG1:YFP line 50
2.8.2 Analysis of the effect of 78GL3:GUS aptamer expression in the *ttg1-13*pTTG1::TTG1:YFP plants 54
2.9 Mapping the mobility domain in TTG1 56
2.9.1 Analysis of AN11 mobility between the tissue layers 58
2.9.2 Swapping non homologous regions in TTG1 and AN11. 61
2.10 Generation of mutants affecting the transport of TTG1 from the subepidermis to the epidermis 61

3 Discussion **65**
3.1 GL3 is required for the TTG1:YFP depletion during trichome pattern formation 66
3.2 GL3 sequesters TTG1:YFP in the nucleus 67
3.3 EGL3 contributes to TTG1 nuclear localization 71
3.4 Is the nuclear import of TTG1 necessary for cell-to-cell transport ? . 73
3.5 Mobility of TTG1:YFP is counteracted by GL3 76
3.6 Paradoxical phenotype of the *ttg1* weak alleles - Does depletion has a role to play ? 78
3.7 Mapping the TTG1 mobility domain 84
3.8 Isolation of TTG1 transport inhibitor mutants 87
3.9 Model for the GL3 dependent TTG1 depletion during the trichome pattern formation 90

4 Materials and Methods **93**
4.1 Chemicals and antibiotics 93
4.2 Enzymes, Kits, Primers and Molecular biological materials 93
4.3 Bacterial strains and Yeast strains 93
4.4 Plant lines used 94
4.5 Vectors, Constructs and Transgenic lines 94
4.6 Creation of pENTRY vectors 100

4.7 Creation destination vectors 101
4.8 Yeast two-hybrid 101
4.9 Nuclear Transportation Trap (NTT) assay 102
4.10 Microscopy and quantification of YFP Fluorescence 103
4.11 Transient expression 103
4.12 Plant growth conditions 104
4.13 Crossing of plants 104
4.14 Plant transformation 105
4.15 Seed sterilisation 105
4.16 Seed coat mucilage staining 105

Bibliography **107**

Erklärung **i**

Acknowledgment

My sincere gratitude goes to my supervisor, **Prof. Dr. Martin Hülskamp**, for his great insights, perspectives and guidance. His encouragement and belief in my strengths and lending me freedom to think, plan and work independently was a great learning experience that I will cherish throughout my life.
I avail this opportunity to thank **Prof. Dr. Siegfried Roth** for being a part of my thesis committee and for evaluating my thesis. I am also grateful to **Prof. Dr. Angelika A. Noegel** for accepting to chair my thesis defense.
My gratitude to **Dr. Martina Pesch** for fruitful discussions, critical comments, useful suggestions and finally for critically reading my thesis, which helped me in molding my thesis into a right shape. I am very grateful to **Dr. Daniel Bouyer** who introduced me into this nice project and was always there to discuss new ideas, problems and progresses in the project and for correcting my thesis.
I am very much thankful to Dr. Swen Schellmann and Dr. Joachim Uhrig for all the scientific discussions. I also thank Prof. Dr. Friedrich Kragler who introduced me to microinjection technique.
Thanks to members of the patterning group for very lively and fruitful discussions. I am very much thankful to Alex Friede for her enormous help in using latex software and for preparing the template for the thesis writing using latex software. Many thanks to all the members of AG Huelskamp for the wonderful atmosphere that made my stay very memorable. Thanks to Frau Rochaz and Frau Thorn for the administrative help. Special thanks to Uschi and very helping technicians Bastian, Birgit, Britta and Irene. I also take this opportunity to thank Klaus and his team in the garden for all the help. I owe my sincere thanks to IGS-GFG, University of Cologne for the graduate fellowship. Special thanks to Dr. Brigitte Wilcken Bergmann for administrative and general help. Many many thanks to Alex, Bastian, Karsten, Philipp and especially Cordula who were very helping every time I bothered them with the german to english translations of my letters and phone calls. My very special thanks to all my friends for all the fun and party. My whole hearted thanks to my parents, In-Laws and all the family members.

Without their boundless love, affection and selfless sacrifice, I would not have been what I am today. From the bottom of my heart I thank my wife Rashmi for her care, support, encouragement and pretty much for everything in my life-thank you so much. Finally I thank everyone who directly or indirectly helped me to achieve this success.

Zusammenfassung

Trichommusterbildung in *Arabidopsis thaliana* ist ein gutes Modellsystem, um zweidimensionale Musterbildung in Pflanzen zu untersuchen. Laterale Inhibition während der Trichommusterbildung kann theoretisch entweder durch aktive Inhibition oder durch Entfernung von Trichom fördernder Aktivität (z.B. Depletion) erreicht werden. Vor kurzem publizierte Daten haben eine Rolle des Aktivator-Depletionsmechanismus in der Trichommusterbildung vorgeschlagen. Es wurde gezeigt, dass das TTG1 Protein in den Trichom umgebenden Epidermiszellen depletiert und in den Trichominitialen akkumuliert wird. In der hier vorliegenden Studie habe ich mich auf die Charakterisierung des molekularen Mechanismus und der Rolle des Festhaltens von TTG1 während der Trichommusterbildung konzentriert.

Ich zeigte, dass die Entfernung des bHLH Faktors GL3 in dem Verlust der TTG1 Depletion resultiert, was deutlich suggeriert, dass die TTG1 Depletion GL3 abhängig ist. Zellen, die ein hohes Level von *GL3* exprimieren, zeigen einen positiven Effekt auf die Kernlokalisation des TTG1 Proteins. Ebenso wirkt GL3 der TTG1 Mobilität sowohl innerhalb als auch zwischen Gewebeschichten entgegen. Koexpression von *GL3* und *TTG1* in der Subepidermis blockiert die Mobilität von TTG1 von der Subepidermis in die Epidermis. Innerhalb der Epidermis ist das TTG1 Protein in Trichominitialen im Vergleich zu anderen Epidermis zellen weniger frei sich zu bewegen. Ähnlich wird TTG1, das in eine Trichominitiale diffundiert ist, effizienter zurückgehalten als TTG1, das in eine andere epidermale Zellen diffundiert ist. Dies korreliert sehr gut mit dem Expressions- und Lokalisationsmuster von *GL3*, welches bevorzugt in Trichominitialen exprimiert wird. Diese Beobachtung wird weiter durch die Tatsache bestärkt, dass in 35S:GL3 Linien die Depletion aufgrund des Festhaltens von TTG1 in allen epidermalen Zellen verloren gegangen ist. Zusammenfassend zeigen diese Daten klar, dass GL3 TTG1 im Kern der Trichominitialen festhält.

Schwache Allele von *ttg1*, die Trichomcluster produzieren, wurden benutzt, um

die biologische Relevanz der Depletion zu testen. Interessanter Weise zeigten die schwachen Allele von TTG1 im Hefesystem entweder eine schwache oder keine Interaktion mit GL3 und waren nicht in der Lage im Kern festgehalten zu werden. Dies führte zu dem Postulat, dass die Interaktion von schwachen TTG1 Allelen mit GL3 zwar ausreichend ist Trichome zu initiieren, aber nicht ausreicht TTG1 in den Kern zu ziehen/ festzuhalten, was zum Verlust der TTG1 Depletion in den Trichomnachbarzellen und damit zur Clusterbildung führt.
Eine Grenzkonzentration von TTG1 im Kern scheint kritisch für die korrekte Verzweigung von Trichomen zu sein. Diese Vermutung korreliert sehr gut mit dem Unterverzweigungsphänotyp von schwachen *ttg1* Allelen, in denen das im Kern lokalisierte TTG1 aufgrund der schwachen/ fehlenden Interaktion mit GL3 als geringer erwartet wird.
Die Mobilitätsdomäne in TTG1, die nicht alleine, aber teilweise verantwortlich für die TTG1 Beweglichkeit zwischen den Gewebeschichten ist, wurde auf wenige Aminosäuren im N-Terminus von TTG1 eingeschränkt.
Eine mögliche TTG1 Transportinhibitor-Mutante (*tti*), die spezifisch den Transport von TTG1 aus der Subepidermis in die Epidermis von Blättern und Samen inhibiert, wurde in einem EMS-Mutagenese-Screen von *ttg1*pRBC:TTG1 Pflanzen isoliert.
Die Anwendung des photokonvertierbaren Markers KikGR1 in Pflanzen wurde zum ersten Mal gezeigt. Dieser wurde dann erfolgreich benutzt, um die Mobilität von TTG1 in der Blattepidermis zu studieren.

Abstract

Trichome patterning in *Arabidopsis thaliana* is a potential model system to study two dimensional patterning. Theoretically, lateral inhibition during trichome patterning can be achieved either by active inhibition or by removal of trichome promoting activity (e.g. depletion). Recent data have suggested a role of this activator depletion mechanism in trichome patterning. It was shown that the TTG1 protein is depleted in the trichome surrounding epidermal cells and accumulates in the trichome initials. In this study I focused on the characterization of the molecular mechanism and the role of TTG1 trapping during trichome patterning.

I showed that the removal of the bHLH factor GL3 results in the abolition of the TTG1 depletion strongly suggesting that TTG1 depletion is GL3 dependent. Cells expressing high levels of *GL3* show a strong positive effect on nuclear localization of the TTG1 protein. GL3 also counteracts the TTG1 mobility both within as well as between the tissue layers. Co-expression of *GL3* and *TTG1* in the subepidermis blocked the mobility of TTG1 from the subepidermis to the epidermis. Within the epidermis the TTG1 protein in the trichome initials is less free to move compared to TTG1 in the other epidermal cells. Similarly the TTG1 entering into the trichome initial is retained more efficiently than the TTG1 entering into other epidermal cells. This correlates with the expression and localization pattern of *GL3* which is predominantly expressed in trichome initials. This observation was further strengthened by p35S::GL3 lines where the depletion was lost because of the trapping of TTG1 in all epidermal cells. Taken together these data are clearly pointing towards a GL3 mediated nuclear trapping of TTG1 in the trichome initials.

Weak alleles of *ttg1*, which produce trichome clusters, were used to test the biological relevance of the depletion. Interestingly the weak allelic forms of *TTG1* showed either a weak or no interaction with GL3 and failed to be trapped in the nucleus in the yeast system. This led to the postulation that in these weak alleles the TTG1 interaction with GL3 might be sufficient enough to initiate trichomes but

not strong enough to attract/trap TTG1 in the nucleus resulting in no depletion of the activator TTG1 in the trichome adjacent cells and thereby leading to cluster formation.
A threshold level of TTG1 concentration in the nucleus appears to be crucial for the correct branching of the trichome. This assumption also correlates nicely with the underbranched phenotype in the weak *ttg1* alleles where also nuclear TTG1 would be expected to be less because of weak/no interaction with GL3.
The mobility domain in TTG1, which is not solely but partially responsible for the TTG1 mobility between the tissue layers was mapped to few amino acids in the N-terminus of TTG1.
A potential TTG1 transport inhibitor (*tti*) mutant was isolated in the EMS mutagenesis screening of the *ttg1*pRBC::TTG1 plants that specifically inhibited the transport of TTG1 from the subepidermis to the epidermis in leaf and the seeds.
The application of the photoconvertible marker KikGR1 in plants was shown for the first time. This was then successfully used to study the mobility of TTG1 in the leaf epidermis.

Publication

Balkunde, R*., Bouyer, D*., and Hülskamp, M., (2011), Nuclear trapping by GL3 controls intercellular transport and redistribution of TTG1 protein in *Arabidopsis*, *Development* 138, (*, equal contribution)

Balkunde, R., Pesch, M. and Hülskamp, M., (2010), Trichome Patterning in *Arabidopsis thaliana*: From Genetic to Molecular Models, *Current Topics in Developmental Biology*, Volume 91, 299-321

Bouyer, D., Geier, F., Kragler, F., Schnittger, A., Pesch, M., Wester, K., **Balkunde, R**., Timmer, J., Fleck, C. and Hülskamp, M. (2008), Two-Dimensional patterning by a Trapping/Depletion mechanism: The role of TTG1 and GL3 in *Arabidopsis* trichome formation, *PLoS Biology* 6(6), e141.

List of Figures

1.1 Mechanisms of biological pattern formation. 4
1.2 Trichome development in *Arabidopsis thaliana*. 8
1.3 Interaction and expression regulatory networks of trichome regulators. 12
1.4 *TTG1* expression and distribution pattern. 13

2.1 Analysis of TTG1:YFP depletion in *gl3* mutant background. 16
2.2 Cellular distribution of TTG1:YFP in different background. 18
2.3 Quantification of nuclear TTG1:YFP in the epidermal cells of the trichome patterning zone expressed under the *TTG1* promoter in different mutant background. 19
2.4 Analysis of TTG1 localization in different bHLH mutants. 21
2.5 Localization analysis of TTG1:YFP in the roots of *gl3* and *gl3 egl3*. . 22
2.6 Yeast two-hybrid analysis of GL3 variants and GL3 fragments (41GL3 and 78GL3 aptamers). 24
2.7 Nuclear Transportation Trap (NTT) assay to test the influence of GL3 on the nuclear transport of TTG1. 26
2.8 Transient expressions studies to show nuclear trapping of TTG1 as influenced by the interaction with GL3. 28
2.9 Intracellular localization analysis of 78GL3:GUS aptamer. 29
2.10 Analysis of the competitin between 78GL3:GUS and GL3 for binding to TTG1 in co-expression studies in onion epidermal cells. 30
2.11 Localization of TTG1△C26 in the leaf epidermis. 31
2.12 Tissue specific expression of *GL3* controls subepidermal TTG1 movement. 33
2.13 Rescue analysis of *ttg1-13*pTTG1::TTG1:KikGR1. 36
2.14 Analysis of transport rates of TTG1:KikGR1 in different epidermal cell types. 38
2.15 Analysis of TTG1:KikGR1(red) transport from trichome neighboring cell. 40
2.16 Seed coat phenotype analysis of the TTG1:YFP nuclear targeted and non-nuclear targeted lines. 42
2.17 Yeast two-hybrid analysis of allelic forms of TTG1 with GL3, EGL3 and TT8. 45
2.18 Nuclear transportation trap (NTT) assay for the allelic forms of TTG1. 46

2.19 Localization of TTG1 allelic forms in the leaf epidermal cells of Columbia wild type plants. 47
2.20 Genetic analysis of overexpression of allelic forms of *TTG1* in Columbia wild type. 48
2.21 Genetic analysis of overexpression of *GL3*, *GL3*△78 and *GL3*△NLS under *p35S* promoter in *ttg1-13*pTTG1::TTG1:YFP. 53
2.22 Effect of p35S::78GL3:GUS aptamer on trichome branching. 55
2.23 Influence of overexpression of 78GL3:GUS aptamer on the cellular distribution of TTG1. 57
2.24 Yeast two-hybrid and NTT assay of AN11. 59
2.25 TTG1 and AN11 protein sequence alignment showing the non homologous domains in the N-terminus. 62
2.26 Analysis of the TTG1 transport inhibitor (*tti*) mutant 63

3.1 Schematic presentation of the effect of tissue specific *GL3* expression on the mobility of *TTG1* expressed in the subepidermal tissue. 77
3.2 GL3 dependent TTG1 depletion model 92

List of Tables

2.1 Yeast two-hybrid analysis of GL3 variants with trichome regulators . 29
2.2 Quantification of TTG1:KikGR1(red) movement in different epidermal cell types 39
2.3 Genetic analysis of trichome phenotypes in the nuclear targeted TTG1:YFP expressing lines 43
2.4 *ttg1* alleles used in this study 44
2.5 Comparsion of trichome phenotypes when *TTG1* / TTG1:YFP is overexpressed in different *ttg1* alleles 49
2.6 Analysis of TTG1:YFP distribution in GL3 variants overexpressing lines 51
2.7 Analysis of leaf trichome phenotypes in the lines expressing *GL3* variants under *p35S* promoter 52
2.8 Comparison of trichome rescue efficiency of *TTG1* and *AN11* and their mutual swapped versions 60

4.1 **List of basic vectors used in this study** 94
4.2 **List of pENTRY/donor vectors used in gateway cloning** 95
4.3 **List of yeast vectors/constructs used in this study** 95
4.4 **List of destination vectors/constructs used in this study** 97

List of Abbreviations

^{0}C	degree celcius
E. coli	*Escherichia coli*
et al.	*et alterni* [Lat.] and others
µ	micro
µg	micro gram
µm	micro meter
AN11	ANTHOCYANINLESS11
AP3	APETALA3
AtML1	*Arabidopsis thaliana* MERISTEM LAYER1
BAN	BANYULS
bHLH	basic Helix-Loop-Helix
bp	base pair
C	DNA conatent of a haploid genome
CaMV	cauliflower mosaic virus
cDNA	complementary DNA
CDS	coding sequence
CFP	CYAN FLUORESCENT PROTEIN
ChIP	chromatin immunoprecipitation
CLSM	Confocal laser scanning microscopy
Col	Columbia
CPC	CAPRICE
DNA	deoxyribonucleic acid

EGL3	ENHANCER OF GLABRA3
ETC1-3	ENHANCER OF TRIPTYCHON and CAPRICE1-3
GEM	GLABRA2 EXPRESSION MODIFIER
GFP	GREEN FLUORESCENT PROTEIN
GL1	GLABRA1
GL2	GLABRA2
GL3	GLABRA3
HD	homeodomain
kb	kilo basepair
KikGR	Kikume green to red (photoconvertible fluorescent marker)
KN	KNOTTED
L*er*	Landsberg *erecta*
MCS	multicloning sites
MP	movement protein
NCAP	Non-cell autonomous protein
OD	optical density
p	promoter
p35S	35S promoter from Cauliflower mosaic virus
pBSK	pBluescript
PCR	polymerase chain reaction
PD	plasmodesmata
RBC	RUBISCO
RFP	RED FLUORESCENT PROTEIN
SCR	SCARECROW
SD	standard deviation
SEL	size exclusion limit
SHR	SHORTROOT

TIS	trichome initiation site
TRY	TRIPTYCHON
TT2	TRANSPARENT TESTA2
TT8	TRANSPARENT TESTA8
TTG1	TRANSPARENT TESTA GLABRA1
TTG2	TRANSPARENT TESTA GLABRA2
UTR	untranslated region
WD	Tryptophan Aspartic acid
WER	WEREWOLF
Wt/wt	wild type
YFP	YELLOW FLUORESCENT PROTEIN

1 Introduction

1.1 Pattern formation in biological system-Role of intercellular communication

The development and maintenance of multicellular organisms largely depend on intercellular communication as a major requirement. Several mechanisms have been established during the evolution for the exchange of signal molecules between the cells. These mechanisms include the intercellular membrane channels called plasmodesmata (PD) which make symplasmic connections between the plant cells (Lucas *et al*., 1995; Olsen, 1979; Ding *et al*., 1992; Turner *et al*., 1994; Bayer *et al*., 2004) and proteinaceous channels called gap junctions in animal cells (White and Paul, 1999; Willecke *et al*., 2002).

Unlike in animals where cell lineage is the main means of specific cell and tissue type development, the cell fate in plants largely depends on the positional informations. The process of intercellular communication is achieved by secreted signal molecules such as polypeptides, RNAs and ribonucleoproteins (RNPs) (Gallagher and Benfey 2005, 2009; Matsubayashi *et al*., 2001). However, the precise mechanism for cell-to-cell trafficking of molecules is largely unknown. Whereas in some cases the transport may be non selective (Wu *et al*., 2002, 2003), in others the developmental regulation of protein or mRNA movement hints at a selective and regulated process (Kim *et al*., 2005a).

The mobility of signal molecules across the PD is tightly regulated by size exclusion

limit (SEL) of PD that varies during the development creating symplastic domains (Gisel *et al*., 1999). By means of regulating the SEL cells maintain a qualitative as well as quantitative control over intercellular communication. All cells of the embryo of higher plants are initially connected as a single symplasmic unit mainly with simple PDs. As a result they have high SEL and increased cell-to-cell transport (Oparka and Turgeon, 1999; Crowford and Zambryski, 2000, 2001; Kim *et al*., 2005b, 2005c). With the advancement of embryogenesis the cell-to-cell transport of macromolecules is downregulated as a result of formation of symplsmic domains. The trafficking of certain proteins is restricted only within this domain (Kim *et al*., 2005; Crowford and Zambryski, 2000). These observations suggest that plants have evolved certain mechanism to restrict the mobility of signalling molecules both spatially and temporally to give correct size and shape to the plant body during growth and development.

Protein movement has been implicated in several pattern formation processes in plants, including radial and epidermal patterning in the root of *Arabidopsis* by SHORTROOT (SHR) mobility from stele into the endodermis, *Arabidopsis* root hair pattern formation by the mobility of the transcription factors CAPRICE (CPC) and GLABRA 3 (GL3) (Berger *et al*., 1998; Nakajima *et al*., 2001; Wada *et al*., 2002). Other examples to support the importance of intercellular transport of proteins include the control of leaf morphology modification by long distance transport of the transcription factor Mouse ears (Me) mRNA and/or protein in tomato, altered plant development due to the silencing or expression of dominant negative form of non-cell autonomous pathway protein 1 (NCAPP1) (Lee *et al*., 2003) and the regulation of flower development by the the cell-to-cell transport of regulatory proteins (Sessions *et al*., 2000; Kim *et al*., 2003; Wu *et al*., 2003).

While the protein mobility is important for proper pattern formation restricting the protein mobility to certain cell types is equally important. One classical example for this is the restriction of SHR mobility in the endodermis thereby

defining a single layer of endodermis (Gallagher *et al*., 2004; Cui *et al*., 2007). Trichome patterning in *Arabidopsis* serves as a potential model system to study the regulated control of intercellular communication during biological pattern formation as it invloves lot of intercellular communication through cell-cell protein trafficking (Schnittger *et al*., 1999; Schellmann *et al*., 2002; Bouyer *et al*., 2008; Wester *et al*., 2008; Zhao *et al*., 2008).

1.2 Models of biological pattern formation

The fundamental question how an organism, which starts as a single cell develops into a finely carved shape and structure has long held the curiosity of the scientific world. Development of pattern in a biological system is a very complex process consisting of numerous interconnected mechanisms operating simultaneously and in a highly ordered fashion. Interaction of complex processes such as spatiotemporal coordination of growth, cell-cell signalling, gene expression, cell differentiation and tissue movement are generally nonlinear and difficult to analyse. But mathematical models have the ability to generate a framework, which facilitates to compute the outcome based on different hypotheses on modes of interactions and also to make predictions that are experimentally testable. Meinhardt and Gierer (1974, 2000) modelled stable pattern formation and morphogenesis in biological systems and was referred to as Activator-Inhibitor mechanism/model (Figure 1.1A) (Koch and Meinhardt, 1994). According to this model the homogenity of a system can be broken to create a pattern. For this the system has to fulfill certain conditions. First local self enhancement of the activators is necessary for the continuous supply of activators themselves that in turn lead to local increase in the concentration of the inhibitors, which depend on the activators for their production. Second, the inhibitors need to diffuse into the surrounding cells and have a long range inhibitory effect. This means the inhibitors have to be mobile but the activators have

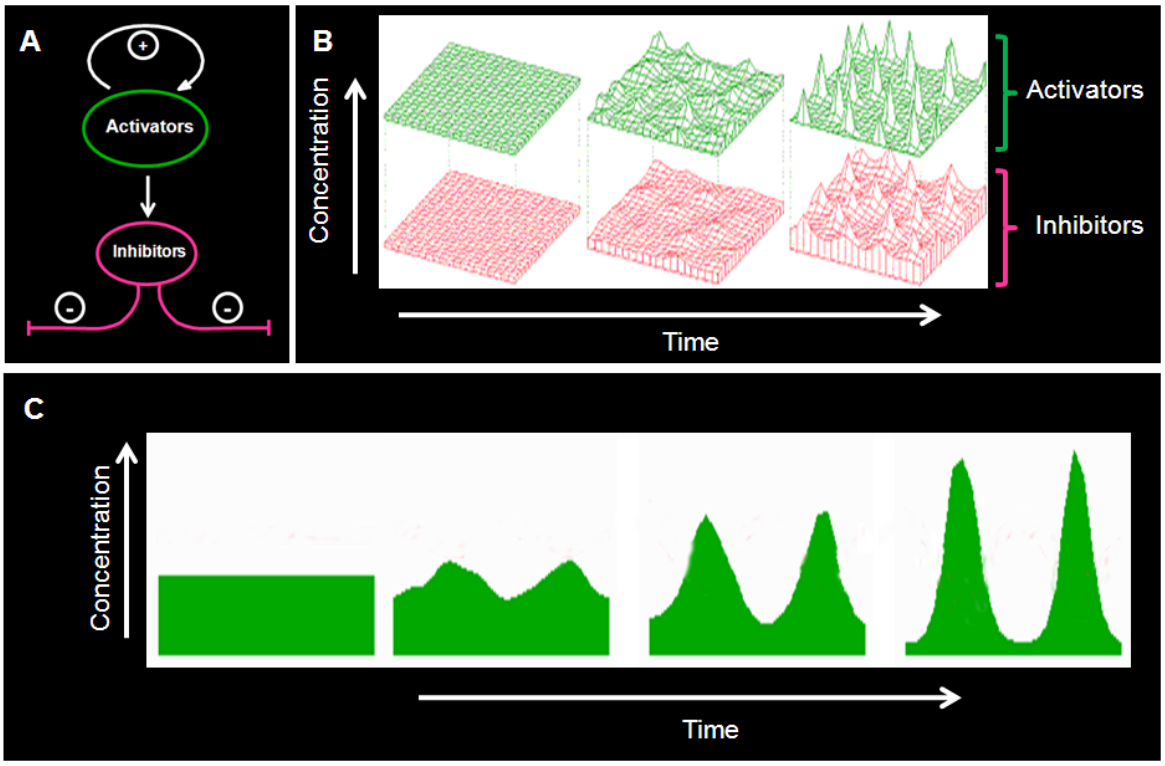

Figure 1.1: Mechanisms of biological pattern formation. (A) Activator-Inhibitor model. (B) Computer simulation using the equations of the activator-inhibitor model for the concentration of the activator (green) and the inhibitor (pink), (Figure from Scholarpedia). (C) Computer simulation for the activator depletion mechanism, green peaks indicate the activator concentration. (Figure modified from Scholarpedia) .

to function locally or at least be less mobile compared to the inhibitors. Computer simulations of the activator-inhibitor process shows that a small increase in the concentration of the activators results in local self-enhancement of the activators. Increase in activators further results in an increase in inhibitors concentration. But due to the high diffusion property of the inhibitors compared to the activators their concentration is increasing throughout the tissue, while the activators which are less mobile are restricted to their production spot. As a result of interaction between two types of components with different diffusion rates complemented with local self enhancement of activators a spatial concentration pattern is generated starting from nearly uniform distributions (Figure 1.1B) (Turing, 1952). The antagonistic effect could be caused by the long range inhibitory signal molecules in

activator-inhibitor mechanism or alternatively inhibitory effect can be caused by the removal of the activator or material required for the self enhancement resulting in a specific pattern by activator depletion mechanism (Figure 1.1C).

1.3 Epidermal pattern formation in *Arabidopsis thaliana*

Trichome formation on leaves, stomata development on the hypocotyl and root hair formation are determined by a common set of genes or corresponding homologues. Development of these three cell types serves as a model to study epidermal patterning in plants (Schellmann *et al*., 2007). Current genetic, biochemical and yeast interaction data suggest that these patterning systems consists of a transcriptionally active complex comprising of R2R3 type MYB related transcription factors, basic helix-loop-helix (bHLH) transcription factors and a WD40 repeat protein. The MYB-bHLH-WD40 trimeric complex forms a positive regulatory unit of trichome fate on leaf, atrichoblast fate in root and non stomata fate in the hypocotyl epidermis (Bernhardt *et al*., 2003; Payne *et al*., 2000; Berger *et al*., 1998; Schellmann *et al*., 2007). Single repeat MYB transcription factors, the expression of which depends on the activator complex lack a transactivation domain. These single repeat MYBs compete with the R2R3 MYBs in the activator complex resulting in formation of transcriptionally inactive complex (Payne *et al*., 2000; Esch *et al*., 2003; Bernhardt *et al*., 2003). Despite very high similarities in gene regulatory networks (GRNs), these three systems differ from each other from the developmental context (Benitez *et al*., 2008). Patterning in the roots and hypocotyl epidermis is predictable based on their position with respect to the underlying cortex cells. Epidermal cells overlying a cortex cell develops into a non root hair while the ones lying on the cleft between two cortex cells develps into a root hair (Berger *et al*., 1998; Dolan *et al*., 1994). Similarly in the hypocotyl

the cells overlying a cleft between two cortex cells are small and can develop into stomata, while large protruding cells present directly above the cortex cell bear no stomata forming ability. On the other hand trichome patterning is considered as a *de novo* pattern formation as trichome position has no correlation with any other landmarks and a cell lineage scenario was excluded by clonal analysis (Pesch and Hülskamp, 2004; Larkin *et al*., 1994; Schnittger *et al*., 1999).

1.4 Trichome patterning in *Arabidopsis thaliana*

Arabidopsis trichomes are single enlarged epidermal cells that have undergone four rounds of endoreduplication without a cytokinesis. As a result a wild type trichome has a DNA content of 32C. Wild type trichomes have three to four branches. Trichome development on the adaxial surface of the leaf starts at the distal end of the leaf and progresses basipetally (Hung *et al*.,1998). The First trichome appears at the tip of the leaf when the leaf size is about 100µm. Trichomes are distributed in a highly ordered fashion indicating a tight mechanism controlling their spacing (Hülskamp *et al*., 1994). Trichome patterning occurs at the base of the young leaves and incipient trichomes are separated by epidermal cell divisions during leaf expansion (Hülskamp *et al*., 1994). Genetic screening studies led to isolation of different mutants, which helped in identification and cloning of over 40 genes controlling the trichome development and patterning (Figure 1.2) (Hülskamp *et al*., 1994; Marks *et al*., 2009). The genes of the core activator and inhibitor complex are broadly grouped into two classes.

1.4.1 Positive regulators or activators

This group includes those genes in the absence of which there are either fewer or no trichomes on the leaf surface. This group includes the R2R3 MYB related transcription factors *GLABRA1* (*GL1*) and its homolog *MYB23* (Openheimer et al.,

1991; Kirik *et al*., 2001). Mutations at the *GL1* locus results in the complete loss of trichomes on the leaf surface but does not affect edge trichomes (Figure 1.2K) (Oppenheimer *et al*., 1991; Kirik *et al*., 2001). On the other hand the *myb23* mutant plants show no obvious effect on the trichome initiation but is affected in branching and production of marginal trichomes and in combintation with *gl1* mutant (*gl1 myb23* double mutant) resulted in complete loss of trichomes including the edge trichomes (Kirik *et al*., 2001, 2005). *GL1* and *MYB23* show similar expression pattern but have spatial and temporal differences at the transcriptional regulation level (Kirik *et al*., 2001, 2005). *MYB23* when expressed under the *GL1* cis-regulatory elements complimented *gl1* mutant phenotype but *GL1* expression under the *MYB23* regulatory elements did not rescue the *gl1* phenotype suggesting that *MYB23* is expressed relatively late compared to *GL1* (Kirik *et al*., 2005).

The second member of the activator group belongs to the basic Helix-Loop-Helix (bHLH) proteins *GLABRA3* (*GL3*) and its homologue *ENHANCER OF GLABRA3* (*EGL3*) (Payne *et al*., 2000; Zhang *et al*., 2003; Bernhardt *et al*., 2003). Mutation at the *GL3* locus results in a moderate effect on trichome number but has a severe negative effect on trichome branching and size (Figure 1.2M) (Hülskamp *et al*., 1994; Payne *et al*., 2000). DNA content in *gl3* trichomes is mostly 16C compared to 32C in wild type trichomes (Hülskamp *et al*., 1994). Mutation in *EGL3* does not lead to an obvious trichome phenotype but *gl3 egl3* double mutant is completely glabrous (Figure 1.2N) (Zhang *et al*., 2003). Because of the presence of the *GL3* homologue *EGL3* that functions redundantly with *GL3*, *gl3* mutants are not completely devoid of trichomes. Apart from their role in trichome patterning both *GL3* and *EGL3* participate in root hair differentiation and patterning and anthocyanin biosynthesis. EGL3 is also required for the seed coat epidermal cells development (Zhang *et al*., 2003; Gonzalez *et al*., 2009).

The third component in this group is a WD40 repeat containing protein *TRANSPARENT TESTA GLABRA1* (*TTG1*) (Koornneef M., 1981; Galway *et al*.,1994; Walker

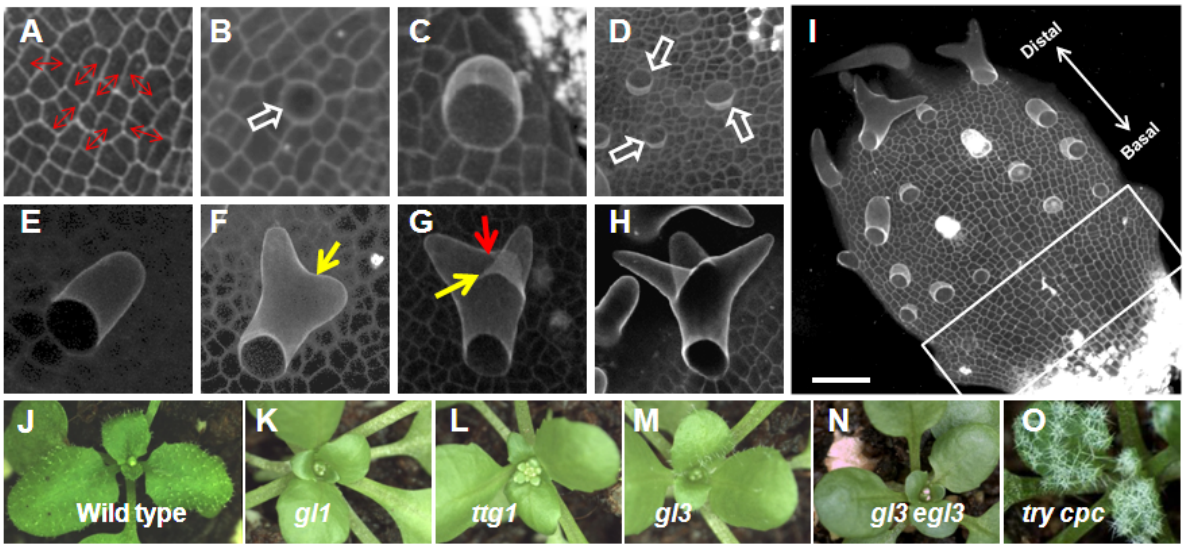

Figure 1.2: Trichome development in *Arabidopsis thaliana*. (A-H) Stages of a trichome development. (A) Undifferentiated epidermal cells, double headed arrow indicates intercellular communication. (B) One epidermal cell enters trichome fate, (arrow). (C) Trichome initial bulging out. (D) New trichomes emerge out from the epidermal cells at certain distance from each other. (E) Outgrowth of a trichome. (F) Primary branch point is indicated by arrow. (G) Primary (yellow arrow) and secondary (red arrow) branch point are indicated. (H) Matured trichome with three branches. (I) Trichome distribution pattern on a leaf, white box indicates patterning zone; scale = 50 µm. (J-O) Trichome phenotype in wild type (J), activator mutants (K-N), inhibitor mutant (O). (A-I) confocal images taken after staining with propidium iodide to mark the cell wall (false colored); (O) taken from Wester K., (2009).

et al., 1999; Larkin *et al*., 1999). Mutation at this locus results in a glabrous phenotype (Figure 1.2L). Apart from the trichome specification, *TTG1* also controls several other phenotypes such as root hair patterning, seed coat proanthocyanidin (PA) biosynthesis, seed coat mucilage production and anthocyanin biosynthesis (Koornneef M., 1981). The trichome phenotype of *ttg1* can be partially rescued by overexpressing *GL3* (Payne *et al*., 2000). Over expression of both *GL3* and *GL1* together can rescue the *ttg1* trichome phenotype to wild type suggesting that TTG1 is not absolutely necessary but is rather playing a regulatory function probably by modulating the GL3-GL1 interaction (Payne *et al*., 2000).

Apart from these three there are at least two other genes that regulate trichome development. *GLABRA2* (*GL2*) encodes a homeodomain leucine zipper transcription

factor of the class HD-Zip IV and *TRANSPARENT TESTA GLABRA 2* (*TTG2*) that encodes a WRKY transcription factor (Rerie *et al*., 1994; Johnson *et al*., 2002). Although *gl2* mutants appear glabrous, they do have underdeveloped trichomes. On the leaves of *gl2* mutant plants epidermal cells that enter into trichome fate exit from the differentiation pathway at various stages of their development and appear as enlarged flat epidermal cells (Hülskamp *et al*., 1994; Srinivas B.P., 2004). Various genetic analysis revealed that GL2 is required not just for the trichome differentiation but is needed for trichome initiation and patterning (Ohashi *et al*., 2002; Srinivas BP., 2004). GL2 is also required to specify hairless cell fate in roots (Rerie *et al*.,1994; Di Cristina *et al*., 1996; Masucci *et al*., 1996). *ttg2* mutants have reduced trichome number, are underbranched and range in structure from rudimentary outgrowth to well developed stage (although underbranched). TTG2 shares some activity with GL2 in trichome development as was evident from the more severe trichome phenotype in *ttg2 gl2* double mutant than in either of the single mutants (Johnson *et al*., 2002).

1.4.2 Negative regulators or inhibitors

This group includes the genes whose product inhibits trichome cell fate hence absence of these gene products results in increase in trichome number/density and/or cluster frequency. Single repeat R3 MYB transcription factors including *TRIPTYCHON* (*TRY*), *CAPRICE* (*CPC*), *ENHANCER OF TRIPTYCHON AND CAPRICE1, 2, 3* (*ETC1, 2, 3*) are the five homologues that make up the negative regulator group (Schnittger *et al*., 1999; Schellmann *et al*., 2002; Wada *et al*., 1997; Kirik *et al*., 2004a, 2004b; Simon *et al*., 2007; Tominaga *et al*., 2008; Wester *et al*., 2008). Members of this group lack the transactivation domain thus likely forming a transcriptionally inactive complex. *try* mutant plants show clusters of trichome where more than one trichome appears from the same trichome initiation site. *try*

mutants also show an overbranching phenotype (Hülskamp *et al*., 1994). Mutation in the *CPC* gene results in increased trichome number/density (Wada *et al*., 1997; Schellmann *et al*., 2002). The *cpc try* double mutants exhibit big clusters consisting of upto 30 trichomes per cluster (Figure 1.2O) (Schellmann *et al*., 2002). The different phenotypes of *try* and *cpc* suggests that TRY and CPC proteins might have different diffusion rates with CPC being more diffusible compared to TRY hence TRY is important for short range inhibition while CPC is required for the long range inhibiton (Schellmann *et al*., 2002). Further three homologues, ETC1-3 were also reported to act as inhibitors redundant with TRY and CPC during trichome patterning (Kirik *et al*., 2004a, 2004b; Simon *et al*., 2007; Wester *et al*., 2008; Tominaga *et al*., 2008). Triple and quadruple mutants show very severe phenotypes. Triple mutant *cpc try etc1* and *cpc try etc3* show incresed cluster size compared to *try cpc* double mutant. The quadruple mutant *cpc try etc1 etc3* shows the entire leaf surface covered with trichomes (Kirik *et al*., 2004a, 2004b; Tominaga *et al*., 2008; Wester *et al*., 2008). These observations further highlights the fact that evey epidermal cell is equally potent to develop into a trichome though not every epidermal cell becomes a trichome, even in the quadrupel-mutant. Apart from inhibition of trichome fate on the leaf epidermis these inhibitors also inhibit atrichoblast cell fate and promote trichoblast formation in the root (Wada *et al*., 1997, 2002; Schellmann *et al*., 2002; Kirik *et al*., 2004a, 2004b; Simon *et al*., 2007; Tominaga *et al*., 2008).

1.5 Expression, interaction and transcriptional regulation of trichome regulators

Binding of GL1 and TTG1 simultaneously to GL3/EGL3 at different binding sites but not interacting with each other was shown by yeast two-hybrid and co-precipitation experiments (Kirik *et al*., 2005; Zhang *et al*., 2003; Payne *et al*., 2000;

Zimmermann et al., 2004; Wang *et al*., 2008; Digiuni *et al*., 2008; Zhao *et al*., 2008; Gao *et al*., 2008). The existance of the GL1-GL3-TTG1 trimeric complex was shown by co-precipitation assay by Zhao *et al*., (2008). The fact that these three proteins share several of the trichome regulators as their common targets supports the existance of the trimeric complex (Zhao *et al*., 2008) (Figure 1.3). Positive action of this complex is counteracted by inhibitors which compete with GL1 for the binding site in GL3 thereby rendering the complex inactive. Competition between the inhibitors and GL1 for the binding site in GL3 was demonstrated by yeast three-hybrid analysis (Payne *et al*., 2000; Wester *et al*., 2008; Esch *et al*., 2003; Bernhardt *et al*., 2003). Physical interaction between TRY and GL1 was surprising but authors clearly showed that this interaction is not relevant for patterning (Digiuni *et al*., 2008). TRICHOMELESS1 (TCL1), which is single-repeat MYB type transcription factor that negatively regulates trichome formation in the inflorescence epidermis was shown to bind to *GL1* promoter by ChIP assay (Wang *et al*., 2007). This hinted at direct regulation of activators at the expression level by the inhibitors .

Apart from *TTG1* all the other patterning genes exhibit a similar expression pattern. They are ubiquitously expressed in all the epidermal cells in the trichome patterning zone of the leaf and show increased expression in the incipient trichomes (Larkin *et al*., 1996; Payne *et al*., 2000; Schellmann *et al*., 2002; Zhang *et al*., 2003; Kirik *et al*., 2004a, 2004b; Tominaga *et al*., 2008; Wester *et al*., 2008; Zhao *et al*., 2008; Bouyer *et al*., 2008). As the leaf matures the expression of both activators and the inhibitors is limited to the trichome. This paradoxical phenomenon fits perfectly with the dynamic nature of the inhibitors expected in the theoratical model by Meinhardt and Gierer (1974). Accordingly the expression of inhibitors must be under the tight control of the activators. Hence highest expression of inhibitors is also at the place where activators are highly expressed (Figure 1.1A, B). Several studies showed that expression of inhibitors is indeed

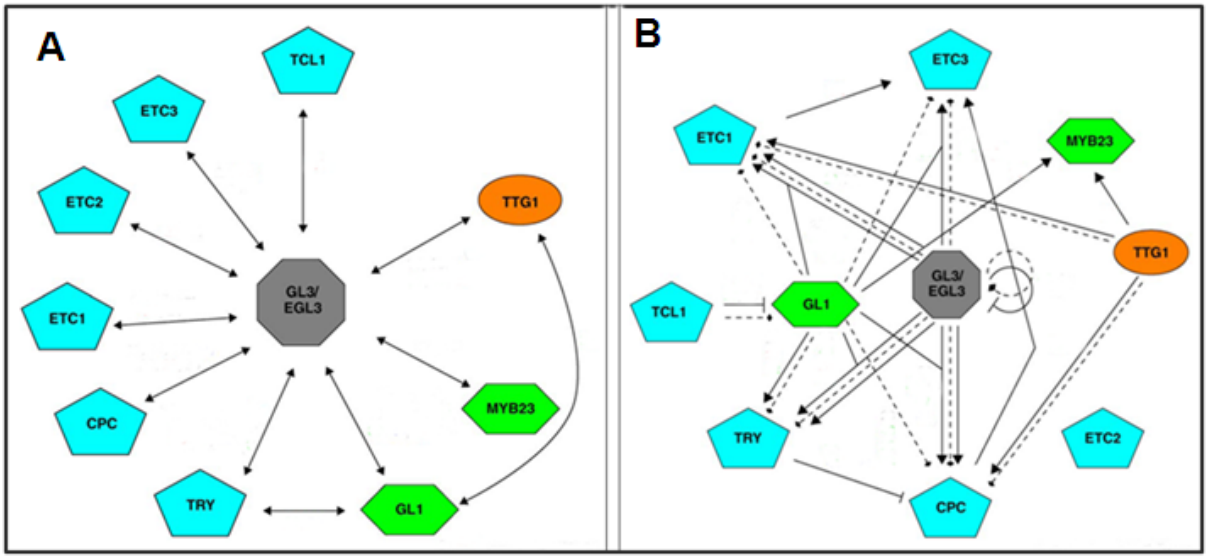

Figure 1.3: Interaction and expression regulatory networks of trichome regulators. (A) Protein-protein interaction network based on yeast two hybrid, GAL4::GUS reporter in co-transformed protoplasts, pull down experiments and BiFC results. (B) Cross regulatory interactions between trichome patterning genes. Arrow, positive regulation; blunted lines, negative regulation; solid lines, evidence based on expression in mutants or overexpression lines; dashed lines, based on indirect evidences such as CHIP experiment. Picture taken from Pesch and Hülskamp, (2009).

controled by activators. Expression of *TRY* was completely absent in *gl3* and *gl1* mutants as shown by GUS analysis (Digiuni *et al.*, 2008). GL3 regulates the expression of *CPC* and *ETC1* by directly binding to their promoters in a GL1 dependent manner while it binds to *TRY* promoter independent of GL1 (Morohashi *et al.*, 2007; Zhao *et al.*, 2008). Apart from binding to the regulatory sequences of inhibitors GL3 was also shown to bind to and activate the expression of *GL2* and *TTG2* in co-operation with GL1 (Morohashi *et al.*, 2007; Zhao *et al.*, 2008). Similarly GL1 and TTG1 were shown to share the same target genes as GL3 thus supporting the existance of GL1-GL3-TTG1 trimeric complex controlling the expression of other regulators of trichome cell fate and patterning (Zhao *et al.*, 2008; Morohashi *et al.*, 2007; Morohashi and Grotewold, 2009). Furthermore, the other requirement of the activator-inhibitor model that the inhibitors are highly mobile compared to activators, was shown by transient expression in leaf epidermis

as well as by expressing them under tissue specific promoters in plants (Digiuni *et al*., 2008; Wester *et al*., 2009; Zhao *et al*., 2008).

1.6 The role of TTG1 in trichome patterning: new findings

Genetic studies have shown that strong *ttg1* alleles (*ttg1-1* and *ttg1-13*) are glabrous whereas weak alleles (*ttg1-9*, *ttg1-10*, *ttg1-11* and *ttg1-12*) show clusters and an underbranched trichome phenotype (Koornneef M. 1981; Koornneef *et al*., 1982; Larkin *et al*., 1999; Walker *et al*., 1999). These paradoxical observations points to a role of TTG1 in both positive and negative regulation of trichome development.

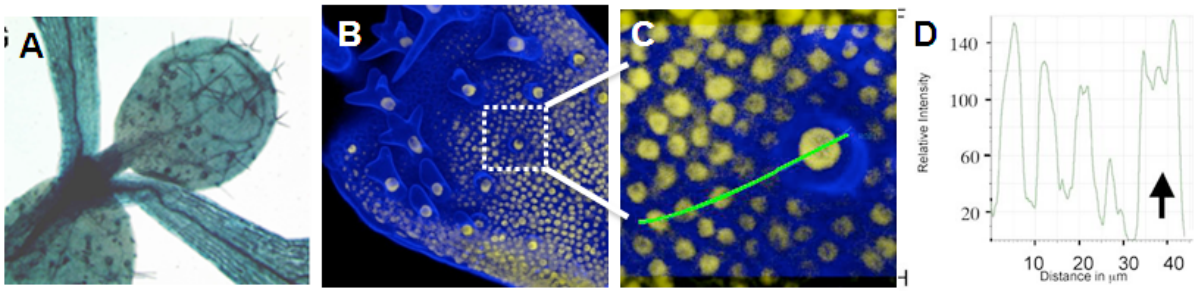

Figure 1.4: *TTG1* expression and distribution pattern. (A) pTTG1::GUS expressing line showing the expression pattern of *TTG1* promoter, taken from Bouyer D., (2004). (B) *ttg1*pTTG1::TTG1:YFP line showing cellular distribution pattern of TTG1:YFP protein. (C) Close look at the marked region in (B) showing distribution of TTG1:YFP in and around a trichome initial (arrow). (D) Graph showing YFP fluorescence intensity along the green line in (C), arrow indicates trichome initial. Yellow, YFP fluorescence; blue, cell wall marked with propidium iodide (false colored); (B-D) taken from Bouyer *et al*., (2008).

TTG1 is needed in the trimeric transcriptional activator complex for proper activation of downstream targets genes. Moreover, Recent findings clearly hinted how TTG1 could fulfill its function as a negative regulator of trichome fate. Bouyer *et.al*., (2008) discovered that during trichome patterning TTG1 protein is accumulated in trichome initials while being depleted from the surrounding cells. Analysis of YFP fluorescence in lines expressing the fusion protein TTG:YFP

driven by the *TTG1* promoter showed an elevated signal in the trichome cell while the signal was 39%, 76% and 93% in the 1st, 2nd and 3rd tiers respectively around the trichome initial (Figure 1.4) (Bouyer *et.al*., 2008).

1.7 Aim of the research

The observation of the TTG1 depletion in the trichome neighboring cells led to the postulation that apart from the widely applied activator inhibitor mechanism, an activator depletion mechanism might play a role in trichome patterning in *Arabidopsis thaliana*. While in an activator inhibitor mechanism TTG1 functions as an activator of a trichome fate, its removal from the trichome neighboring cells in the activator depletion mechanism renders a negative effect on these cells, which is equivalent to the active inhibition by the inhibitors. Hence my Ph.D thesis was aimed to investigate the molecular mechanism involved in TTG1 depeletion and to analyse the role of depletion in trichome pattern formation. The other objectives were to characterize the mobilty domain in TTG1 and to isolate TTG1 transport inhibitor mutants by EMS mutagenesis of the *ttg1*pRBC::TTG1 plants.

2 Results

2.1 Analysis of TTG1:YFP depletion in *gl3* mutant

Although *TTG1* is expressed ubiquitously at all stages of leaf and trichome development the cellular distribution pattern of TTG1 protein is not consistent with the expression pattern. It was shown that TTG1 protein is accumulated in the nucleus of the developing trichome and is depleted from the cells surrounding it (Bouyer *et al*., 2008). TTG1 is a mobile protein, however, it is not specifically transported into the trichome. These observations raised the question what makes TTG1 to accumulate in the trichome nucleus while being depleted from the surrounding cells. The *GL3* expression pattern, GL3 protein localization and its strong interaction with TTG1 as shown in yeast two-hybrid and co-precipitation experiments hints at possible role of the GL3 protein in regulating the cellular distribution of TTG1 (Payne *et al*., 2000; Zhang *et al*., 2003; Zhao *et al*., 2008; Bouyer D., 2004). These properties of the GL3 led to the hypothesis that TTG1 might be trapped by GL3 in the trichome initials where *GL3* is highly expressed.
In order to test the hypothesis of GL3 mediated TTG1 trapping, TTG1:YFP fusion protein was expressed under the *TTG1* promoter in *gl3* mutant background. TTG1:YFP fusion protein is uniformly distributed in all cells in the young leaf epidermis in the *gl3* mutant background (Figure 2.1). Using confocal laser scanning microscopy (CLSM) the cellular distribution of TTG1:YFP was analysed in the trichome patterning zone. YFP signal along the green line in (Figure 2.1A)

starting from trichome initial (marked by red arrow) was measured. Quantification revealed a slightly elevated level of YFP specific fluorescence in the trichome initials and the fluorescence was at similar levels in the surrounding cells. The relative intensity of YFP fluorescence corresponding to TTG1:YFP specific signal was 79% in the first tier of trichome surrounding cells, 77% in the second tier and was 79% in the third tier showing the loss of the depletion in trichome neighboring cells (Figure 2.1B, compare with Figure 1.4). These values were obtained using 40 samples.

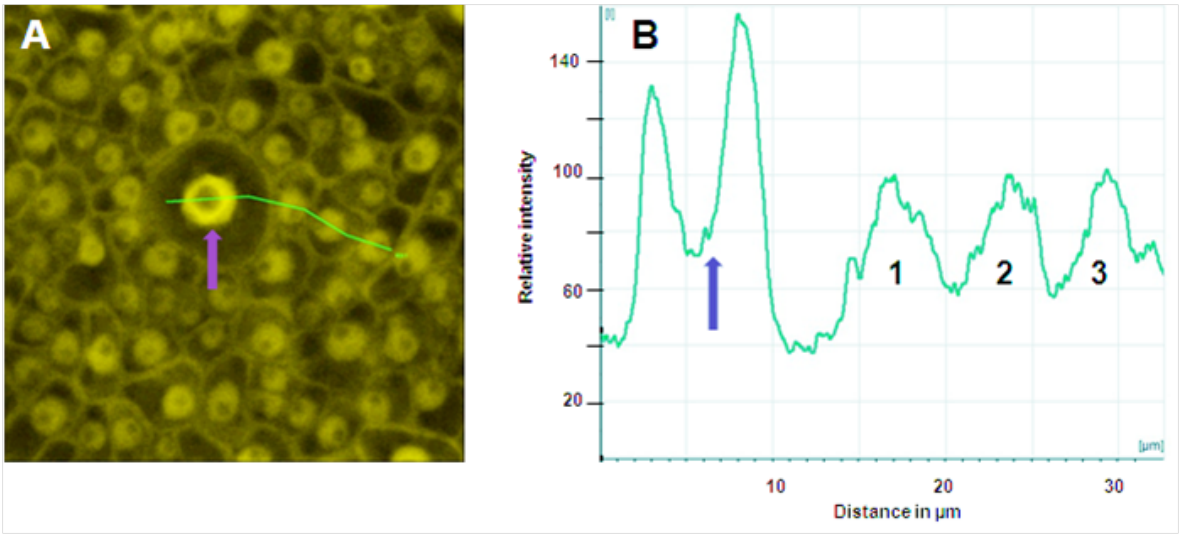

Figure 2.1: Analysis of TTG1:YFP depletion in *gl3* mutant background. (A) pTTG1::TTG1:YFP in *gl3* mutant shows clear nuclear and cytoplasmic YFP signal in the epidermal cells of the patterning zone. (B) Quantification of fluorescence intensity along the green line in (A). Yellow, YFP fluorescence; arrow, points to incipient trichome; 1, 2 and 3 in (B) indicates the YFP fluorescence intensity in first, second and third tier cells around the incipient trichome.

2.2 Effect of trichome patterning related bHLH proteins on the subcellular distribution of TTG1:YFP

Loss of depletion and qualitative observation that more TTG:YFP shifts to cytoplasm in the absence of GL3 hinted at a GL3 mediated trapping of TTG1 in the nucleus. One straight forward experiment for this would be to quantify the sub-

cellular localization of TTG1:YFP expressed under the *TTG1* promoter in the *gl3* mutant and in the *GL3* overexpression background.

2.2.1 GL3 is the main modulator of TTG1 intracellular localization

In *gl3* mutants the TTG1:YFP distribution is more diffuse compared to TTG1:YFP in the wild type background indicating a shift of the protein from the nucleus to the cytoplasm resulting in a more or less equal distribution of TTG1:YFP between cytoplasm and the nucleus. Detailed analysis at the cellular level in the patterning zone revealed clear differences in the intracellular distribution of TTG1:YFP in wild type and *gl3* (Figure 2.2A and 2.2B). I further looked at the intracellular localization of TTG:YFP when *GL3* is overexpressed under a strong promoter. To test this, I observed the distribution of TTG1:YFP in lines expressing *GL3* under the constitutively active *CaMV 35S* promoter. Expectedly TTG:YFP fluorescence was more or less restricted to nuclei in p35S::GL3 background (Figure 2.2C) compared to wild type (Figure 2.2A) and *gl3* mutant nuclei (Figure 2.2B). Interestingly in the *GL3* overexpressing lines TTG1:YFP depletion is lost. Three dimensional (3D) analysis of TTG1:YFP in all the three backgrounds further confirmed our observation (Figure 2.2D-F). In 3D pictures intensity of YFP fluorescence is indicated by height of the peaks. In wild type background YFP specific peaks of different heights indicate different amount of TTG1:YFP protein in cells. Clearly the immediate neighbors of the trichome shows the smallest peaks and with distance from the trichome initial the height of the YFP specific peak also increases (Figure 2.2D). In *gl3* mutant all the peaks appears to have fused at the base compared to discrete peaks with valleys in the wild type. This is due to equal distribution of TTG1:YFP in the cytoplasm and the nucleus (Figure 2.2E). Finally in p35S::GL3 lines each epidermal cell shows a very clear, bright and individual peak of almost the same height confirming the loss of TTG1 depletion (Figure 2.2F).

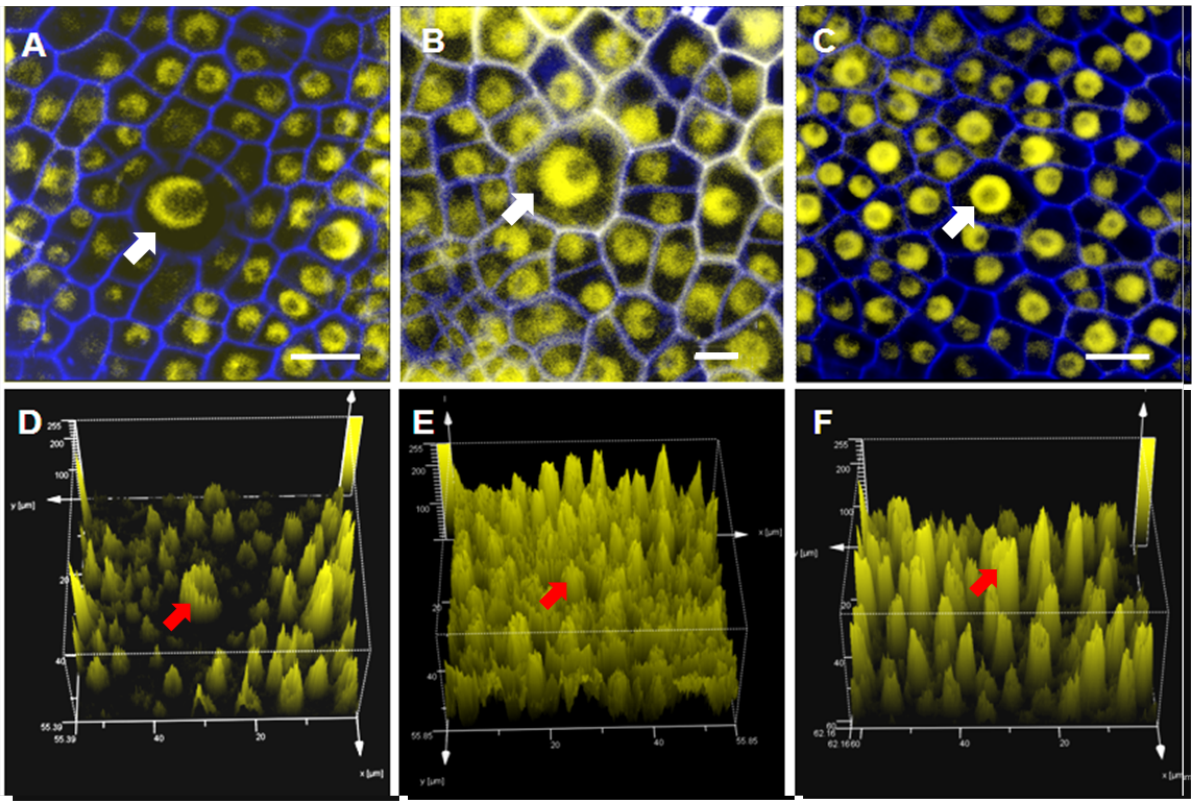

Figure 2.2: Cellular distribution of TTG1:YFP in different background.TTG1:YFP distribution in the epidermal cells of the trichome patterning zone was analyzed. (A) *ttg1*pTTG1::TTG1:YFP, YFP fluorescence is found in the nucleus and the cytoplasm. (B) *ttg1 gl3*pTTG1::TTG1:YFP, YFP fluorescence in the cytoplasm appears to be increased at the expense of nuclear intensity. (C) p35S::GL3pTTG1::TTG1:YFP, YFP fluorescence is predominantly found in the nucleus. (D-F) Three-dimensional illustration of YFP signals strength in (A-C) respectively. The fluorescence intensity is indicated by size of the peaks. White arrow, points to incipient trichome; red arrow, points to the nucleus of trichome initials; yellow, YFP specific fluorescence; Blue, cell wall stained with propidium iodide (false colored). Scale=10 µm.

Furthermore, using the CLSM quantification tool nuclear YFP fluorescence in the epidermal cells within the trichome patterning zone was quantified as percentage of the total fluorescence in the analyzed cell (Figure 2.3D). Quantitative analysis confirmed the observed impression. In wild type 72% of the TTG1:YFP fluorescence was found in the nucleus. In *gl3* mutants TTG1:YFP nuclear fraction is reduced to 49% and in p35S::GL3 lines the nuclear localized TTG1:YFP is increased to 93% (Figure 2.3D). Comparing intracellular localization of TTG1:YFP in wild type, *gl3*

mutant and p35S::GL3 expressing leaves clearly indicated a strong influence of the amount of GL3 on the intracellular localization of TTG1:YFP.

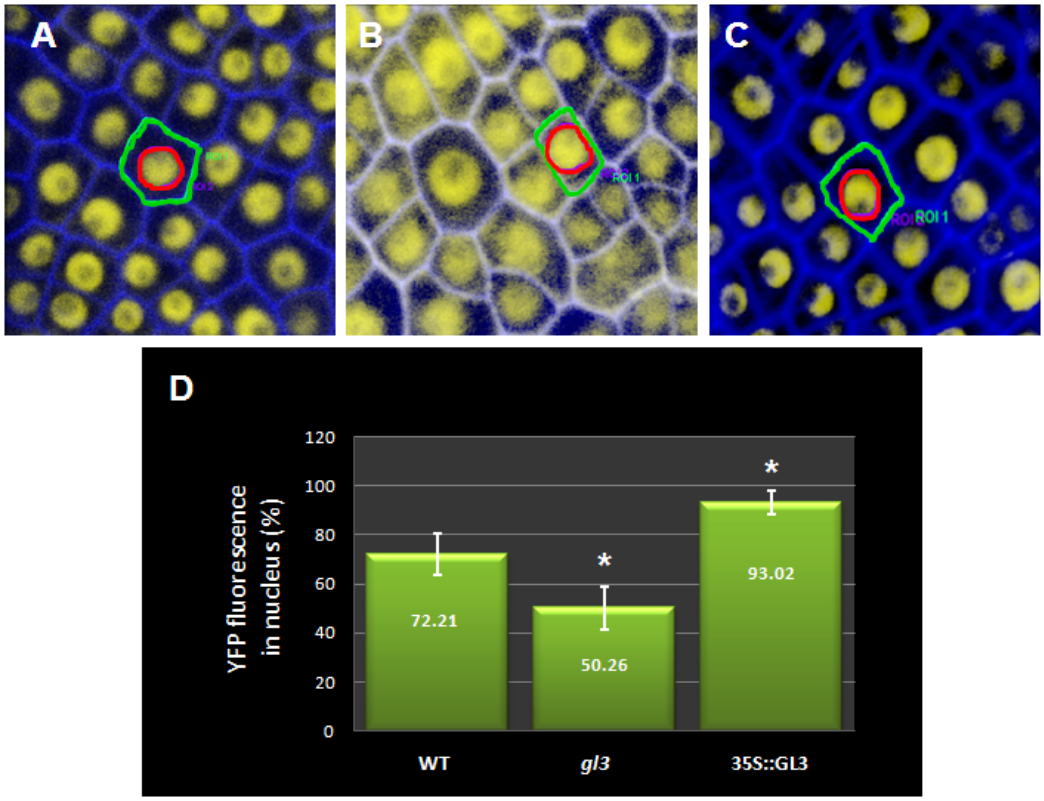

Figure 2.3: Quantification of nuclear TTG1:YFP in epidermal cells of the trichome patterning zone when expressed under *TTG1* promoter in different mutant background. (A) Wild type. (B) *gl3* mutant background. (C) p35S::GL3 background. (D) Percentage of nuclear YFP fluorescence. All values are based on at least 188 single cell measurements. * the values are statistically highly significantly different from wild type, t-test, $p < 0.0001$; yellow, YFP-specific fluorescence; blue, cell wall marked with propidium iodide (false colored); ROIs are used to quantify YFP intensity; ROI1 (green), region of interest that marks the entire cell; ROI2 (red), region of interest that marks the nucleus.

2.2.2 Additive effect of GL3 homologues on the subcellular localization of TTG1:YFP

In the absence of a functional GL3 protein nuclear TTG1 was reduced but was not exclusively cytoplasmic. This could be explained by the redundancy of bHLH genes regulating trichome fate in *Arabidopsis thaliana*. Indeed apart from GL3 at least another two bHLH proteins namely EGL3 and TT8 have been reported to

play a role in trichome development (Zhang *et al*., 2003; Maes *et al*., 2008). These proteins interact with TTG1 and MYBs and can form MYB-bHLH-WD40 trimeric complexes similar to that of GL3 (Zhang *et al*., 2003; Baudry *et al*., 2004; Maes *et al*., 2008). Hence it is likely that EGL3 and TT8 also contribute to the retention of TTG1 in the nucleus.

To test this I quantified the subcellular localization of TTG1:YFP in the trichome patterning zone of the leaf epidermis in single (*gl3*) double (*gl3 egl3*) and triple (*gl3 egl3 tt8*) mutants. Like I observed previously TTG1:YFP is partially delocalized to cytoplasm in *gl3* (Figure 2.4E-H) mutant compared to wild type situation (Figure 2.4A-D). Removal of more trichome regulating bHLH factors further enhanced the cytoplasmic fraction of TTG1. Quantification of nuclear fractions in these mutants revealed that nuclear TTG1:YFP was 48% in *gl3 egl3* double mutant (Figure 2.4I-L) compared to 56% in *gl3* ($p < 0.0001$). There was no significant effect on the subcellular distribution of TTG1:YFP upon additional removal of TT8, the third member of the bHLH family in trichome development (Figure 2.4M-P). In *gl3 egl3 tt8* triple mutant 49% of TTG1:YFP fusion protein was accounted in the nucleus, which was not significantly different from that of nuclear TTG1:YFP amount in *gl3 egl3* ($p > 0.05$). TTG1:YFP in the control line *ttg1*pTTG1::TTG1:YFP was mainly in the nucleus (Figure 2.4A-D). It showed 68% nuclear TTG1:YFP protein which was significantly higher than the nuclear fraction observed in *gl3*, *gl3 egl3* and *gl3 egl3 tt8* ($p < 0.0001$) (Figure 2.4Q).

2.2.3 TTG1:YFP subcellular localization analysis in the roots of *gl3* and *gl3 egl3* mutants

Similar to the observation in the leaf epidermis an influence of bHLH proteins on the TTG1 localization would be expected in the root cells as well due to their involvement in root hair patterning. Qualitative analysis indeed revealed that TTG1:YFP fluorescence was clearly shifted to cytoplasm in *gl3* and *gl3 egl3*

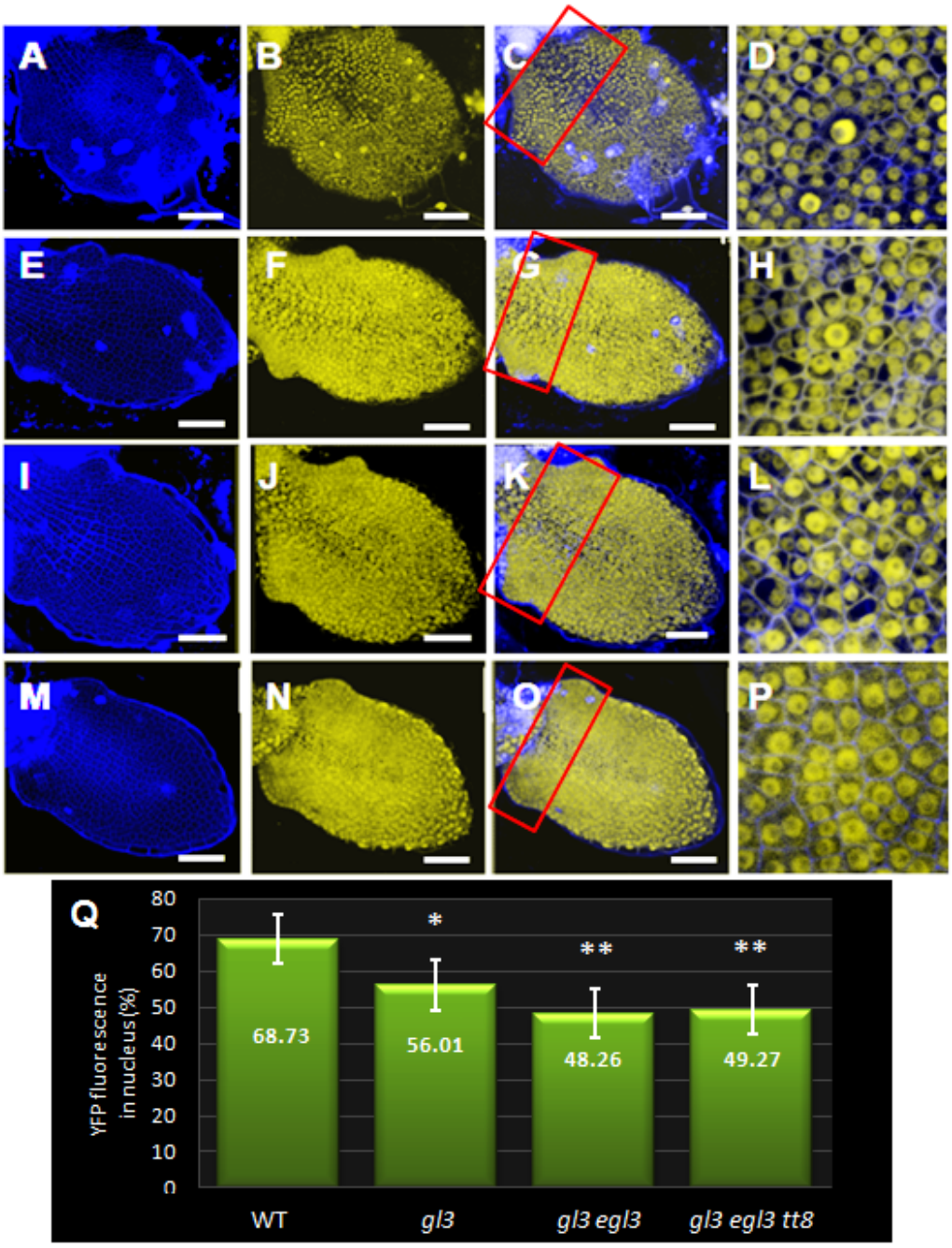

Figure 2.4: Analysis of TTG1 localization in different bHLH mutants. (A-D) *ttg1*pTTG1::TTG1:YFP. (E-H) *gl3*pTTG1::TTG1:YFP. (I-L) *gl3 egl3*pTTG1::TTG1:YFP. (M-P) *gl3 egl3 tt8*pTTG1::TTG1:YFP. (A, E, I, M) Cell wall stained with propidium iodide. (B, F, J, N) YFP specific fluorescence. (C, G, K, O) Overlay of propidium iodide channel and YFP channel. (D, H, L, P) Close up look at the localization of TTG1:YFP in the epidermal cells of the patterning zone. (Q) Graph showing the nuclear TTG1:YFP presented as a percentage of total YFP fluorescence in the cell, * the values are statistically highly significantly different from wild type, (t-test, $p < 0.0001$); ** the values are statistically highly significantly different from wild type and *gl3*, (t-test, $p < 0.0001$); yellow, YFP fluorescence; blue, cell wall stained with propidium iodide (false colored). Scale=50µm.

mutants (Figure 2.5). Triple mutant *gl3 egl3 tt8* was not included in this analysis as *TT8* is not expressed in roots (Baudry *et al.*, 2006). However, in future detailed CLSM based quantitative analysis would be more convincing whether GL3 and EGL3 have additive effect on the subcellular localization of TTG1:YFP in roots as well similar to the observations in the leaves.

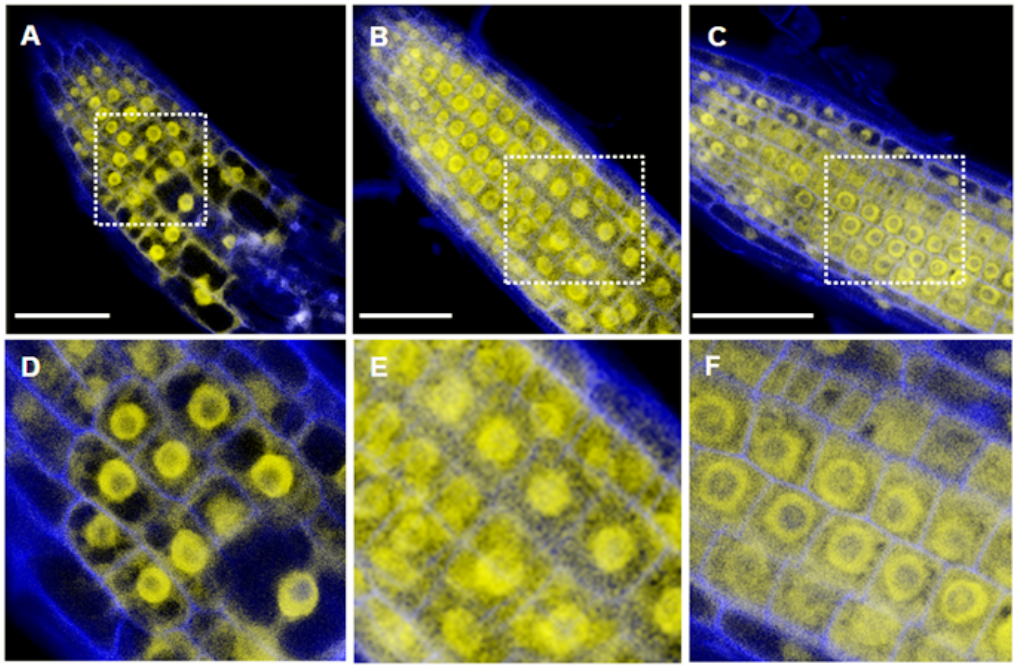

Figure 2.5: Localization analysis of TTG1:YFP in the roots of wild type (wt), *gl3* and *gl3 egl3*. (A) wtpTTG1::TTG1:YFP. (B) *gl3*pTTG1::TTG1:YFP. (C) *gl3 egl3*pTTG1::TTG1:YFP. (D-F) higher magnification of the marked region in (A-C) respectively.

2.3 Influence of GL3 on the nuclear trapping/ transport of TTG1

TTG1 is predominantly localized in the nucleus in spite of not having any predictable nuclear localization sequences (Bouyer *et al.*, 2008; Zhao *et al.*, 2008). On the other hand analysis of the cellular localization of AN11, an orthologue of TTG1 from *Petunia hybrida*, had revealed a cytoplasmic targeting of the AN11 protein in cell fractionation experiments (de Vetten *et al.*, 1997). Moreover, the

TTG1 subcellular localization shows that in the epidermal cells of the young region of the leaf TTG1:YFP fusion showed strong nuclear localization in all cells including trichomes, whereas in the older leaf tissue/region it was predominantly cytoplasmic in epidermal cells and nuclear in trichomes (Bouyer D., 2004). These observations raised a question as to what is modulating the TTG1 subcellular localization changes in the cells. In the previous experiment I could show that nuclear amount of TTG1 is strongly influenced by bHLH factors with GL3 being the most important. Moreover, the TTG1 orthologue PFWD from *Perilla frutescens* when co-expressed with the GL3 homologue from the same species in onion epidermal cells by biolistic transformation showed a clear localization to nucleus, which otherwise is present both in cytoplasm and the nucleus when expressed alone (Sompornpailin *et al*., 2002). From the previous experiment it is likely that GL3 and TTG1 also share a similar relationship (Figure 2.3). Hence I wanted to check the specificity of GL3 and TTG1 interaction for TTG1 trapping in the nucleus.

2.3.1 Mapping mutual interaction domains in TTG1 and GL3

To demonstrate that the specific interaction between TTG1 and GL3 is responsible for TTG1 nuclear targeting it was planned to use the respective variants lacking the mutual interaction as control. For this I created TTG1 and GL3 variants that disturb their interaction. A TTG1 variant lacking the C terminal 26 aa (here after referred to as TTG1$\triangle$C26) was earlier shown not to interact with GL3 in yeast two-hybrid (Figure 2.17A) (Payne *et al*., 2000). For GL3, I mapped the TTG1 interaction domain to an internal 78 amino acid spanning region between 360-437 amino acids in GL3. This region was mapped based on the corresponding domain in EGL3, which was previously shown to interact with TTG1 in yeast two-hybrid screens (Zimmermann, 2004). This 78 amino acid region from GL3 was deleted to create a GL3 deleted version (here after referred to as GL3$\triangle$78) that does not interact with TTG1 as I could show in yeast two-hybrid assays (Figure 2.6A). To test the

specificity of the deleted 78 amino acid region from GL3 for interaction with TTG1, I fused the 78 amino acid GL3 fragment N-terminally to GUS in order to ensure the stability of the small fragment (here after referred as 78GL3:GUS) and found a strong interaction with TTG1 that was comparable to full length GL3 in yeast two-hybrid (Figure 2.6A). Furthermore, based on the previous report that N-terminal

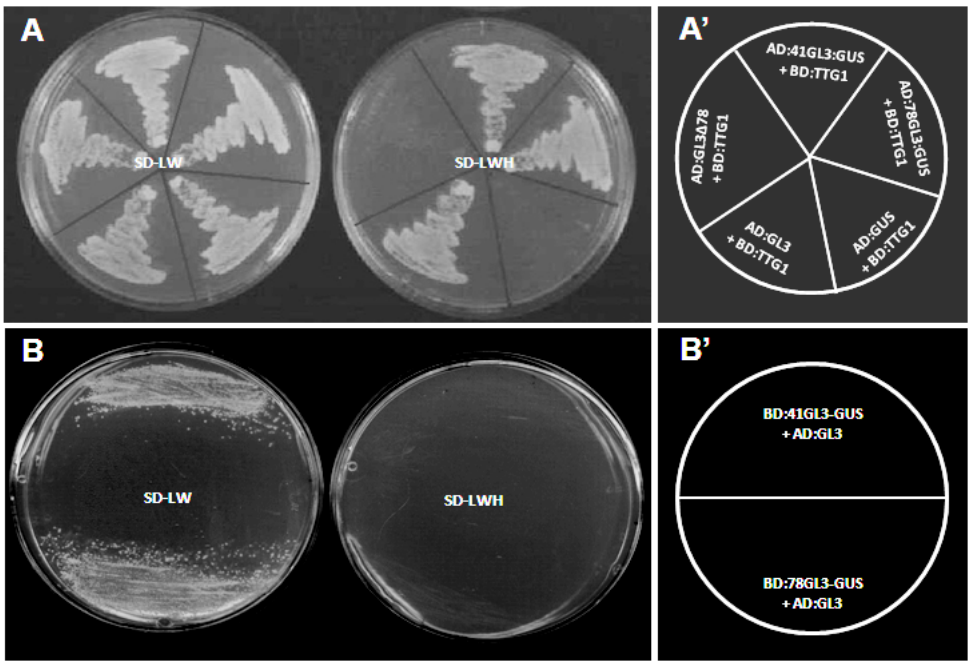

Figure 2.6: Yeast two-hybrid analysis of GL3 variants and GL3 fragments (41GL3 and 78GL3 aptamers). (A, B) Shows yeast growth on two amino acid drop medium for selection (SD-LW) and three amino acid drop out medium for interaction (SD-LWH). (A', B') Schematic presentations showing the positions of different interactions tested in yeast two-hybrid analysis in (A, B) respectively. Proteins were fused to either GAL4 transactivation domain (AD); or fused to GAL4 DNA binding domain (BD); yeast growth indicates positive interactions; no growth indicates lack of interaction; the interaction on interaction medium contained 5mM 3-aminotriazole (3-AT).

region (1- 400 amino acids) but not the C-terminal (400-637 amino acids) fragment of GL3 showed interaction with TTG1 (Payne *et al.*, 2000) I further reduced the TTG1 interaction domain to a 41amino acid region between 360 to 400 amino acid. This 41 amino acid fragment of GL3 was fused N-terminally to GUS (41GL3:GUS) to stabilize the small peptide. Yeast two-hybrid analysis showed that 41amino acid fragment of GL3 is sufficient to show interaction with TTG1 as strong as the

78 amino acid fragment and the full length GL3 (Figure 2.6A). For the further *in planta* studies it was necessary that these fragments were specific for TTG1 interaction and they did interact with the endogenous GL3. It was indeed observed that these fragments showed no interaction with GL3 in yeast two-hybrid analysis (Figure 2.6B). For further studies I used the GL3△78 variant and the aptamer 78GL3 fused N-terminally to GUS (78GL3:GUS). The aptamers are small protein fragment that compete with the binding of two proteins under consideration and the method is referred as an aptamer approach.

2.3.2 TTG1 lacks any functional nuclear localization signals (NLS)

The regulation of nuclear targeting of GL3 and TTG1 was analyzed using a yeast based nuclear transportation trap (NTT) assay, a selection system for nuclear targeted proteins (Ueki *et al*., 1998). Here the protein of interest is expressed as a fusion to an artificial transactivator LexAD fused to a nuclear export signal (NES) at its N-terminal (NES:LexAD). Due to the presence of the NES non-nuclear targeted proteins that lack a functional NLS remain in the cytoplasm or are exported out of the nucleus. On the other hand nuclear targeted proteins can overcome the NES mediated nuclear export and enter the nucleus thereby activating the reporter gene (Ueki *et al*., 1998). I used this method first to test if TTG1 has any functional NLS. In this assay TTG1 and GL3 were fused to create NES:LexAD:TTG1 and NES:LexAD:GL3 respectively. This assay clearly demonstrated that TTG1 did not enter the nucleus suggesting that it is not actively transported into the nucleus (Figure 2.7A). By contrast, GL3 behaved as a nuclear protein in this assay (Figure 2.7A). In the second experiment, the NTT assay was slightly modified where NES:LexAD:TTG1 fusion protein was co-expressed with *GL3* protein. Upon co-expression of NES:LexAD:TTG1 and GL3, TTG1 was clearly targeted to the nucleus suggesting GL3 mediated transport

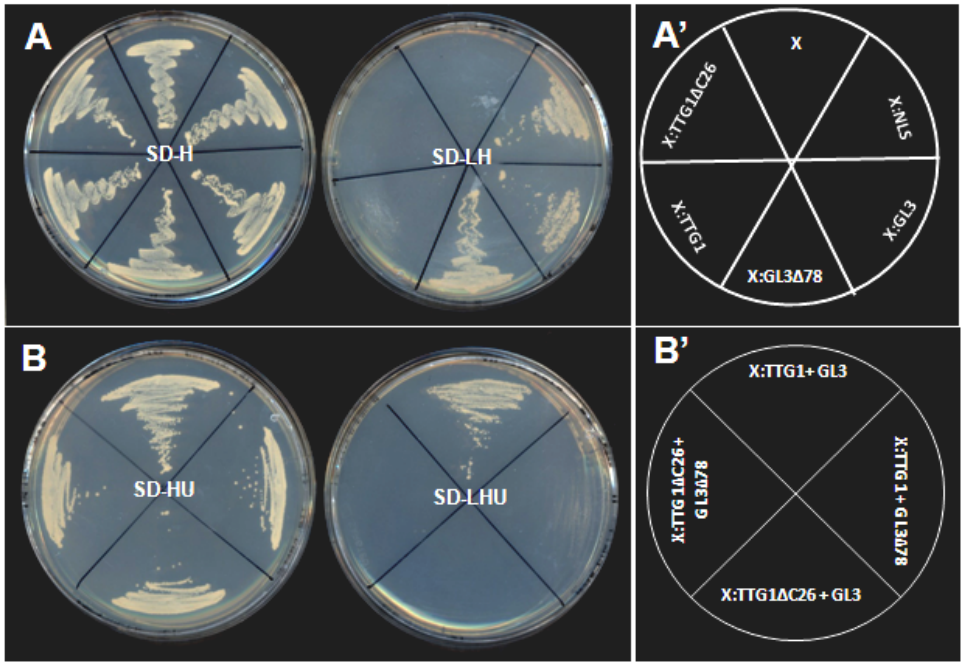

Figure 2.7: Yeast based Nuclear Transportation Trap (NTT) assay to test GL3 influence on TTG1 nuclear transport. (A) NES based nuclear transportation trap (NTT) assay demonstrating that GL3 and GL3△78 but not TTG1 and TTG1△C26 can enter into the nucleus. X (NES:LexAD) was used as a negative control and X:NLS where SV40 viral NLS was fused to NES:LexAD was used as positive control. (B) NTT assay showing TTG1 is transported into nucleus in the presence of GL3. (A' and B') Schematic presentation of the positions of fusion proteins tested for nuclear transport in (A and B) respectively. Yeast growth, fusion protein is in the nucleus; no growth, fusion protein is exported out of the nucleus; SD-H and SD-HU, amino acid drop out medium for the selection of yeast cells transformed with one and two constructs respectively; SD-LH and SD-LHU, amino acid drop out medium for the selection of nuclear transport of a protein fused to NES:LexAD when expressed alone (A) and in the presence of GL3 (B) respectively.

of TTG1 into the nucleus (Figure 2.7B). I further confirmed the specificity of the interaction between GL3 and TTG1 for the nuclear transport of TTG1 by using GL3△78 and TTG1△C26 in various combinations in the NTT assay (Figure 2.7B). First NES:LexAD:GL3△78 and NES:LexAD:TTG1△C26 were tested for their localization by NTT assay in yeast. As expected NES:LexAD:GL3△78 was clearly in the nucleus while NES:LexAD:TTG1△C26 was not (Figure 2.7A). Though GL3△78 is localized in the nucleus (Figure 2.7A), it failed to trap TTG1 in the nucleus when co-expressed in NTT assay (Figure 2.7B). Similarly TTG1△C26

that lacks interaction with GL3 also failed to be transported into the nucleus upon co-expression with GL3 in this assay (Figure 2.7B).

2.3.3 *In planta* analysis of the GL3 and TTG1 interaction specificity for TTG1 nuclear trapping

A. Transient expression in onion epidermal cells

In micropojectile bombardment experiments in onion epidermal cells all used fusion proteins were expressed under control of the *CaMV 35S* promoter. In one set of experiment I co-expressed TTG1:YFP and CFP:GL3. While TTG1:YFP alone is localized in the nucleus and the cytoplasm (Figure 2.8B), co-expression with CFP:GL3, which is in the nucleus (Figure 2.8C) causes a predominantly nuclear localization of TTG1:YFP (Figure 2.8E). Next CFP:GL3△78, which is in the nucleus (Figure 2.8H) but lacks TTG1 interaction (Figure 2.8A) was used in a similar co-expression analysis. Co-expression of CFP:GL3△78 (Figure 2.8H) had no effect on the localization of TTG1:YFP (Figure 2.8G). To test the localization of TTG1:YFP when GL3 is targeted to the cytoplasm the NLSs from GL3 were deleted to create CFP:GL3△NLS. Deletion of NLS in GL3 did not affect its interaction with TTG1 in yeast two-hybrid (Figure 2.8A) but its localization in the cell is completely shifted to the cytoplasm (Figure 2.8D). Co-expression of TTG1:YFP (Figure 2.8I) and CFP:GL3△NLS (Figure 2.8J) revealed that significant amount of TTG1:YFP is still in the cytoplasm (Figure 2.8I) unlike in the co-expression of CFP:GL3 and TTG1:YFP where TTG1:YFP was predominantly in the nucleus (Figure 2.8E). TTG1:YFP is not targeted to the nucleus anymore instead it is distributed in nucleus and cytoplasm (Figure 2.8I) much like TTG1:YFP expressed alone (Figure 2.8B). Nevertheless, I cannot rule out the quantitative differences in the cytoplasmic concentration of TTG1:YFP when TTG1:YFP is expressed alone and when it is expressed together with CFP:GL3△NLS.

As deletions may cause aberrant protein functions I tested the functionality of the

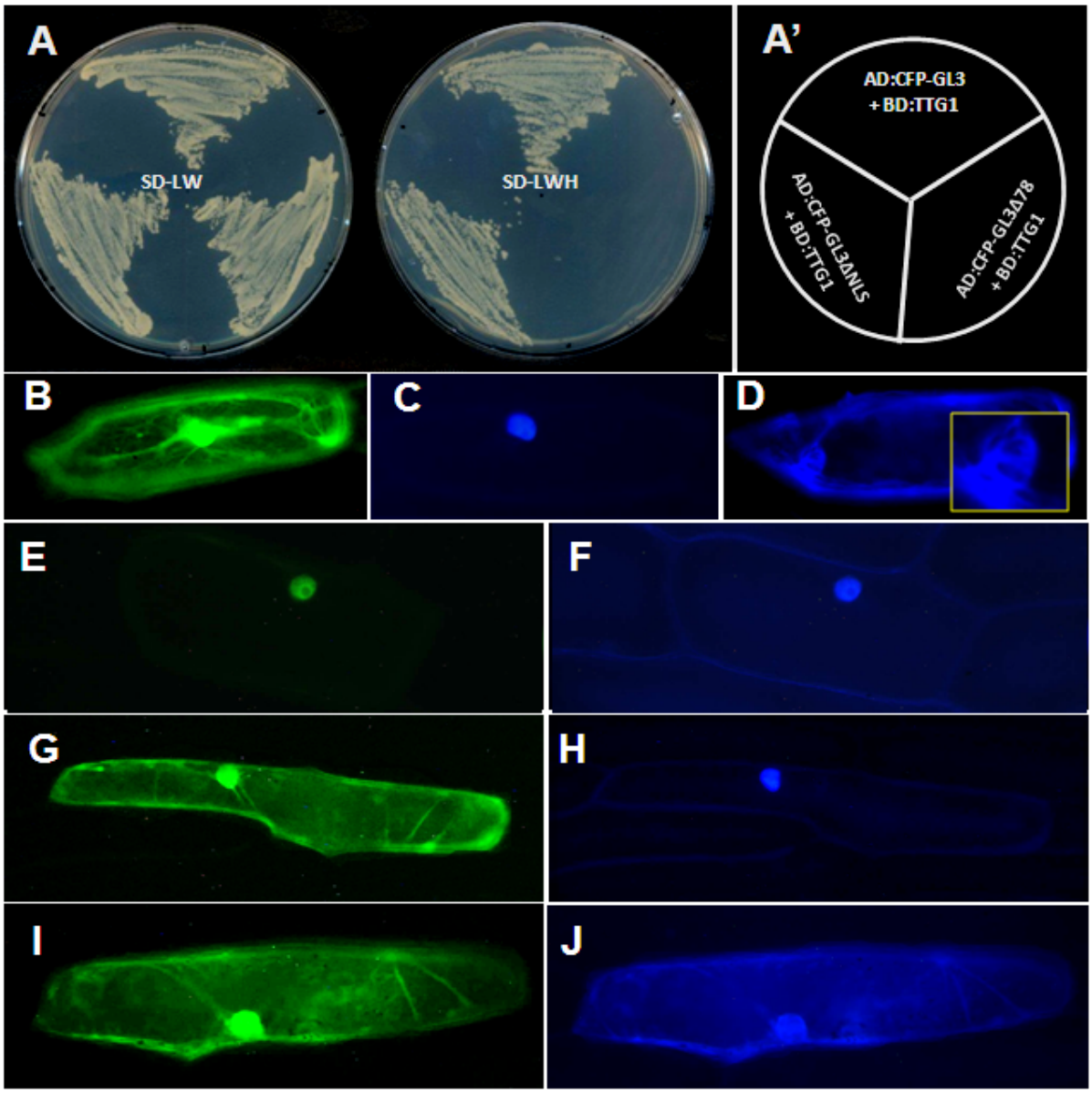

Figure 2.8: Transient expressions studies to show nuclear trapping of TTG1 as influenced by the interaction with GL3. (A) Yeast two-hybrid analysis to test the TTG1 interaction with CFP fused GL3 variants. (A') Schematic presentation showing the positions of different interactions tested. TTG1 was fused to GAL4 DNA binding domain; CFP fused GL3 variants were fused to GAL4 transactivation domain. (B-I) Transient expression using microprojectile bombardment in onion epidermal cells. (B) TTG1:YFP, fluorescence is found in the nucleus and the cytoplasm. (C) CFP:GL3, fluorescnece is found only in the nucleus. (D) GL3△NLS, fluorescence is found only in the cytoplasm. Inset showing the magnification of nucleus. (E) Co-expression of TTG1:YFP and CFP:GL3, bulk of the TTG1:YFP fluorescence is restricted to nucleus. (F) Same cell as in (E) showing the CFP:GL3 localization. (G) Co-expression of TTG1:YFP and CFP:GL3△78, TTG1:YFP is localized in the cytoplasm and the nucleus. (H) Same cell as in (G) showing the CFP:GL3△78 localization. (I) Co-expression of TTG1:YFP and CFP:GL3△NLS, TTG1:YFP is localized in cytoplasm and nucleus. (J) Same cell as in (I) showing CFP:GL3△NLS localization. All the constructs in the bombardment experiment were expressed under *p35S* promoter.

GL3 variants (GL3△NLS and GL3△78) with two experimental approaches. First I could show that GL3△78 and GL3△NLS as well as their N-terminal CFP fused versions (CFP:GL3△78 and CFP:GL3△NLS) interact with other trichome regulators such as GL1, CPC and TRY (Table 2.1) which have been shown to interact with GL3 (Payne *et al.*, 2000; Zhang *et al.*, 2003; Zhao *et al.*, 2008). The second

Table 2.1: Yeast two-hybrid analysis of GL3 variants with trichome regulators.

	BD:TRY	BD:CPC	BD:GL1	BD:TTG1
AD:GL3	+++	+++	+++	++++
AD:GL3△78	+++	+++	+++	-
AD:GL3△NLS	+++	+++	+++	++++
AD:CFP:GL3	+++	+++	++	++++
AD:CFP:GL3△78	++	+++	++	-
AD:CFP:GL3△NLS	++	+++	++	++++

+, indicates the strength of the interaction; **-**, is no interaction; AD, is the transactivation domain; BD, is the DNA binding domain.

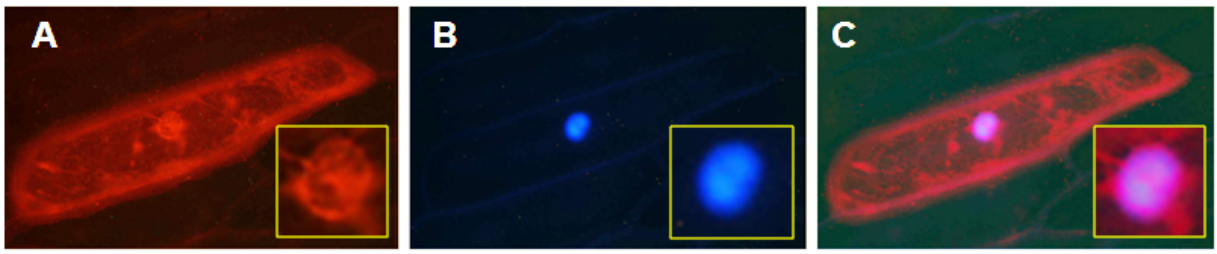

Figure 2.9: Aptamer 78GL3:GUS is localized exclusively in the cytoplasm. Localization of the 78GL3:GUS was studied by expressing transiently in onion epidermal cells. (A) RFP:78GL3:GUS. (B) CFP:GL3. (C) Overlay of (A) and (B). Inset in (A-C) shows magnification of the nucleus.

approach was aimed to demonstrate the relevance of TTG1 and GL3 interaction by an aptamer approach. Here I used 78GL3:GUS as an aptamer to disturb the interaction between TTG1 and GL3. First I tested the localization of 78GL3:GUS

by fusing red fluorescent protein (RFP) at its N-terminus and co-expressed it with CFP:GL3 in onion epidermal cells. Here I could show that RFP:78GL3:GUS is localized in the cytoplasm and did not alter the localization of CFP:GL3 (Figure 2.9). RFP:78GL3:GUS was then co-expressed with CFP:GL3 and TTG1:YFP. Here RFP:78GL3:GUS fluorescence was observed in the cytoplasm (Figure 2.10B) and efficiently interfered with the ability of CFP:GL3 (Figure 2.10A) to recruit TTG1:YFP (Figure 2.10C) to the nucleus. On the contrary in the control experiment where RFP:GUS (Figure 2.10E) instead of RFP:78GL3:GUS was co-expressed with CFP:GL3 (Figure 2.10D) and TTG1:YFP (Figure 2.10F) the nuclear targeting of TTG1:YFP by CFP:GL3 was not affected (Figure 2.10D-F). This clearly demonstrates that TTG1 localization to the nucleus is triggered by GL3 through direct binding.

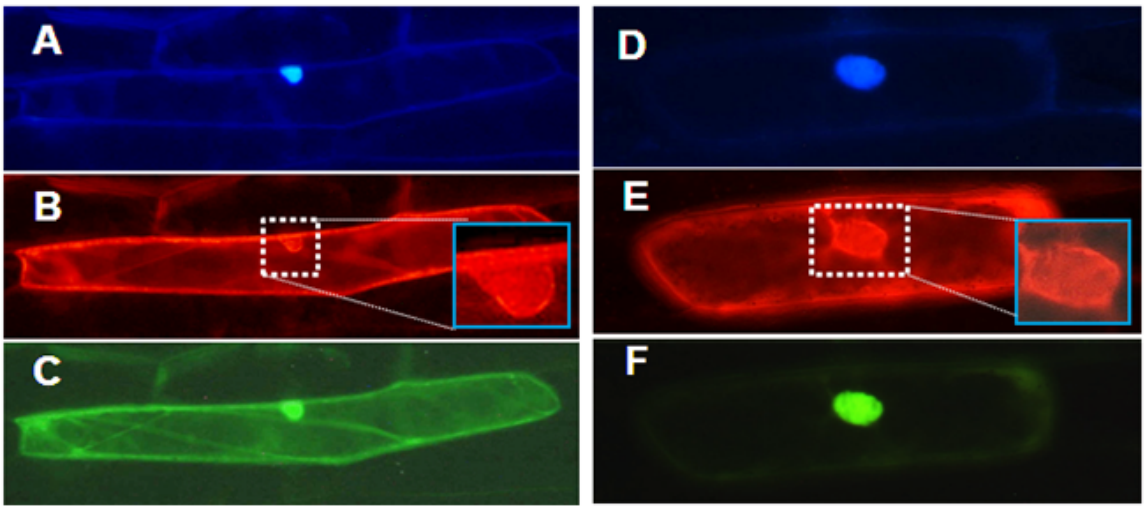

Figure 2.10: Aptamer 78GL3:GUS competes with GL3 for binding to TTG1 in aptamer experiment. (A-C) Co-expression of CFP:GL3, RFP:78GL3:GUS and TTG1:YFP, showing the localization of CFP:GL3 in the nucleus (A), RFP:78GL3:GUS in the cytoplasm (B) and TTG1:YFP in the cytoplasm and the nucleus (C). (D-F) Co-expression of CFP:GL3, RFP:GUS and TTG1:YFP, showing the localization of CFP:GL3 in the nucleus (D), RFP:GUS in the cytoplasm (E) and TTG1:YFP predominantly in the nucleus (F). Insets in (B, E) shows the magnification of the nucleus; all the constructs were expressed under the *p35S* promoter.

B. TTG1△C26:YFP is exclusively cytoplasmic

TTG1△C26 was shown not to interact with GL3 in yeast two-hybrid assay (Figure 2.17A) (Payne *et al.*, 2000). I further tested the interaction of TTG1△C26 with the other bHLH factors EGL3 and TT8 whose role was also implicated in trichome development (Zhang *et al.*, 2003; Maes *et al.*, 2008). TTG1△C26 did not interact with GL3, EGL3 and TT8 in yeast two-hybrid assay (Figure 2.17). Further the localization of TTG1△C26 was analysed in plants. Transgenic plants expressing pTTG1::TTG1△C26:YFP variant showed exclusively cytoplasmic localization while lines expressing pTTG1::TTG1:YFP showed predominantly nuclear YFP fluorescence indicating that for the nuclear localization of TTG1 interaction with the bHLH proteins is necessary (Figure 2.11A).

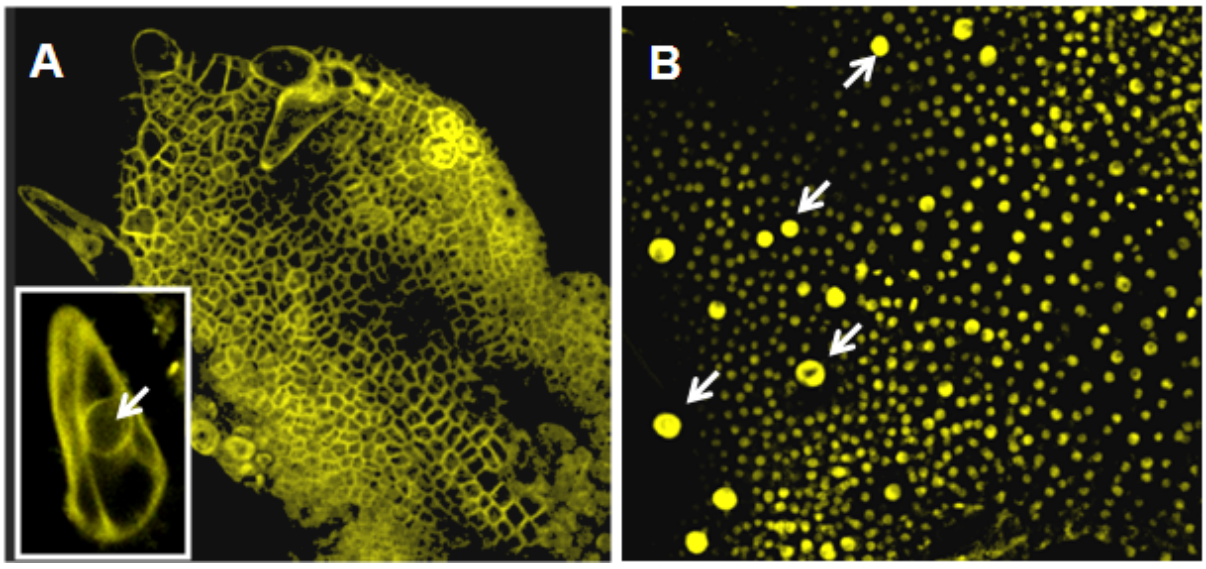

Figure 2.11: Localization of TTG1△C26 in the leaf epidermis. (A) pTTG1::TTG1△C26:YFP in *ttg1-12* showing exclusively cytoplasmic localization of TTG1△C26:YFP fusion protein in the young leaf epidermis. Inset picture of a trichome showing absence of YFP fluorescence in the nucleus marked by arrow. Note, TTG1△C26 is a *ttg1-1* allelic form of TTG1 hence shows no rescue. trichomes observed in (A) are the trichomes present in the *ttg1-12* allele used for the localization study. (B) pTTG1::TTG1:YFP in *ttg1-12* TTG1:YFP is mainly localized in the nucleus in young leaf epidermal cells and the trichomes; trichome nucleus marked with arrow.

2.4 GL3 counteracts TTG1 mobility between the tissue layers

The previous finding that the TTG1 protein depletion is not found in *gl3* mutants led to the hypothesis that TTG1 binding to GL3 leads to a trapping of TTG1 in trichome cells due to elevated GL3 levels. One prediction of this hypothesis is that the mobility of TTG1 should depend on the presence of GL3. It was shown previously that *TTG1* can rescue *ttg1-1* mutant phenotype when expressed in the subepidermis using the *pPCAL* promoter (Bouyer *et al*., 2008). If the hypothesis of TTG1 trapping/ attracting by GL3 is correct one would expect that tissue specific *GL3* expression modulates the rescue ability of *ttg1-1* mutant phenotype by *TTG1* expressed in the subepidermis. Experiments were designed to test this in two directions.

First does epidermal GL3 promote the rescue by trapping TTG1 in the epidermis. In order to address this question, I tested the rescue ability of subepidermal TTG1 in the absence or abundance of epidermal GL3. As shown before with the *pPCAL* promoter (Bouyer *et al*., 2008), also subepidermal TTG1 expression driven by the *RUBISCO* small sub unit promoter (*pRbcS2b*/*pRBC*) completely rescued *ttg1-1* mutant trichome phenotype (Figure 2.12D). Expression of pRBC::TTG1:YFP in *ttg1* and *gl3* resulted in TTG1:YFP localization in both, subepidermis as well as the epidermis demonstrating that the TTG1:YFP protein movement between cell layers is independent of GL3 (Figure 2.12E, G). The effect of the absence of GL3 in the epidermis was assayed by studying the rescue ability of subepidermal TTG1 in *ttg1 gl3* double mutant. If the presence of GL3 in the epidermis is not relevant, a moderate rescue equivalent to *gl3* mutant phenotype would be expected in *ttg1 gl3*pRBC::TTG1:YFP expressing line. However, the rescue efficiency of pRBC::TTG1:YFP in *ttg1 gl3* double mutant (Figure 2.12F) was much less effective than pRBC::TTG1:YFP in *ttg1* single mutant (Figure 2.12D). While

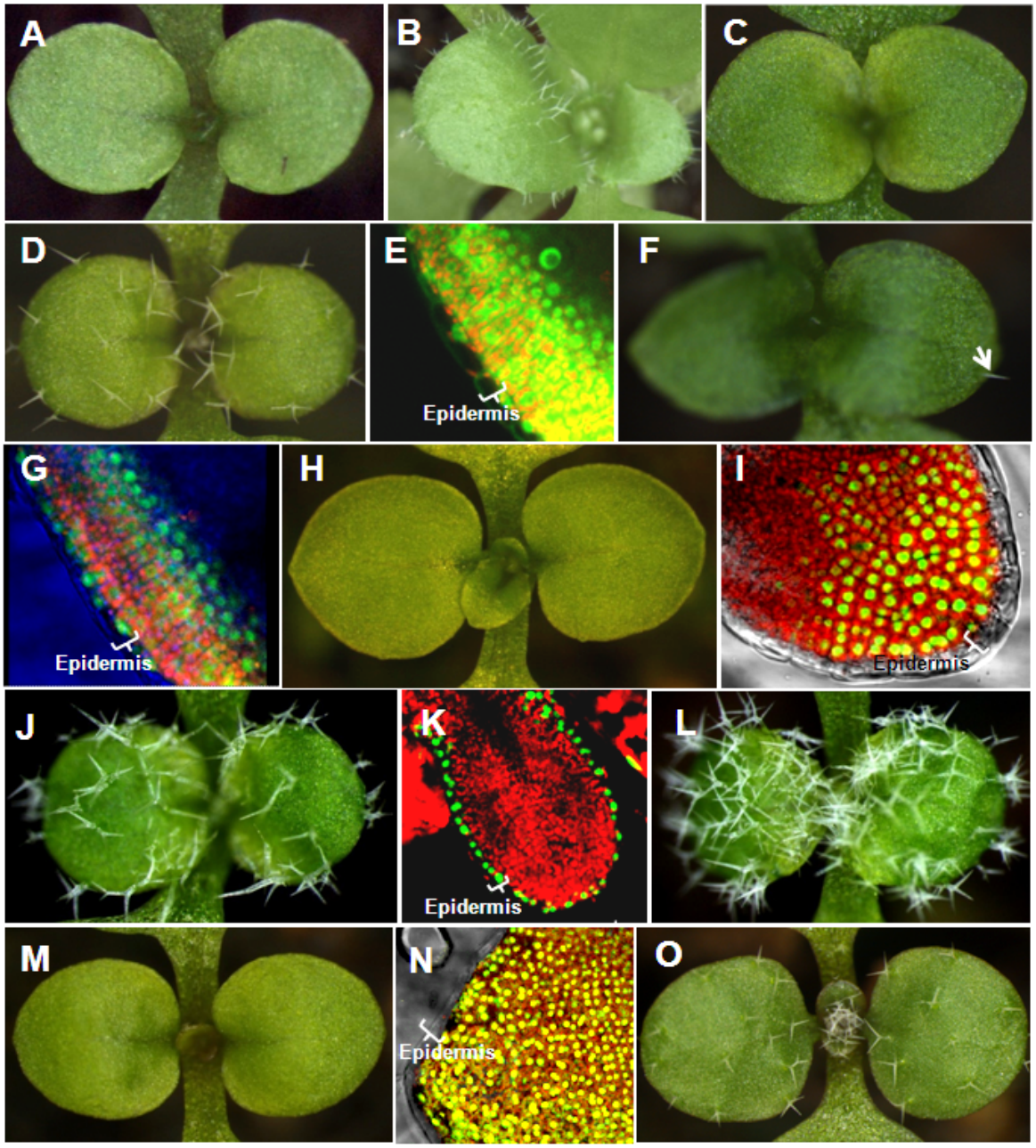

Figure 2.12: Tissue specific expression of *GL3* controls subepidermal TTG1 movement. (A) *ttg1*, no trichomes are found. (B) *gl3*, trichomes are small in size and underbranched. (C) *ttg1 gl3*, no trichomes are found. (D) *ttg1*pRBC::TTG1:YFP, wild type trichome phenotype is restored. (E) *ttg1*pRBC::TTG1:YFP, YFP signal is found in the subepidermis and the epidermis. (F) *ttg1 gl3*pRBC::TTG1:YFP, weak rescue of the trichome phenotype, arrow depicts a trichome. (G) *ttg1 gl3*pRBC::TTG1:YFP, YFP fluorescence is found in the subepidermis as well as in the epidermis. (H) *ttg1 gl3*pRBC::GFP:GL3, no trichomes are found. (I) *ttg1 gl3*pRBC::GFP:GL3, GFP fluorescence is found exclusively in the subepidermis. (J) *ttg1 gl3*pAtML1::GFP:GL3, moderate trichome rescue. (K) *ttg1 gl3*pAtML1::GFP:GL3, GFP fluorescence is found exclusively in the epidermis. (L) *ttg1 gl3*pAtML1::GFP:GL3pRBC::TTG1:YFP, strong overproduction of trichomes. (M) *ttg1 gl3*pRBC::GFP:GL3pRBC::TTG1:YFP, no trichomes are found. (N) *ttg1 gl3*pRBC::GFP:GL3pRBC::TTG1:YFP, both YFP and GFP signals co-localize and are restricted to the subepidermis. (O) L*er* wild type

*ttg1*pRBC::TTG1:YFP could rescue to wild type situation (compare FigureD and O), *ttg1 gl3*pRBC::TTG1:YFP did not show a rescue upto *gl3* situation (compare Figure 2.12B and F). This indicates that epidermal GL3 strongly promotes the rescue efficiency of subepidermal TTG1. In order to exclude that GL3 promotes the rescue through co-movement from the subepidermis or by modification of TTG1 function I analyzed the rescuing ability of subepidermal TTG1:YFP by expressing GFP:GL3 specifically either in the subepidermis or in the epidermis. GFP:GL3 was found specifically in the respective layers indicating that it cannot move between the layers in either direction (Figure 2.12I, K). In the first approach I tested the lines in which epidermal GL3 level was increased by providing GFP:GL3 under the epidermal specific *Arabidopsis thaliana MERISTEM LAYER 1* (*pAtML1*) promoter. This promoter was previously reported to show tissue specific expression (Takada and Juergens, 2007; Bai *et al*., 2009). GFP:GL3 was found specifically in the epidermis in *ttg1 gl3* double mutant (Figure 2.12K). This epidermal specific expression of GFP:GL3 resulted in a moderate rescue of trichomes in *ttg1 gl3* (Figure 2.12J) but led to a drastic increase in trichome number in *ttg1 gl3*pRBC::TTG1:YFP background (Figure 2.12L) suggesting that GL3 promotes rescue efficiency of subepidermal TTG1 by trapping /attracting it in the epidermis.

In a second experiment I tested whether exogenous supply of subepidermal GL3 inhibits/ reduces the rescue ability of TTG1 from the subepidermis. First I could show that the GFP:GL3 expressed under the *pRBC* promoter is restricted to subepidermis (Figure 2.12I). Then I compared the phenotypes of *ttg1 gl3*pRBC::TTG1:YFP and *ttg1 gl3*pRBC::TTG1:YFPpRBC::GFP:GL3 lines (Figure 2.12F, M). Rescuing ability of subepidermal TTG1 seems to be further reduced by addition of subepidermal GL3 in *ttg1 gl3*pRBC::TTG1:YFPpRBC::GFP:GL3 line. Occasional trichome formation in *ttg1 gl3*pRBC::TTG1:YFP (marked by arrow in Figure 2.12F) was at a much higher frequency than in *ttg1 gl3*pRBC::GFP:GL3pRBC::TTG1:YFP.

2.5 Analysis of TTG1 transport rates in different epidermal cell types using the photoconvertible marker KikGR1

The *GL3* expression level is elevated in the trichome cells compared to the pavement cells as soon as the trichome fate of a cell is determined resulting in accumulation of the GL3 protein in the trichome cells (Zhang *et al*., 2003; Zhao *et al*., 2008; Yoshida *et al*., 2009). If GL3 restricts the mobility of TTG1 by sequestering it in a complex in the nucleus, the TTG1 protein in the trichome nucleus should be less mobile compared to the mobility in the surrounding cells. To determine this I used the photoconvertible marker KikGR1 (Kikume Green to Red 1) as a translational fusion at the C-terminal end of TTG1 to get the TTG1:KikGR1 fusion protein (Tsutsui *et al*., 2005). This fusion protein was expressed under the *TTG1* promoter that was previously reported to be sufficient for the full rescue of the *ttg1* phenotype (Bouyer *et al*., 2008). The pTTG1::TTG1:KikGR1 construct was transformed into the *ttg1-13* null allele and it completely rescued trichome, seed coat color and seed coat mucilage phenotype of the *ttg1-13* mutant (Figure 2.13). Root hair phenotype and anthocyanin synthesis that are also regulated by TTG1 were not analysed.

2.5.1 Standardization of the conditions for the photoconversion of TTG1:KikGR1

KikGR1 is a photoconvertible marker which irreversibly changes from green to bright red by a process known as β-elimination reaction upon irradiation with UV or violet light (360-420nm) (Tsutsui *et al*., 2005). It was shown that *Escherichia coli* (*E. coli*) cells expressing KikGR1 showed green to red conversion when exposed to natural light for one hour following a 12 hours of dark incubation after transformation (Tsutsui *et al*., 2005). This posed a big hindrance for using

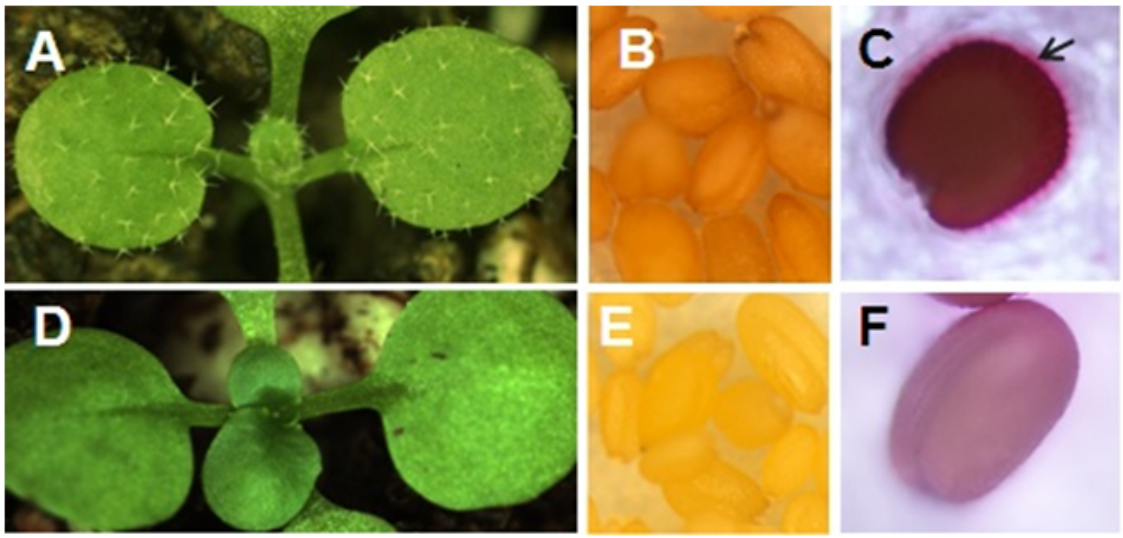

Figure 2.13: Rescue analysis of *ttg1-13*pTTG1::TTG1:KikGR1. (A, D) Trichome phenotype in *ttg1-13*pTTG1::TTG1:KikGR1 (A) and *ttg1-13* (D). (B, E) Seed coat color in *ttg1-13*pTTG1::TTG1:KikGR1 (B) and *ttg1-13* (E). (C, F) Seed coat mucilage production in *ttg1-13*pTTG1::TTG1:KikGR1 (C) and *ttg1-13* (F) seen by ruthenium red staining. Arrow in (C) points to mucilage layer seen as a diffused red stained zone and it is absent in (F).

KikGR1 marker in plants as plants need light for their growth and development. It was indeed found that significant amount of green protein was converted into red in the plants expressing TTG1:KikGR1 thereby making it impossible to make quantitative analysis. To avoid this problem, seedlings grown under the normal long day conditions were shifted to dark when the first pair of rosette leaves has emerged out. After about 24 hours exposure to dark, leaf number 3 and 4 that are approximately about 300µm in length were used for the photoconversion in specific cell types using the pulse of diode laser.

2.5.2 Analysis of TTG1:KikGR1(red) transport rate in different epidermal cell types

To compare the different mobility rates of TTG1 in different epidermal cell types TTG1:KikGR1 was converted from green to red in three different types of epidermal cells namely, trichome initial (Figure 2.14A) trichome neighboring epidermal cell (Figure 2.14B) and an epidermal cell away from the trichome initial (Figure

2.14C) using same set of conditions in the CLSM. Hereafter the photoconverted form of TTG1:KikGR1 is referred to as TTG1:KikGR1(red) and unconverted form as TTG:KikGR1(green). Pictures were taken at 0 and 2 minutes after photoconversion using the CLSM. I chose to make the observation at 2 minutes after photoconversion based on the previous studies using the microinjection in mesophyll cells of *Nicotiana benthamiana* (Bouyer *et al*., 2008) (Daniel Bouyer and Fritz Kragler, personal communication). Because TTG1:KikGR1 is converted into red only in a single cell, appearance of any red signal in the surrounding cells should be from the cell where it was converted. Therefore the red signal was quantified at 0 and 2 minutes after photoconversion in the converted cell and the cells that are immediate neighbors to it. Difference in the red signal intensity in a cell at these two time points is the gain or loss of TTG:KikGR1(red) fusion protein.

In general due to very small amounts of the TTG1:KikGR1(red) protein in the cells neighboring to photoconverted cells it was not possible to observe the red signal in the images. Nevertheless, quantifications with the quantification tool in CLSM using same pictures clearly showed differences in the red fluorescence at 0 and 2 minutes time points after photoconversion. It was interesting to note that loss of TTG1:KikGR1(red) was only 2.38% of the total in the trichome cells compared to 22.27% and 16.9% in the trichome neighboring cell and epidermal cell away from the trichome, respectively (Table 2.2). Gain of TTG:KikGR1(red) in the immediate neighboring cells was analyzed in all three situations. The lost TTG:KikGR1(red) in the photoconverted cells was set to 100. Interestingly total gain of red signal in all the immediate neighboring cells under all three different situations was relatively similar and accounted for 32.8%, 32.48% and 28.14% of the total loss in trichome, trichome neighboring cell and epidermal cell away from the trichome respectively (Table 2.2). The transport of TTG1:KikGR1(red) far away than only one neighboring cell could be the reason why 100% of the lost TTG1:KikGR1(red) was not accounted in the immediate neighboring cells. This is supported by the

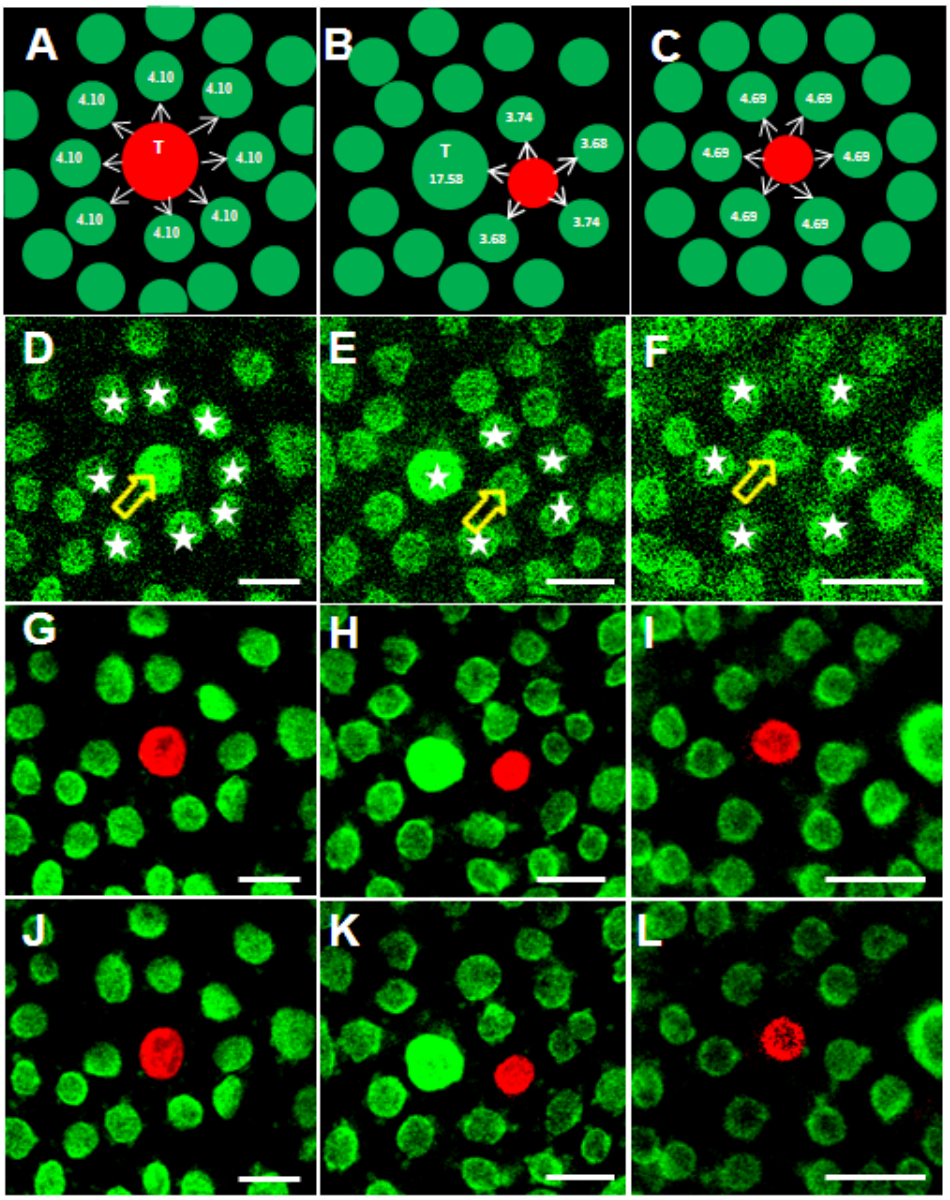

Figure 2.14: Analysis of transport rates of TTG1:KikGR1 in different epidermal cell types. (A-C) Schematic presentation of a field of epidermal cell nuclei (circles) where red represents photoconverted nuclei in trichome cell (A), trichome neighboring cell (B) and epidermal cell away from trichome initial (C). Other surrounding cells nuclei are shown in green. Values in the circles indicate the percentage gain of the red fluorescence 2 minutes after photoconversion; arrows indicate the directionality of TTG1:KikGR1(red) transport; trichome nucleus is depicted with letter T. (D-F) Field of epidermal cells before photoconversion. (G-I) field of epidermal cells 0 minutes after photoconversion in trichome initial (G), trichome neighboring cell (H) and epidermal cell away from trichome (I). (J-L) field of epidermal cells 2 minutes after photoconversion in trichome initial (J), trichome neighboring cell (K) and epidermal cell away from trichome (L). Red, photoconverted TTG1:KikGR1 referred as TTG1:KikGR1(red); green, unconverted TTG1:KikGR1 referred as TTG1:KiKGR1(green); yellow arrows, points to the nucleus selected for photoconversion; star, denotes nuclei of the immediate neighbors of the photoconverted cell. Scale= 10µm.

Table 2.2: Quantification of TTG1:KikGR1(red) movement in different epidermal cell types

Photoconverted cell type	Loss of red signal 2 minutes after photoconvertion, expressed as a percentage of the red signal at 0 minutes	Gain of red signal in all immediate neighbors 2 minutes after photoconvertion, expressed as a percentage of loss in photoconverted cell (Number of neighboring cells)	n
Trichome	2.38	32.80 (8)	57
Trichome neighbor	22.27	32.48 (5)	53
Epidermal cell	16.9	28.14 (6)	24

observation that TTG1 moves several cells distance in microinjection experiments within 2 minutes. All the immediate neighboring cells of the trichome initials are of the same type. Similarly the immediate neighboring cells of the epidermal cell that are away from the trichome initial also are of same type. Hence under these two situations the gain in all the immediate neighbors is comparable (Figure 2.14A, C). On the other hand the trichome neighboring cell has three different cells types as its immediate neighbors including the trichome initial, neighboring cells that are also immediate neighbors of trichome initial and the cells that are in the second row from the trichome initial (Figure 2.14B). Therefore I further analysed the gain of red fluorescence in these cell types separately to see if there is a difference in the gain of TTG1:KikGR1(red). Measuring the gain of TTG1:KikGR1(red) in these cells showed that of the 32.48% (sum of gains in all the immediate neighbors), 17.58% was accounted only in the trichome cell whereas two neighboring cells that are also immediate neighbors to trichome accounted for 3.74% each and the two

cells which are in the second tier of cells from trichome accounted for 3.68% each (Figure 2.14B). Due to the relatively higher amount of TTG1:KikGR1(red) in the trichome initial from the photoconverted neighboring cell it was occasionally possible to see the red fluorescence in them (Figure 2.15).

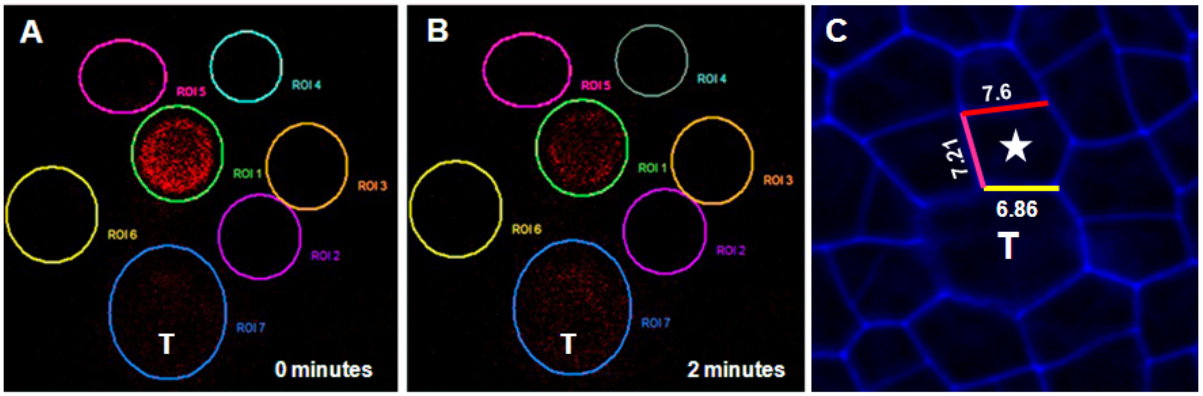

Figure 2.15: Analysis of TTG1:KikGR1(red) transport from trichome neighboring cell. (A) TTG1:KikGR1(red) in the photoconverted cell nucleus (ROI 1) at 0 minutes after photoconversion. (B) Distribution of TTG1:KikGR1(red) 2 minutes after photoconvertion in trichome neighboring cell (ROI1), note that red fluorescence in ROI1 is reduced while it is increased in ROI7. Red, is the photoconverted TTG1:KikGR1 referred to as TTG1:KikGR1(red); ROI 1, photoconverted cell nucleus; ROI 2-7, nuclei of the immediate neighboring cells of the photoconverted cell; ROI7, nuclei of the trichome initial, which is one of the immediate neighboring cells to the photoconverted cell. Note that red signal in ROI7 in (B) is higher than in (A) due to the gain from ROI1. (C) Shows comparison of contact lengths (in µm) of photoconverted cell (marked with star) with its neighbors, trichome cell is marked with letter T.

In order to exclude the possibility that the observed differences were due to differences in the contact length/area of the different types of neighboring cells with the photoconverted cell, contact lengths of the photoconverted cell with the neighboring cells were compared. The contact length of photoconverted trichome neighboring cell with trichome initial, trichome neighbor and epidermal cell in the second tier of cells from the trichome was 6.86, 7.21 and 7.6 µm respectively (Figure 2.15C). Considering this information and no specific directional transport as was reported earlier (Bouyer *et al.*, 2008), the total TTG1:KikGR1(red) protein that is lost from the photoconverted trichome neighboring cell should be transported

into its five neighbors as 18.78% into the trichome initial, 19.73% into each of the two trichome neighboring cells and 20.81% into each of the neighboring cells in the second tier from the trichome initial. But in contrast to this my observations after two minutes clearly suggests that almost everything that entered into the trichome initial is trapped in the nucleus while from the other neighboring cells the TTG1:KikGR1(red) moved further away into the other cells (Figure 2.14B). I want to point out that this is consistant with the high *GL3* expression in the trichome initial and drastically reduced expression of *GL3* in the pavement cells. (Zhang *et al*., 2003; Zhao *et al*., 2008).

2.6 Nuclear targeted TTG1:YFP is able to move

It was reported that pTTG1::NLS:TTG1 leads to formation of trichome clusters comparable to pTTG1::TTG1:YFP expressing plants while pTTG1::TTG1 alone does not result in any cluster formation (Bouyer D., 2004). This suggested that nuclear targeted TTG1 might be reduced in its mobility similar to the decrease in the mobility rate of TTG1:YFP fusion protein that makes the fusion protein size bigger than the TTG1 alone. To look into more details whether nuclear targeted TTG1 is impaired in its mobility, rescue efficiency and the pattern formation, I compared pTTG1::TTG1:YFP with pTTG1::NLS:TTG1:YFP and pRBC::NLS:TTG1:YFP expressed in *ttg1-13* (Table 2.3). I used the SV40 NLS to target TTG1:YFP to the nucleus. It was shown previously that the SV40 NLS fused to GFP was exclusively in the nucleus (Bouyer et al., 2008). Also a GFP:GUS construct fused to an NLS was shown to target the protein exclusively to the nucleus (Chytilova *et al*., 1999). Trichome rescue efficiency experiments clearly showed that NLS:TTG:YFP fusion protein is as efficient as TTG1:YFP when expressed under the endogenous promoter as well as under control of the subepidermal specific *pRBC* promoter. Expression of the pTTG1::NLS:TTG1:YFP showed 128 $\pm$ 18 trichomes compared to

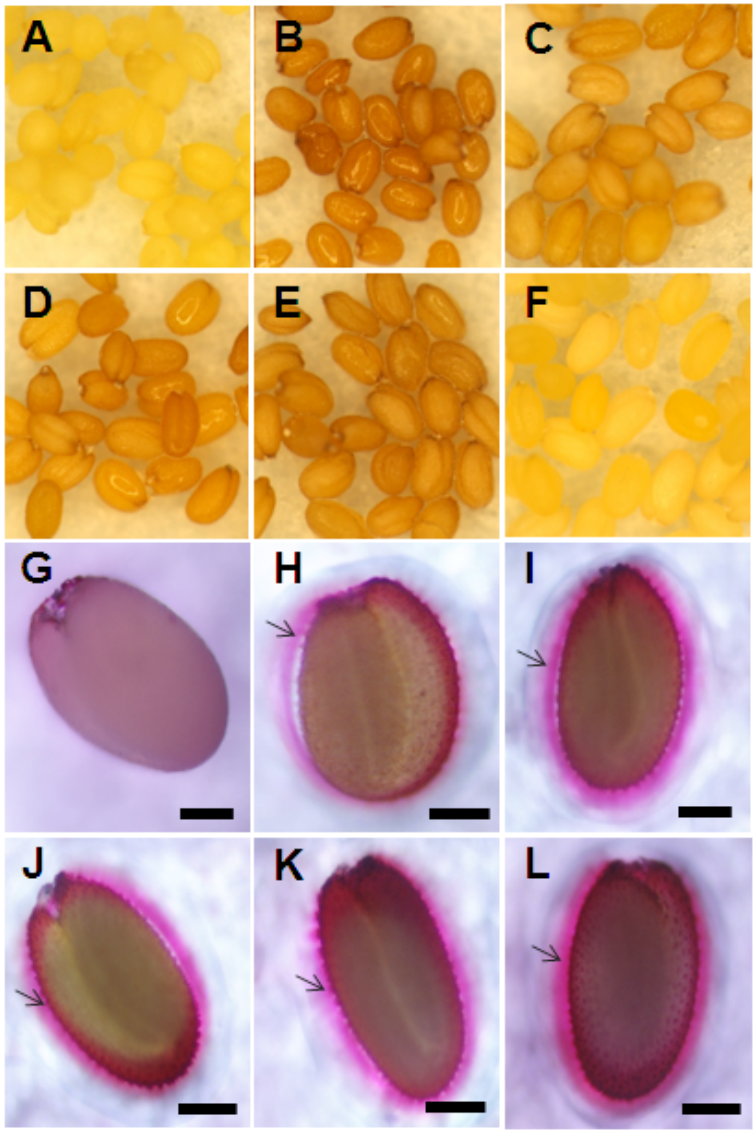

Figure 2.16: Seed coat phenotype analysis of the TTG1:YFP nuclear targeted and non-nuclear targeted lines. (A-F) Seed coat color phenotype. (G-L) Ruthenium red staining for seed coat mucilage phenotype. Mucilage is visualized by ruthenium red stain as a diffusely stained zone around the seed indicated by arrow. (A, G) *ttg1-13*. (B, H) RLD wild type. (C, I) *ttg1-13*pTTG1::TTG1:YFP. (D, J) *ttg1-13*pRBC::TTG1:YFP. (E, K) *ttg1-13*pTTG1::NLS:TTG1:YFP. (F, L) *ttg1-13*pRBC::NLS:TTG1:YFP. Scale=100µm.

127 ± 20 in the lines expressing pTTG1::TTG1:YFP. The lines carrying the construct pRBC::NLS:TTG1:YFP produced 124 ± 30 trichomes suggesting that the subepidermal NLS:TTG1:YFP is as efficient as NLS:TTG1:YFP and TTG1:YFP expressed under the endogenous promoter. Analysis of the cluster frequency further revealed that the mobility of NLS:TTG1:YFP is comparable to TTG1:YFP. The lines carrying pTTG1::TTG1:YFP resulted in formation of 3.68% ± 2.40 trichome clusters, which is marginally less but not significantly different from the lines expressing pTTG1::NLS:TTG1:YFP and pRBC:: NLS:TTG1:YFP that produces 4.69% ± 1.84 and 5.37% ± 2.04 clusters respectively (p= 0.095 and 0.197 respectively) (Table 2.3).

Table 2.3: Genetic analysis of trichome phenotypes in the nuclear targeted TTG1:YFP expressing lines

Background	Trichome number±SD	Cluster frequency (%)±SD	n
*ttg1-13*pTTG1::NLS:TTG1:YFP	128 ±18	4.69 ± 1.84	26
*ttg1-13*pRBC::NLS:TTG1:YFP	124 ± 30	5.37 ± 2.04	26
*ttg1-13*pTTG1::TTG1:YFP	127 ± 20	3.68 ± 2.40	26
*ttg1-13*pRBC::TTG1:YFP	98	4.59	1

SD, standard deviation; trichome phenotypes were scored on the adaxial surface of the third and fourth true leaves of the seedlings from the T1 generation and the control lines; cluster frequency was mean percentage of the trichomes adjacent to another trichome.

Surprisingly pRBC::TTG1:YFP and pRBC::NLS:TTG1:YFP when expressed in *ttg1-13* exhibited different effects on seed coat color (Figure 2.16A-F). The proanthocyanidin (condensed tannin synthesis) pathway seems to be affected when nuclear

targeted TTG1:YFP (NLS:TTG1:YFP) was expressed under the *pRBC* promoter hence this construct failed to rescue the seed coat color phenotype in *ttg1-13* mutant. To test whether nuclear targeted TTG1:YFP is functional in seeds I tested for the seed coat mucilage synthesis, which is another seed property controlled by TTG1. Here I found that seed coat mucilage synthesis is not affected confirming that NLS:TTG1:YFP fusion protein is functional in seeds (Figure 2.16G-L).

2.7 Genetic analysis of the *ttg1* alleles

We recently explained the paradoxical phenotype of *ttg1* alleles where strong alleles show glabrous and weak alleles have underbranched and clustered trichome phenotype by a theoretical model based on the GL3 dependent TTG1 depletion (Bouyer et al., 2008). Hence in this study I looked into more details on the relation of TTG1 and its allelic forms with GL3 during trichome patterning. The *ttg1* alleles used in this study are listed in (Table 2.4). Physical interaction studies using yeast

Table 2.4: *ttg1* alleles used in this study (Koornneef, 1981; Larkin *et al*., 1994, 1999)

ttg1 allele	*ttg1-1*	*ttg1-9*	*ttg1-10*	*ttg1-11*	*ttg1-12*	*ttg1-13*
Type of mutantion	TTG1 △C26	TTG1 (S282F)	TTG1 (g-49a)	TTG1 (G149R)	TTG1 (G43R)	deletion

Note, in *ttg1-10* mutation indicated is base change in the 5'UTR at -49 position.

two-hybrid analysis showed that except TTG1(S282F) (*ttg1-9* allele), which showed weak physical interaction, no other allelic form of TTG1 interacted with GL3 (Figure 2.17A). None of the alleles interacted with EGL3 and TT8 (Figure 2.17B, C). Further, using NTT assay I tested how these allelic forms of TTG1 compared to wild type TTG1 behave with respect to their nuclear transport. NTT assay showed

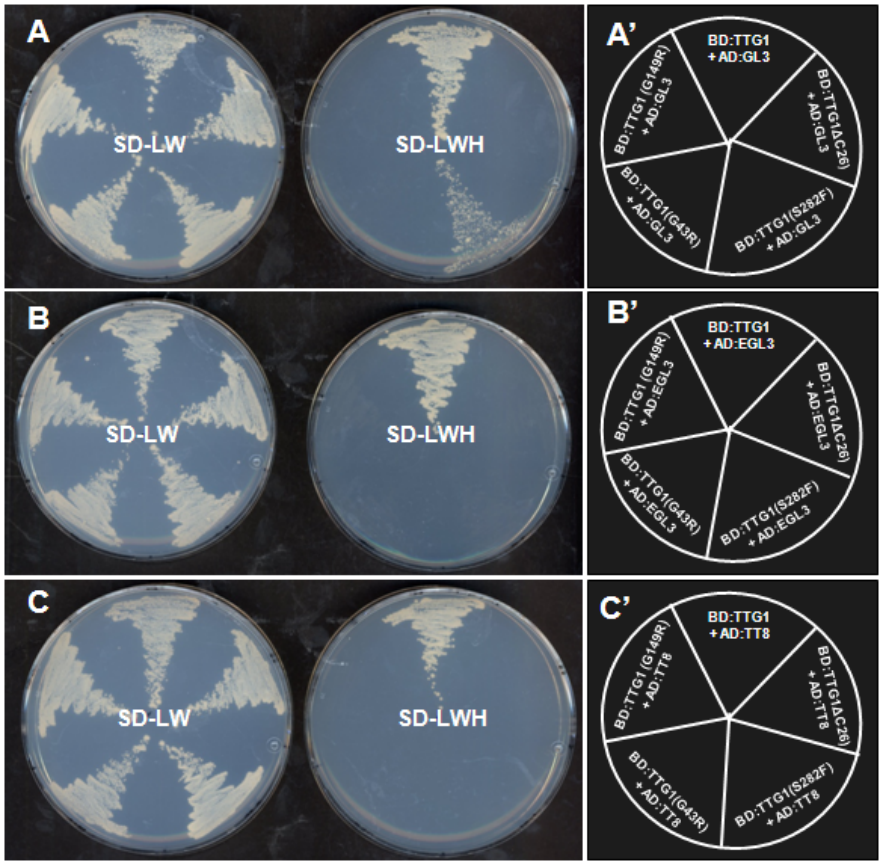

Figure 2.17: Yeast two-hybrid analysis of allelic forms of TTG1 with GL3, EGL3 and TT8. (A-C) Yeast two-hybrid to test physical interaction of TTG1 allelic forms with GL3 (A), with EGL3 (B) and TT8 (C). (A'-C') Schematic presentation of the positions of different interaction partners in (A-C) respectively. BD, GAL4 DNA binding domain; AD, GAL4 transactivation domain; SD-LW, SD-LWH in (A-C) are two and three amino acid drop out medium for the selection of transformation and interactions respectively; interaction plates were supplied with 5mM 3AT; yeast growth, positive interactions; no growth, lack of interaction.

that like TTG1 all the allelic forms of TTG1 also failed to enter into the nucleus (Figure 2.18A). Interestingly none of the allelic forms of TTG1 was trapped in the nucleus by GL3 (Figure 2.18B). Subcellular localization studies by stable transformation in plants revealed that TTG1△C26:YFP expressed under the *TTG1* promoter is exclusively in the cytoplasm (Figure 2.11A). Transgenic plants expressing TTG1(S282F):YFP, TTG1(G149R):YFP and TTG1(G43R):YFP under the *TTG1* promoter in Columbia plants showed that the cellular localization is consistant with the interaction data in yeast. TTG1(S282F):YFP, which interacted weakly

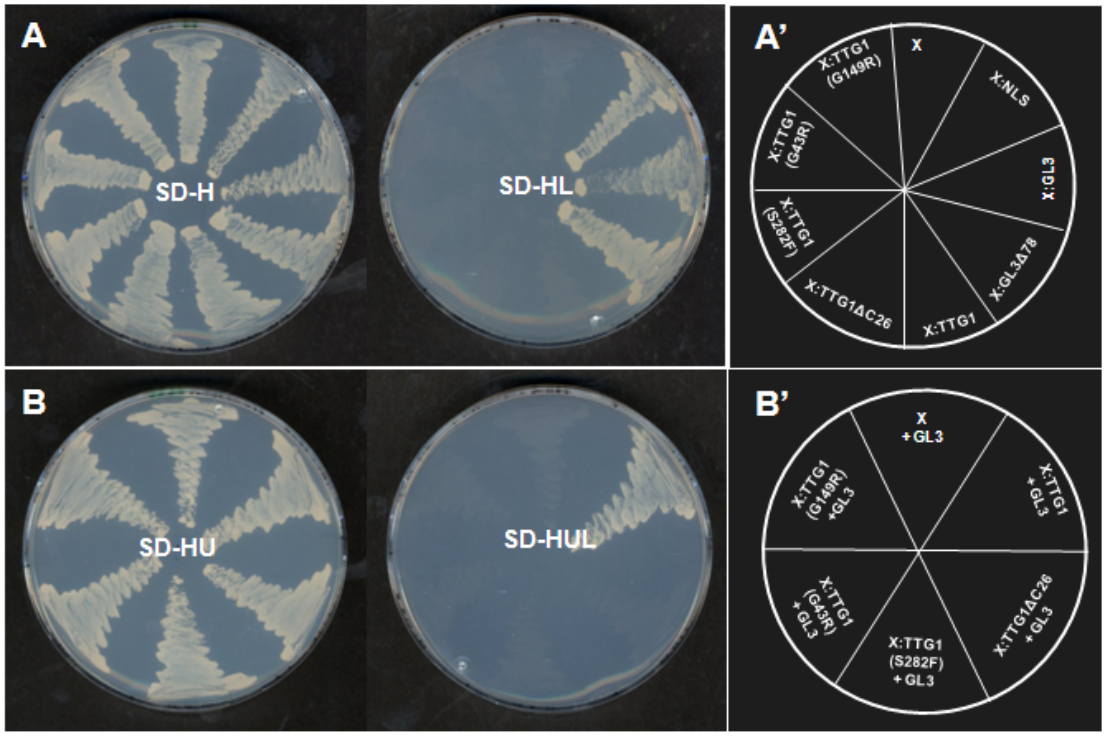

Figure 2.18: Nuclear transportation trap (NTT) assay for the allelic forms of TTG1. (A) NTT assay shows neither TTG1 nor any of the TTG1 allelic forms can enter into the nucleus. (B) NTT assay shows only TTG1 but none of the TTG1 allelic forms is trapped by GL3 in the nucleus. TTG1, TTG1 allelic forms, GL3 and GL3△78 were provided as a translational fusion C-terminal to NES:LexAD in (A). In co-expression assays (B) GL3 protein was provided without any fusion. X, NES:LexAD; LexAD, LexA DNA binding domain + GAL4A transactivation domain; SD-H and SD-HU are one and two amino acid drop out media for the selection of single (A) and double transformations (B) respectively; SD-LH and SD-LHU, amino acid drop out media for the selection of nuclear transport of a protein fused to NES:LexAD when expressed alone (A) and in the presence of GL3 (B) respectively.

with GL3 in yeast showed a weak nuclear localization while TTG1(G43R):YFP and TTG1(G149R):YFP, which did not interact with GL3 in yeast are in the cytoplasm (Figure 2.19). However, their nuclear localization below the detection levels under the CLSM settings used in this study can not be completely excluded. Expression under the constitutively active *p35S* promoter in wild type Columbia plants showed that all the allelic forms of TTG1 tested had a dominant negative effect with varying degree (Figure 2.20). Trichome frequency in TTG1:YFP expressing lines was comparable to wild type. The lines expressing TTG1(S282F):YFP had about 83%

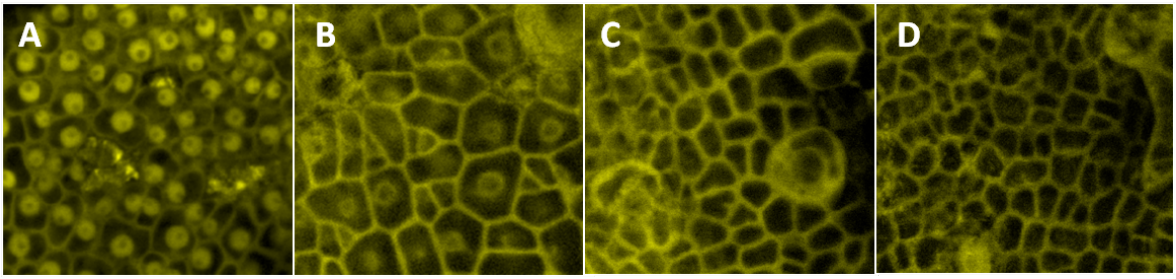

Figure 2.19: Localization of TTG1 allelic forms in the leaf epidermal cells of Columbia wild type plants. (A) pTTG1::TTG1:YFP. (B) pTTG1::TTG1(S282F):YFP. (C) pTTG1::TTG1(G43R):YFP. (D) pTTG1::TTG1(G149R):YFP. Yellow, YFP fluorescence

$\pm$ 28 trichomes rescue while TTG1(G43R):YFP and TTG1(G149R):YFP expressing lines showed 65% $\pm$ 17 and 65% $\pm$ 16 rescue of trichome number compared to wild type Columbia (Figure 2.20A). Cluster frequency was 6.81% $\pm$ 3.04, 4.84% $\pm$ 2.52, 2.65% $\pm$ 2.51 and 2.98% $\pm$ 2.40 in Columbia plants expressing p35S::TTG1:YFP, p35S::TTG1(S282F):YFP, p35S::TTG1(G43R):YFP and p35S::TTG1(G149R):YFP respectively as against 0.05% $\pm$ 0.10 in wild type (Figure 2.20B). A reciprocal experiment was also conducted where p35S::TTG1 and p35S::TTG1:YFP constructs were transformed into all the *ttg1* alleles and analyzed for the rescuing ability and allelic interaction (Table 2.5). Both TTG1 and TTG1:YFP fusion proteins could rescue the trichome number almost to wild type (Table 2.5). But TTG1:YFP fusion protein expressing lines form an irregular distribution of trichome on the leaf surface. Therefore I analysed the cluster frequency in detail to see if this difference is due to the fusion that makes the protein size larger and there by hindering its mobility or whether it is due to allelic interaction. TTG1 and TTG1:YFP in the null allele *ttg1-13* was taken as a control since the complete genomic region of the TTG1 locus is deleted in this allele. The Landsberg erecta allele *ttg1-1* was considered as second control as this is also a strong allele. Therefore any phenotype in these two backgrounds would be solely due to the introduced transgene. Interestingly in both backgrounds (*ttg1-1* and *ttg1-13*) introduction of p35S::TTG1 resulted in a very small frequency of trichome clusters that was not significantly

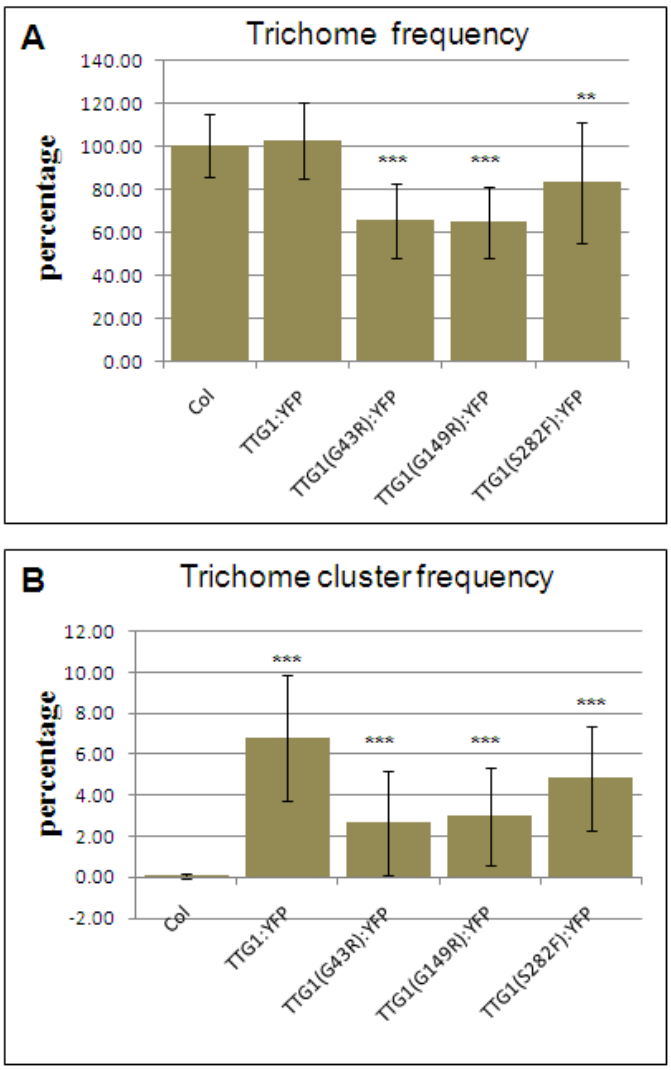

Figure 2.20: Genetic analysis of overexpression of allelic forms of *TTG1* in Columbia wild type. (A) Trichome frequency presented as the percentage of trichome number compared to wild type. (B) Cluster frequency presented as the percentage of trichome number in the respective background. Note, mean values of first four rosette leaves in T1 generation plants compared to wild type were used for the analysis; error bars, standard deviations; t-test, ** $p < 0.01$, *** $p < 0.001$.

Table 2.5: Comparsion of trichome phenotypes when *TTG1* / TTG1:YFP is overexpressed in different *ttg1* alleles

background	Construct transformed	Trichome frequency ± SD	Cluster frequency ± SD
L*er*	-	100 ± 15	0.08 ± 0.35
Col	-	100 ± 16	0.00 ± 0.00
RLD	-	100 ± 14	0.00 ± 0.00
ttg1-1	p35S::TTG1	93 ± 26	0.39 ± 0.90
	p35S::TTG1:YFP	89 ± 37	5.33 ± 5.10
ttg1-9	p35S::TTG1	96 ± 23	0.30 ± 0.61
	p35S::TTG1:YFP	89 ± 42	3.87 ± 2.58
ttg1-10	p35S::TTG1	111 ± 18	1.51 ± 2.36
	p35S::TTG1:YFP	89 ± 26	5.77 ±2.77
ttg1-11	p35S::TTG1	96 ± 21	1.21 ± 1.46
	p35S::TTG1:YFP	100 ±30	6.54 ±4.51
ttg1-12	p35S::TTG1	109 ± 18	1.90 ± 1.64
	p35S::TTG1:YFP	89 ± 24	8.11 ±4.01
ttg1-13	p35S::TTG1	89 ± 18	0.04 ± 0.16
	p35S::TTG1:YFP	87 ± 23	1.20 ±1.28

SD, standard deviation; trichome frequency is the mean of the trichome number expressed as a percentage of the trichome number in the corresponding wild type control; cluster frequency is the mean percentage of the trichomes found adjacent to another trichome; trichomes were counted on the adaxial surface of the first four true leaves; atleast 22 T1 generation lines were used in each background for the analysis.

different from the cluster formation in the corresponding wild type backgrounds (p= 0.1550 and p= 0.2225 for *ttg1-1* and *ttg1-13* respectively) (Table 2.5). On the other hand introduction of p35S::TTG1:YFP resulted in a significantly higher cluster frequency in both backgrounds compared to the corresponding wild type ($p < 0.0001$ for *ttg1-1* and $p< 0.001$ for *ttg1-13*). Among *ttg1-1*p35S::TTG1:YFP and *ttg1-13*p35S::TTG1:YFP, *ttg1-1*p35S::TTG1:YFP showed much higher cluster frequency compared to *ttg1-13*p35S::TTG1:YFP (Table 2.5). Similar analysis in other alleles of *ttg1* revealed that TTG1 and TTG1:YFP both showed significantly higher cluster frequency compared to wild type. In these alleles as well p35S::TTG1:YFP resulted in much higher cluster frequency than p35S::TTG1(Table 2.5). These data suggest that allelic forms of TTG1 with various mutations are functional, not fully though.

2.8 Effect of altering nuclear TTG1 concentration on trichome patterning and morphogenesis

2.8.1 Analysis of overexpression of CFP:GL3, CFP:GL3△78 and CFP:GL3△NLS in *ttg1*pTTG1::TTG1:YFP line

Being a part of transcription regulating complex it is evident that TTG1 protein is required in the nucleus, but I could show that TTG1 lacks any functional NLS. Hence as observed in different experimental approaches described before it seems that plants have adapted a mechanism where GL3 traps and retains TTG1 in the nucleus. Therefore I studied the effect of altering the nuclear concentration of TTG1 on the trichome development and pattern formation in *Arabidopsis*.

In the first approach TTG1:YFP was trapped either in the nucleus or in the cytoplasm using p35S::CFP:GL3 and p35S::CFP:GL3△NLS respectively to alter the nuclear to cytoplasmic ratio of TTG1:YFP. p35S::CFP:GL3△78 was also used to study how the GL3 variant not interacting with TTG1 hence having no effect on the subcellular distribution of TTG1 can influence trichome patterning compared

to GL3 form that does interact. These constructs were transformed in *ttg1-13*pTTG1::TTG1:YFP that was described before (Bouyer *et al.*, 2008). In all the genetic and molecular analysis *ttg1-13*pTTG1::TTG1:YFP was used as control. Nuclear TTG1:YFP was quantified using CLSM in the epidermal cells of the trichome patterning zone on the adaxial surface of leaf 3 and 4 of the T1 generation plants carrying the transformed GL3 variants (Table 2.6). Nuclear TTG1:YFP

Table 2.6: Subcellular distribution of TTG1:YFP in *ttg1*pTTG1::TTG1:YFP lines overexpressing CFP fused GL3 variants.

Background	Nuclear TTG:YFP±SD (%)
*ttg1*pTTG1::TTG1:YFP	60.20 ± 10.74
*ttg1*pTTG1::TTG1:YFPp35S::CFP:GL3	74.73 ± 7.74
*ttg1*pTTG1::TTG1:YFPp35S::CFP:GL3△78	61.63 ± 9.83
*ttg1*pTTG1::TTG1:YFPp35S::CFP:GL3△NLS	50.32 ± 8.17

SD, is the standard deviation; seedlings from the transformation of CFP fused GL3 variants in *ttg1*pTTG1::TTG1:YFP bacground and the control *ttg1*pTTG1::TTG1:YFP were used for the quantification; atleast 140 cells were measured in each case.

amount was 74.73% ± 7.74 in lines with p35S::CFP:GL3 whereas it was reduced to 50.32 % ± 8.17 in the lines carrying p35S::CFP:GL3△NLS. As expected there was no significant difference in the control plants (*ttg1-13*pTTG1::TTG1:YFP) and the lines carrying p35S::CFP:GL3△78, which had 60.20% ± 10.74 and 61.63% ± 9.83 nuclear TTG1:YFP respectively. The nuclear concentration of TTG1:YFP in this experiment is much less than the one which was observed before (Figure 2.3). This could possibly be due to different growing conditions as here I used the plants selected on Murashige and Skoog (MS) medium while soil grown plants were used in the previous experiment. The heterozygous situation of

the CFP:GL3 could be the other reason as T1 generation plants were used for this experiment. Nevertheless, this result also clearly showed that nuclear concentration of TTG1:YFP is GL3 dependent and showed a similar trend as before in different backgrounds. Furthermore the effect of GL3 variants on the trichome phenotype was determined. Parameters such as trichome number, trichome cluster frequency and over/underbranched trichome frequency were considered for the analysis. In all three GL3 variants expressing lines there was a significant increase in trichome number and cluster frequency (Table 2.7) (Figure 2.21)

Table 2.7: Analysis of leaf trichome phenotypes in the lines expressing *GL3* variants under *p35S* promoter

*ttg1*pTTG1::TTG1:YFP transformed with	n	Trichome number ± SD	Cluster frequency ± SD (%)	Overbranching ± SD (%)
-	25	103 ± 15	1.08 ± 0.71	0.65 ± 0.88
p35S::CFP:GL3	26	175 ± 34	3.01 ± 3.11	4.18 ± 4.13
p35S::CFP:GL3 △78	27	183 ± 37	3.76± 2.01	5.36 ± 4.87
p35S::CFP:GL3△NLS	27	124 ± 24	3.20 ± 1.73	0.20 ± 0.29

SD, is the standard deviation; trichome phenotypes were scored on the adaxial surface of the third and fourth true leaves of the seedlings from the T1 generation plants; cluster frequency is the mean percentage of the trichomes adjacent to another trichome; overbranching was expressed as the mean percentage of the trichomes with more than four branches.

This observation was consistent with earlier reports showing overexpression of *GL3* leads to increase in trichome number and that *GL3* overexpression can bypass the need of TTG1 for trichome formation (Payne *et al*., 2000; Digiuni *et al*., 2008). As expected the increase in trichome number was much higher in p35S::CFP:GL3 and p35S::CFP:GL3△78 lines compared to p35S::CFP:GL3△NLS. However, significant increase in trichome number in the lines expressing the *GL3*

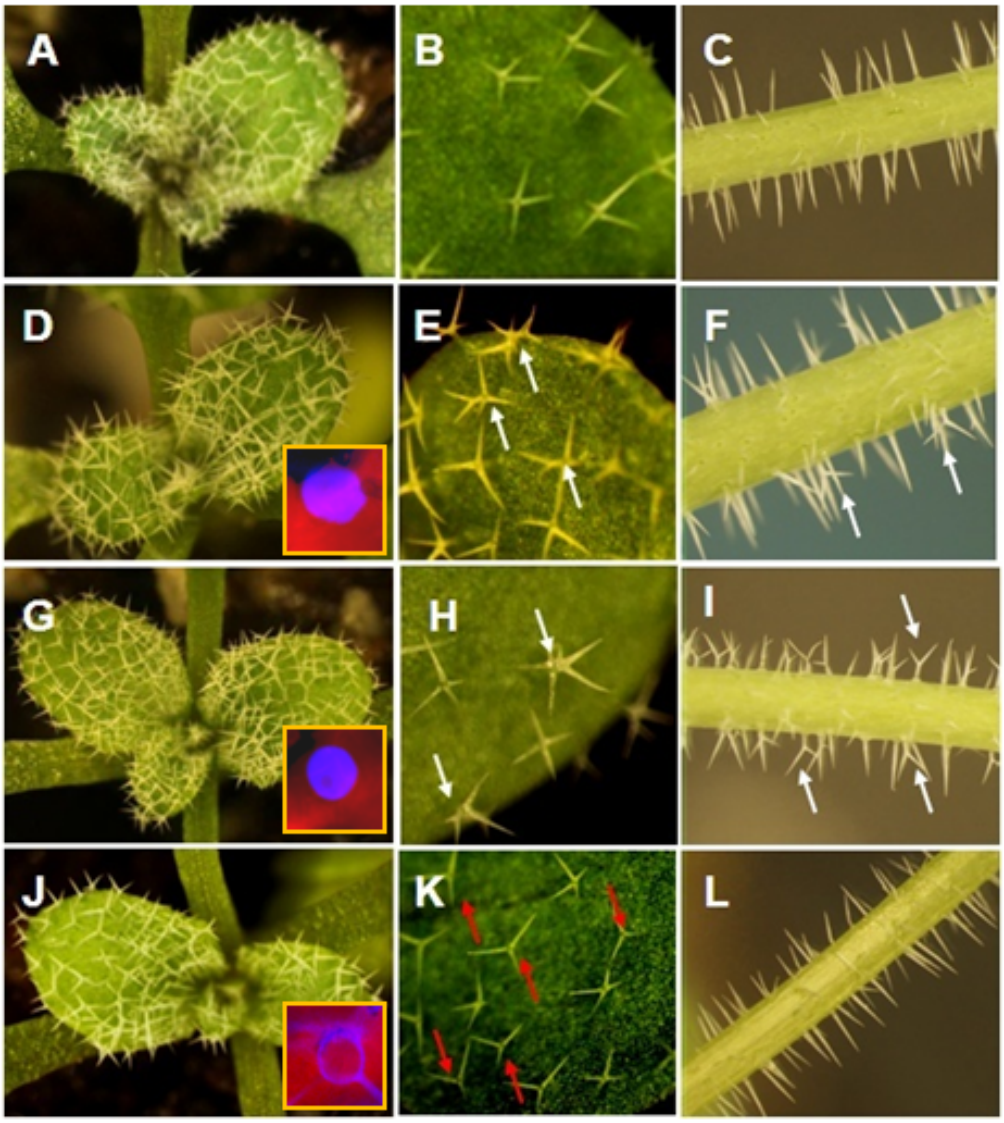

Figure 2.21: Genetic analysis of overexpression of *GL3*, *GL3*△78 and *GL3*△NLS under *p35S* promoter in *ttg1-13*pTTG1::TTG1:YFP. (A-C) *ttg1-13*pTTG1::TTG1:YFP, most of the leaf trichomes are four branched (B) and stem trichomes are unbranched (C). (D-F) *ttg1-13*pTTG1::TTG1:YFPp35S::CFP:GL3, overbranched trichomes with more than four branches on leaves (E) and occasional two or more branched trichomes on stem (F). (G-I) *ttg1-13*pTTG1::TTG1:YFPp35S::CFP:GL3△78, overbranched trichomes with more than four branches on leaves (H) and occasional two or more branched trichomes on stem (I). (J-L) *ttg1-13*pTTG1::TTG1:YFPp35S:CFP:GL3△NLS, trichomes are underbranched on leaves (K) and are unbranched on the stem (L). (A, D, G, J) Overview of trichome distribution on leaf three and four. (B, E, H, K) Higher magnification of the leaf showing trichome morphology. (C, F, I, L) Trichome distribution and morphology on the stem. Insets in A, D and J shows the localization of CFP:GL3, CFP:GL3△78 and CFP:GL3△NLS respectively in tobacco epidermal cell nucleus; white arrow, points to overbranched trichomes; red arrow, points to underbranched trichome.

variant targeted to cytoplasm was unexpected. Surprisingly the cluster frequency was comparable in all three cases suggesting that all three variants of GL3 share a common mechanism that has a slightly negative effect on the trichome patterning (Table 2.7).

Interestingly the trichome branching phenotype seems to be affected by decreasing the nuclear TTG1. There was a small but significant decrease in overbranched (>4branches) trichome frequency from 0.65% ± 0.88 in control to 0.20 %± 0.29 in p35S::CFP:GL3△NLS expressing lines (p= 0.016). On the other hand 4.18% ± 4.13 and 5.36% ± 4.87 overbranched trichome frequency was observed in p35S::CFP:GL3 and p35S::CFP:GL3△78 expressing lines that were significantly higher than the overbranching in the control line (*ttg1-13*pTTG1::TTG1:YFP) and p35S::CFP:GL3△NLS expressing line (Table 2.7). Stem trichome phenotype was also affected in lines expressing the *GL3* variants. Over expression of CFP:GL3 and CFP:GL3△78 led to increase in trichome branching (Figure 2.21).

2.8.2 Effect of expression of 78GL3:GUS aptamer in *ttg1-13*pTTG1::TTG1:YFP plants

Reduction in the trichome branching in p35::CFP:GL3△NLS expressing lines could well be due to reasons other than altering the nuclear TTG1 concentration. Indeed CFP:GL3△NLS is exclusively cytoplasmic but can still interact with GL1, TRY and CPC (Table 2.1) and possibly also with endogenous GL3 as it retains the bHLH interaction/dimerization domain (Feller *et al*., 2006; Payne *et al*., 1999). To exclude the possibility that the underbranched phenotype in p35::CFP:GL3△NLS is due to interaction with any other regulators of trichome development than the interaction with TTG1 I used the 78aa domain of GL3 that I mapped for the specific interaction with TTG1 (Figure 2.6A). 78GL3:GUS was expressed under the *p35S* promoter in *ttg1-13*pTTG1::TTG1:YFP line and for comparisions *ttg1-13*pTTG1::TTG1:YFP was used as a control.

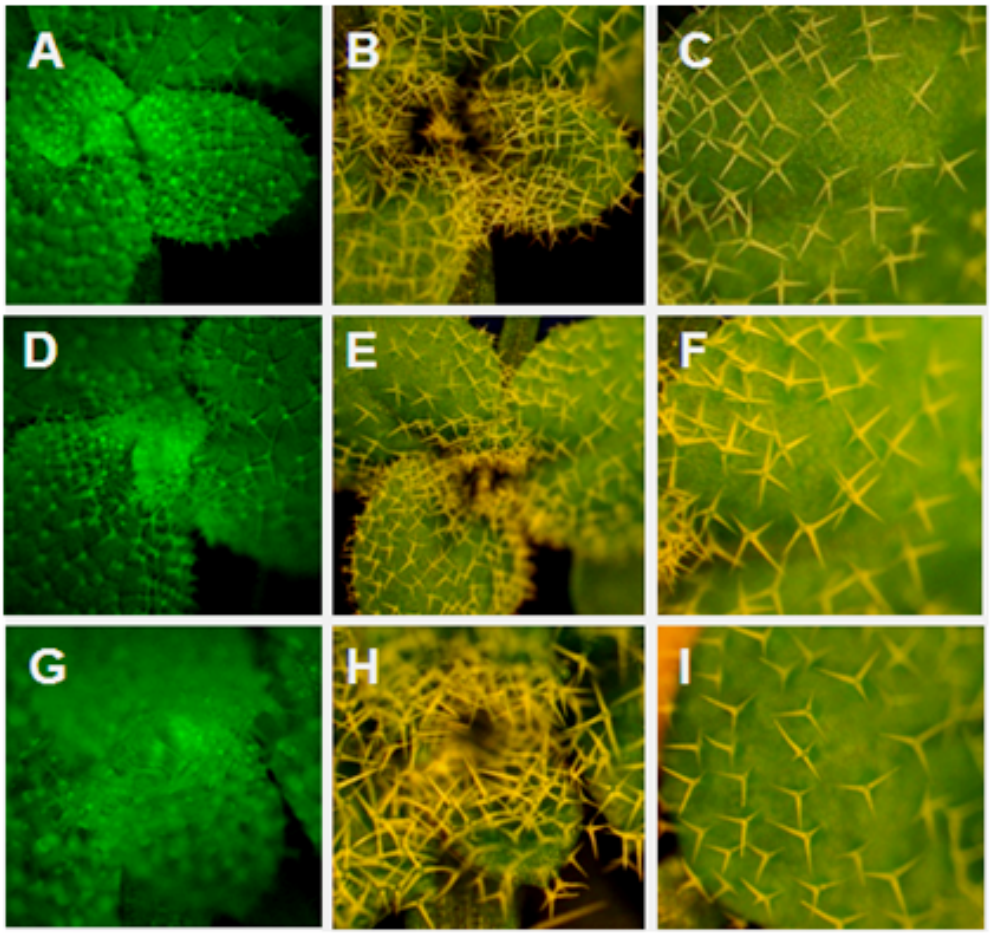

Figure 2.22: Effect of p35S::78GL3:GUS aptamer on trichome branching. (A-C) Control line *ttg1-13*pTTG1::TTG1:YFP where the majority of the trichomes are four branched (C) and nuclear TTG1:YFP is seen clearly as bright yellow dots (A). (D-I) *ttg1-13*pTTG1::TTG1:YFPp35S::78GL3:GUS, overexpression of the aptamer resulted in weak (D-F) and strong (G-I) phenotypes. (D-F) TTG1:YFP localization and trichome distribution in *ttg1-13*pTTG1::TTG1:YFPp35S::78GL3:GUS line showing weak phenotype has clear nuclear TTG1:YFP dots (D) and four branched trichomes (F). (G-I) TTG1:YFP localization and trichome phenotype in *ttg1-13*pTTG1::TTG1:YFPp35S::78GL3:GUS line showing a strong effect on trichome branching shows mostly cytoplasmic YFP as overall leaf appears bright yellow with no clear bright nuclear TTG1:YFP dots (G), Here most of the trichomes are three branched (I). (A, D, G) Epifluorescence images. (B, E, H) White light images of (A, D, G) respectively. (C, F, I) White light images with higher magnification to visualize trichome morphology.

Plants expressing the aptamer 78GL3:GUS resulted in trichome branching phenotypes ranging from wild type (Figure 2.22F) to a strong reduction in branching (Figure 2.22I). Plants with wild type trichomes were four branched (Figure 2.22F). Aptamer expressing plants with a strong phenotype had most trichomes with three branches (Figure2.22I). Observation under the epifluorescence microscope showed that control lines had clear YFP specific dots representing the nuclei (Figure 2.22A). The plants transformed with 78GL3:GUS aptamer also showed a clear specific YFP dots in the lines that showed no underbranching phenotype similar to the control (Figure 2.22D). On the other hand the aptamer expressing lines with a strong trichome branching phenotype showed diffuse YFP specific fluorescence with no specific nuclear dots (Figure 2.22G). Closer look on the subcellular TTG1:YFP by qualitative analysis revealed that TTG1:YFP was partially shifted to the cytoplasm (Figure 2.23A, A' marked by red arrows) compared to the control (Figure 2.23B, B').

Interestingly TTG1:YFP depletion is not affected (compare Figure 2.23 A' and B') though there may be quantitative differences in the depletion between the control and the aptamer expressing lines. I could not observe severe changes in the trichome clustering phenotype in these backgrounds. Detailed quantitative genetic analysis as well as the comparison of degree of depletion will give more insight into the relationship between the subcellular distribution of TTG1 and trichome patterning and morphogenesis.

2.9 Mapping the mobility domain in TTG1

TTG1 is able to act in a non-cell autonomous manner in *Arabidopsis* both within and across the cell layers (Bouyer *et al.*, 2008). AN11 an orthologue of TTG1 from *Petunia hybrida* functions in anthocyanin production together with

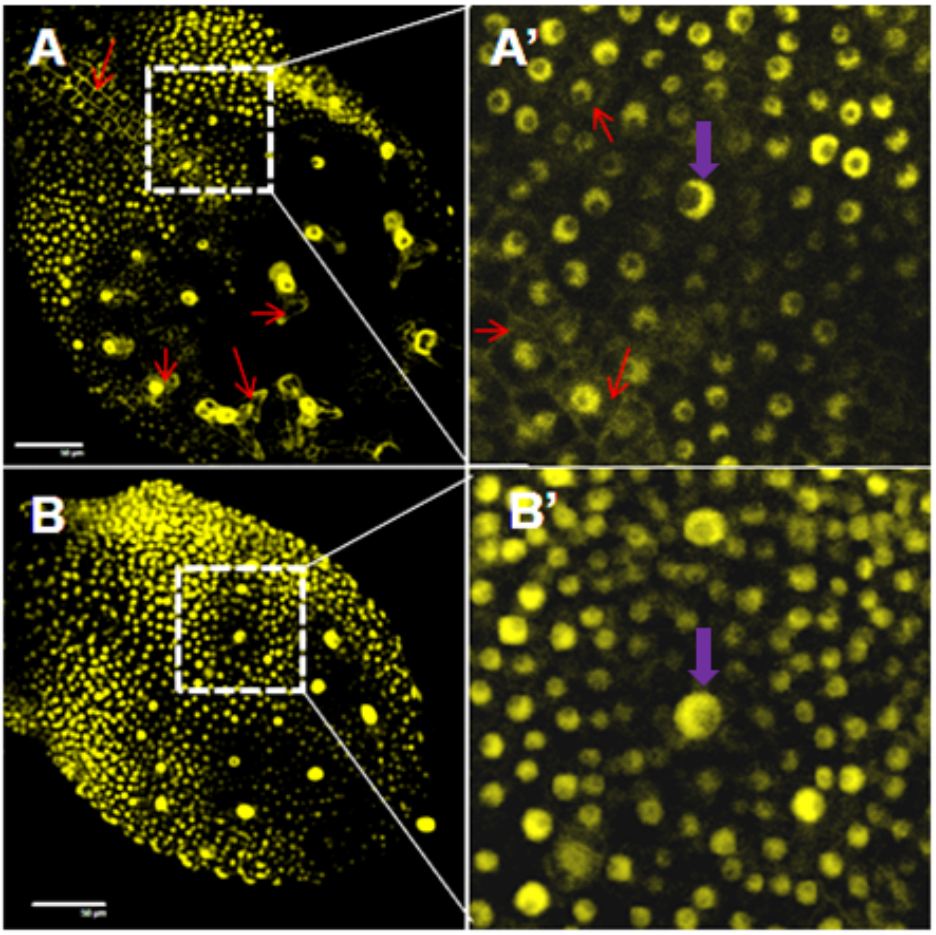

Figure 2.23: Influence of overexpression of 78GL3:GUS aptamer on the cellular distribution of TTG1. (A)*ttg1-13*pTTG1::TTG1:YFPp35S::78GL3:GUS, note that the YFP fluorescence is clearly visible in the cytoplasm of trichome and the epidermal cells (red arrows). (B) *ttg1-13*pTTG1::TTG1:YFP, note that unlike in (A) cytoplasmic YFP fluorescence is too weak to be seen. (A', B') Magnification of a region marked with discontinous square box in (A, B) respectively showing TTG1:YFP depletion around the trichome initial. Yellow, YFP fluorescence; red arrow, points to cytoplasmic YFP fluorescence; solid purple arrow, points to trichome initials around which TTG1:YFP is depleted. Scale= 50µm.

MYB and MYC like transcription factors AN2 and JAF13 respectively (de Vetten *et al*., 1997; Quattrocchio *et al*., 1998; Walker *et al*., 1999). *TTG1* and *AN11* share 78.1% identity and 89.8% similarity at the amino acid level. Preliminary results suggested that AN11 functions in a cell autonomous manner (A.Walker, unpublished results) in contrast to TTG1 (Bouyer *et al*., 2008). I used this fundamental difference between AN11 and TTG1 to map the mobility domain in TTG1 protein.

2.9.1 Analysis of AN11 mobility between the tissue layers

AN11 interacts with GL3 in yeast two-hybrid (Figure 2.24A). Loss of interaction between AN11 and GL3△78 showed that AN11 also binds to GL3 at the same site as TTG1 (Figure 2.24B). Analysis of nuclear transport behaviour of AN11 by NTT assay showed that like TTG1, AN11 is also not actively transported into the nucleus on its own (Figure 2.24C). This observation was consistent with the previous report by cell fractionation assay that AN11 is predominantly in the cytoplasm (de Vetten et a., 1997). Furthermore, AN11 is also trapped in the nucleus by GL3 similar to TTG1 in NTT system (Figure 2.24D). Therefore due to these similarities between AN11 and TTG1 with respect to their relation with GL3 in the yeast system it was expected that AN11 also behaves similar to TTG1 in *Arabidopsis*. To test this I analysed the trichome rescue ability of *AN11* when expressed under different promoters. *AN11* expressed under the *TTG1* promoter showed either no rescue or a very weak rescue of trichome density in *ttg1-1* plants. On the other hand under the p35S promoter *AN11* could fully rescue *ttg1-1* trichome number (106%) that was comparable to the rescue efficiency of p35S::TTG1 (93%) (Table 2.8).

Fusion of YFP to TTG1 in either orientation does not drastically affect its function (Bouyer *et al*, 2008; Zhao *et al*., 2008; Bouyer D., 2004). Therefore I tested the YFP fusion to AN11 also in both orientations. p35S::AN11:YFP

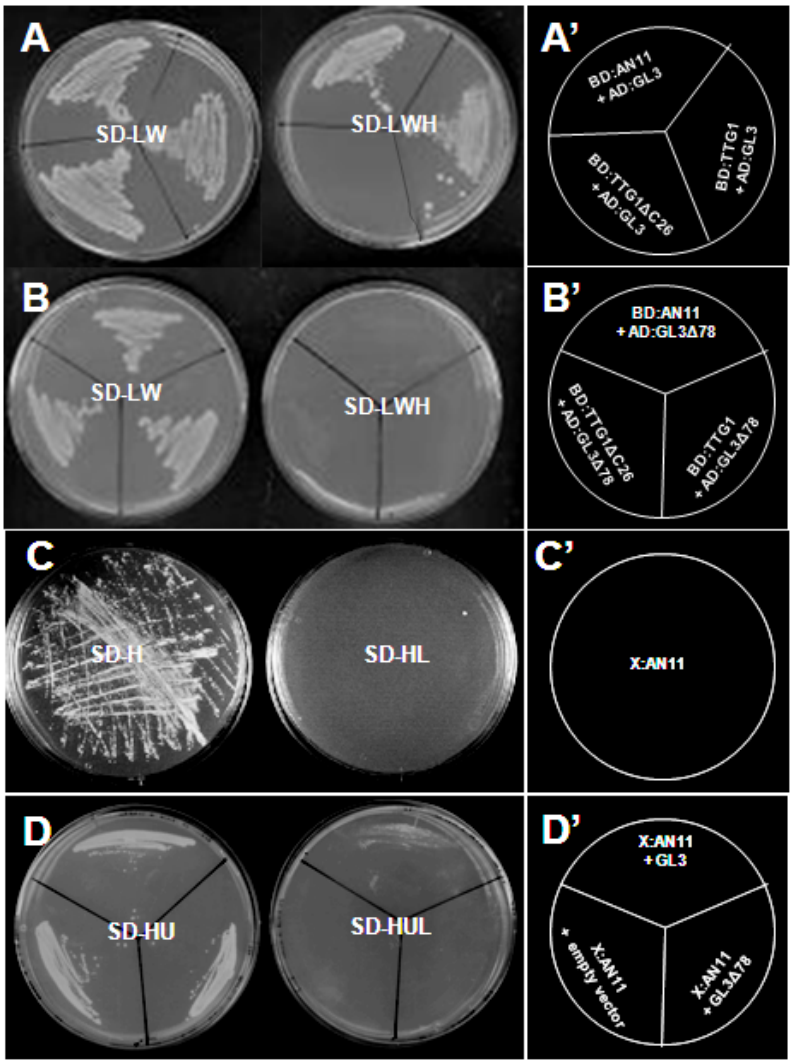

Figure 2.24: Yeast two-hybrid and NTT assay of AN11. (A, B) Yeast two-hybrid analysis of AN11 and TTG1 with GL3 (A) and GL3△78 (B). (C) NTT assay of AN11 shows that AN11 cannot enter into the nucleus. (D) NTT assay showing AN11 is in the nucleus in the presence of GL3 but not when co-expressed with GL3△78. Yeast growth in SD-LWH plates, positive interaction; no yeast growth in SD-LWH, no interaction; yeast growth in SD-HL/SD-HUL plates, X:AN11 fusion protein enters the nucleus; no yeast growth in SD-HL/SD-HUL, X:AN11 fusion protein does not enter the nucleus; AD, GAL4 transactivation domain; BD, GAL4 DNA binding domain; X, NES:LexAD; plates on the left are amino acid drop out medium for the selection of yeast transformed with one (SD-H) or two (SD-LW/SD-HU) vectors; plates on the right side are the amino acid drop out medium for the selection of positive interaction (SD-LWH) or for the proteins entering into the nucleus (SD-HL/SD-HUL); 5mM 3-AT was used for the selection of positive interactions in (A, B); (A'-D'), schematic presentation of the various combinations of the interactions tested in (A-D) respectively.

Table 2.8: Comparison of trichome rescue efficiency of TTG1 and AN11 and their mutual swapped versions expressed under *35S* and *pRBC* promoters

Construct	mutant	*p35S*		*pRBC*	
		Trichome no±SD .	Trichome frequency %of WT±SD	Trichome no.±SD	Trichome frequency %of WT±SD
TTG1	*ttg1-1*	44 ± 7.19	93 ±15.36	40 ±15.38	85 ±32.68
AN11	*ttg1-1*	50 ± 8.45	106 ±17.91	13 ±8.62	28 ±18.33
TTG1:YFP	*ttg1-1*	41 ± 10.25	87 ±21.75	42 ±5.15	89 ±10.91
AN11:YFP	*ttg1-11*	165 ±40	93 ±22.30	17 ±5.5	10 ±3.08
YFP:AN11	*ttg1-1*	43 ±6.77	92 ±14.48	8 ±14.83	17 ±31.51
TTG1:YFP (swap)	*ttg1-1*	48 ±8.94	102 ±18.99	20 ±11.07	43 ±23.55
YFP:AN11 (swap)	*ttg1-1*	45 ±19.5	96 ±41.6	17 ±23	36 ±48.70
-	L*er*	47 ±4.03	100 ±8.57	47 ±4.03	100 ±8.57
-	col	178 ±22	100 ±12.36	178 ±22	100 ±12.36

SD, standard deviation; trichome phenotypes were scored on the adaxial surface of the third and fourth true leaves of the seedlings from the T1 generation and the untransformed control lines; trichome frequency is the mean percentage of the trichomes expressed as a percentage of the corresponding wild type control; 25 plants were used for the analysis; *ttg1-1* is in L*er* ecotype; *ttg1-11* is in Col ecotype.

rescued the trichome number to a wild type situation when expressed in *ttg1-11* (93%) and this rescue efficiency was comparable to p35S::YFP:AN11 expressed in *ttg1-1* (92%) (Table 2.8). Next, expression under the subepidermal specific promoter *pRBC* clearly showed a difference in the rescue ability of *TTG1* and *AN11*. While pRBC::TTG1 could completely rescue the trichome number in *ttg1-1* (85%), pRBC::AN11 failed to do so and could only rescue about 28% trichomes compared to wild type L*er*. Furthermore, pRBC::AN11:YFP and pRBC::YFP:AN11 expreesed in *ttg1-11* and *ttg1-1* respectively showed a very low rescue efficiency

(10% and 17% respectively) (Table 2.8). These observations clearly suggested that the AN11 protein mobility was inefficient to move from the subepidermis to the epidermis.

2.9.2 Swapping non homologous regions in TTG1 and AN11.

The major difference between TTG1 and AN11 protein is observed in the N-terminal region (Figure 2.25). These non homologous regions were swapped between the coding sequences of *TTG1* and *AN11* genes to create TTG1:YFP(Swap) and AN11:YFP(swap) (Figure 2.25). Swapped versions of *TTG1* and *AN11* were then expressed under *p35S* and *pRBC* promoters in *ttg1-1* mutants. Both the swapped proteins could rescue trichome numbers as efficient as the corresponding non swapped versions when expressed under the *p35S* promoter. However, the effect was reversed when they were provided in the subepidermis under *pRBC* promoter. pRBC::TTG1:YFP(swap) could rescue about 43% of the trichome number compared to 89% in pRBC::TTG1:YFP compared to wild type, which means a domain swapping resulted in a decrease of 46% rescue efficiency. On the contrary pRBC::AN11:YFP(swap) showed a rescue of 36% trichome number while pRBC:: AN11:YFP and pRBC::YFP:AN11 had resulted in 10- 17% rescue, which means the TTG1 domains swapped into AN11 helped to increase the rescue efficiency of subepidermal AN:YFP by 19-26% (Table 2.8).

2.10 Generation of mutants affecting the transport of TTG1 from the subepidermis to the epidermis

Arabidopsis plants expressing pRBC::TTG1 completely rescues the *ttg1* trichome phenotype (Figure 2.26B). Microinjection studies in *Nicotiana benthamiana* mesophyll cells suggested that TTG1 can actively open the PD and traffick between the cells (Bouyer *et al.*, 2008). Hence in *ttg1*pRBC::TTG1 lines TTG1 transport from the subepidermis to the epidermis is most likely through active regulation of

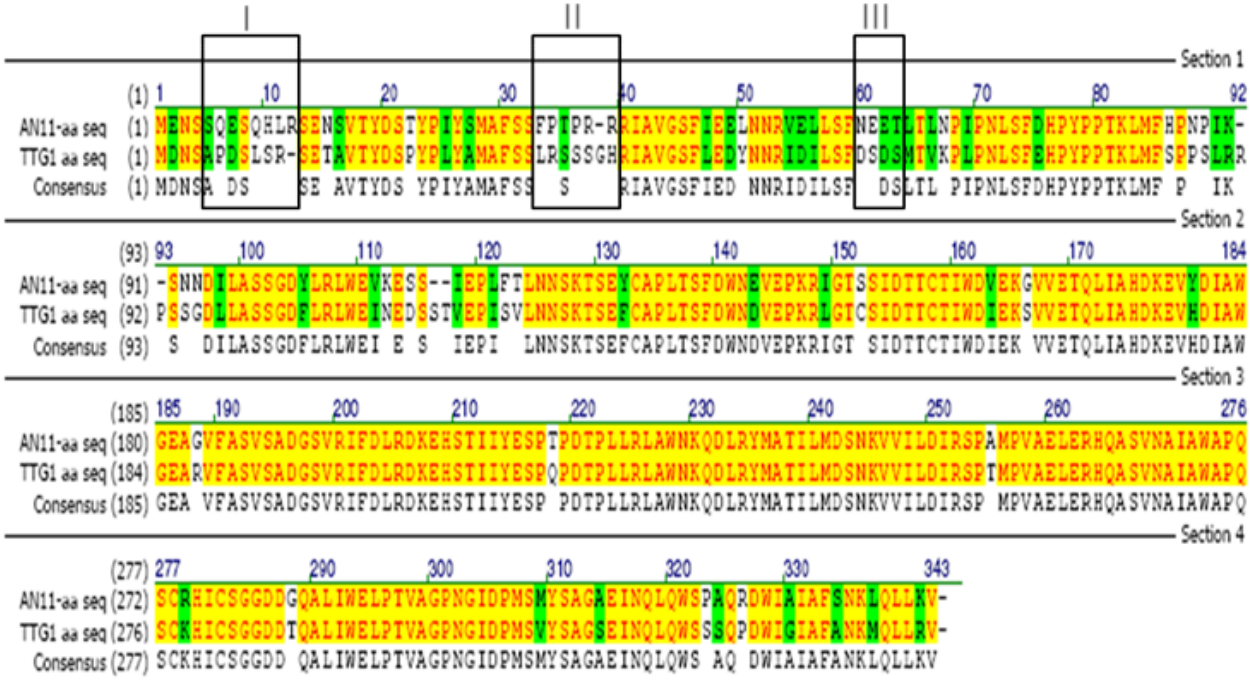

Figure 2.25: TTG1 and AN11 protein sequence alignment showing the non homologous domains in the N-terminus. Black boxes numbered I, II, III denote the three domains that were swapped between TTG1 and AN11 for the gain of function experiments in plants.

PD SEL. Therefore to identify potential candidates that regulate the TTG1 transport in *Arabidopsis ttg1*pRBC::TTG1 plants were mutagenised with ethyl methyl sulphonate (EMS). Mutants inhibiting the transport of the TTG1 protein from the subepidermis to the epidermis should result in a loss of trichomes on the adaxial surface of the leaves. Hence I isolated eight glabrous plants as putative mutants for the TTG1 transport regulators. After complementation experiments with the existing trichome activator mutants (*gl1*, *ttg1* and *gl3*) to exclude the mutations at the same loci, I selected one mutant as a putative TTG1 transport inhibitor (here after referred as *tti*) mutant.

The *tti* mutant is affected in the trichome formation showing completely glabrous leaves (Figure 2.26A) and also shows a defect in seed mucilage synthesis (Figure 2.26C). However, proanthocyanidin synthesis is not affected as shown by the

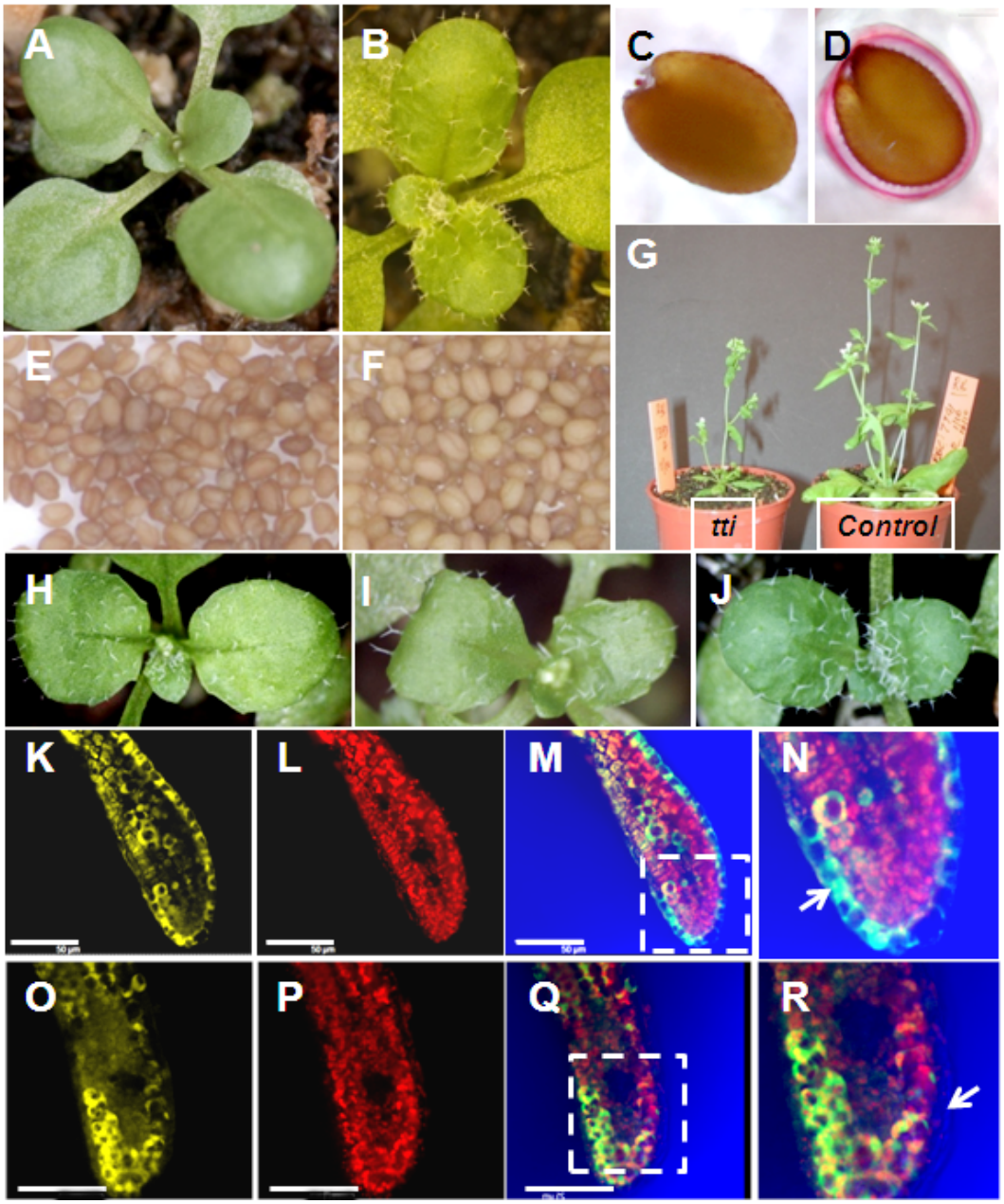

Figure 2.26: Analysis of the TTG1 transport inhibitor (*tti*) mutant isolated in screening of EMS mutagenised pRBC::TTG1 plants. (A, C, E) Phenotypes of *tti* mutant, leaf trichomes (A), seed coat mucilage synthesis (C) and seed coat color (E). (B, D, F) Phenotype of control plant pRBC::TTG1 leaf trichome (B), seed coat mucilage (D) and seed coat color (F). (G) Comparison of general growth of *tti* mutant and control plant. (H-J) Complementation experiment showing the trichome rescue in the F1 from the *tti* mutant crossed to *gl3* (H), *gl1* (I) and *ttg1* (J). (K-N) *ttg1*pRBC::TTG1:YFP, TTG1:YFP moved from the suepidermis to the epidermis (N, marked by arrow). (O-R) *tti*pRBC::TTG1:YFP, TTG1:YFP protein is restricted to the subepidermis and no YFP fluorescence was observed in the epidermis (R, marked by arrow). (N, R) Magnification of the boxes marked with dotted lines in M and Q respectively. Yellow, YFP fluorescence; red, cholorophyll; green, YFP fluorescence in overlay pictures (false colored); arrows in (N, R) points to epidermal layer. Scale=50µm.

brown seed coat color similar to seeds from the wild type plant (Figure 2.26E, F). Genetic complementation experiments were performed by crossing the *tti* mutant with *gl3*, *gl1* and *ttg1* mutants. It was observed that the F1 plants from the *tti* crossed to *gl3*, *gl1* and *ttg1* rescued the trichome phenotype. (Figure 2.26H-J). The F1 from the cross between *tti* and *gl1* resulted in a partial rescue (Figure 2.26I). In order to verify that the specific transport of the TTG1 from the subepidermis to the epidermis is affected in the *tti* mutant TTG1:YFP was expressed specifically in the subepidermis using the *pRBC* promoter. This line was created by crossing the *tti* mutant with the *ttg1*pRBC::TTG1:YFP homozygous line. It was observed that the TTG1:YFP was restricted to the subepidermis in the homozygous F2 plants (Figure 2.26O-R). On the other hand YFP fluorescence was clearly seen in both epidermal as well as the subepidermal tissues in the control line *ttg1*pRBC::TTG1:YFP (Figure 2.26K-N).

3 Discussion

While the mobility of signalling molecules and transcription factors is important for proper pattern formation, restricting their mobility to certain cell types is as important as their active transport. Restricting the mobility of these molecules could be achieved by targeting the proteins to specific cellular compartments (Crawford and Zambryski, 2000) or by complexing them with other factors in the cell. The latter mechanism can be applied to APETALA3 (AP3) and PISTILLATA (PI), which are known to form complexes between them and with other members of the MADS box protein group during floral organ identity specification (McGonigle *et al*. 1996; Riechmann *et al*., 1996; Egea-Cortines *et al*., 1999; Honma and Goto 2001). The other example for this is the restriction of SHR mobility in the endodermis as a result of sequestering by SCR thereby defining a single layer of root endodermis (Gallagher *et al*., 2004; Cui *et al*., 2007).

Trichome patterning in *Arabidopsis* is a *de novo* pattern formation process and is explained by the activator-inhibitor model (Pesch and Hülskamp 2004; Meinhardt and Gierer, 1974). Recent study has shown that apart from the transcrption factors the WD40 protein TTG1 is able to function in a non-cell autonomous manner (Bouyer *et al*., 2008). TTG1 is depleted in the trichome neighboring cells and is accumulated in the trichome initial hinting at a role of activator depletion mechanism during trichome pattern formation. Here I show that TTG1 depletion depends on GL3. Further I characterized the molecular mechanism of the GL3

dependent TTG1 depletion and highlight on the importance of TTG1 depletion on the trichome development and patterning.

3.1 GL3 is required for the TTG1:YFP depletion during trichome pattern formation

The TTG1:YFP fusion protein is able to move within the epidermal tissue as well as between the cell layers (Bouyer *et al*., 2008). It was also demonstrated that TTG1 can move into the trichome cells from the surrounding epidermal cells. Furthermore, TTG1:YFP is depleted in the trichome neighboring cells in such a way that the immediate neighboring cells show the least TTG1:YFP amount in the nuclei and this amount increses in the cells with increasing distance from the trichome initial (Bouyer *et al*., 2008). These findings raised the question whether TTG1:YFP was specifically transported into trichomes in wild type situation, something similar to the directional transport of auxin through PIN1 transporter during the primordia positioning in the meristematic region (Smith *et al*., 2006; Reinhardt D. 2003). However, the possiblity of directional transport was excluded by Bouyer *et al*., (2008) where it could be shown that TTG1:YFP is actively transported not just into the trichomes but is also free to move into other epidermal cells. Taking all these into account it can be hypothesized that a trapping/attracting mechanism is responsible for restricting TTG1 in the trichome nucleus. Similar mechanism was shown to be operating during radial pattern formation in roots where SHR is sequestered by SCARECROW (SCR) in the endodermis nuclei. *SHR* is expressed in stele of the root and moves into the endodermis where it is required in a positive feedback loop for the local enhancement of the SCR pool and for the expression of the common targets of SHR and SCR to define a single layer of endodermis in plants (Cui *et al*., 2007; Gallagher *et al*., 2004).

Similarly the depletion of TTG1:YFP during trichome pattern formation on the adaxial surface of the *Arabidopsis* rosette leaves was thought to be GL3 dependent. The *Gl3* expression, GL3 localization pattern and its strong interaction with TTG1 makes GL3 a potential candidate to cause the TTG1:YFP depletion (Payne *et al*., 2000; Zhang *et al*., 2003; Zhao *et al*., 2008). Moreover, it is proposed that TTG1 forms a part of the activator complex involving GL3 and GL1 that is required to trigger a protodermal cell into trichome pathway (Zhang *et al*., 2003; Zhao *et al*., 2008; Yoshida *et al*., 2009; Payne *et al*., 2000; Esch *et al*., 2003; Digiuni *et al*., 2008; Gao *et al*., 2008). To verify this thought, I analysed TTG1:YFP distribution in the leaf adaxial epidermal cells in the absence of GL3 (Figure 2.1). Mutations in *Gl3* have moderate effect on trichome initiation (Hülskamp *et al*., 1994; Payne *et al*., 2000). Taking advantage of this property of *gl3* mutant, cellular distirbution of TTG1:YFP under the *TTG1* promoter was analysed in *gl3* mutant. Interestingly TTG1:YFP depletion was completely abolished in the absence of GL3 and was uniformly distributed in all epidermal cells with slightly higher concentration in the trichome initials (Figure 2.1) (Bouyer *et al*., 2008). The slightly higher levels of nuclear TTG1:YFP in the trichome initials in *gl3* mutant could be due to the presence of the EGL3 protein which also interacts with TTG1. This experiment clearly suggested that TTG1 depletion depends on the GL3 protein.

3.2 GL3 sequesters TTG1:YFP in the nucleus

TTG1 and GL3 control the expression of the same set of target genes during trichome cell fate specification and in the anthocyanin biosynthetic pathway (Zhao *et al*., 2008; Gonzalez *et al*., 2008). GL1 is required to recruit GL3 to the promoters of two major trichome targets *GL2* and *CPC* (Ishida *et al*., 2007a, 2007b; Wang and Chen 2008). It is interesting to note that GL3 protein forms subnuclear speckles in the absence of TTG1 or GL1 suggesting the presence of TTG1 and GL1 is necessary

for proper distribution of GL3 in the nucleus (Zhao *et al*., 2008; Yoshida *et al*., 2009). These data strongly suggest that TTG1 is required in the nucleus. However, *TTG1* is not a transcription factor and predictions showed no NLS sequences in TTG1 (Walker *et al*., 1999). Moreover, cell fractionation studies showed that AN11 an orthologue of TTG1 from *Petunia hybrida* was cytoplasmic (de Vetten *et al*., 1997) hinting that TTG1 could also be cytoplasmic in *Arabidopsis*. Surprisingly TTG1:YFP fusion protein is predominantly localized in the nucleus in the young region of the leaf whereas in the matured region towards the tip of the leaf it seems to shift to the cytoplasm (Bouyer *et al*., 2008). Loss of depletion and appearance of more cytoplasmic TTG1:YFP in the *gl3* mutant pointed towards the GL3 influence on the TTG1:YFP localization in a cell. Here I could show with several methods that it is indeed GL3 that greatly influence the TTG1:YFP localization in the cell. First *in planta* analysis of TTG1:YFP expressed under the *TTG1* promoter in wild type, *gl3* mutant and in plants expressing *GL3* under the *p35S* promoter showed a clear positive influence of GL3 on the nuclear TTG1:YFP amount (Figure 2.2, 2.3). Detailed quantification of subcellular localization of TTG1:YFP using CLSM in these backgrounds was in complete agreement with the observations (Figure 2.3). Interestingly because of the trapping of TTG1:YFP in all the epidermal cells by GL3 in p35S::GL3 expressing lines, it resulted in a loss of TTG1 depletion in these lines (Figure 2.2C). This means there is a TTG1-GL3 activator complex in all the epidermal cells, which explains the overproduction of trichomes in wild type plants transformed with p35S::GL3. This quantitative analysis of the GL3 influence on the nuclear trapping of TTG1 was further supported by co-expression of CFP:GL3 and TTG1:YFP in onion epidermal cells that resulted in relocalization of a bulk of the TTG1:YFP into the nucleus (Figure 2.8E) compared to the nuclear and cytoplasmic localization when TTG1:YFP is expressed alone (Figure 2.8B). Moreover, the specific interaction between GL3 and TTG1 is needed because GL3$\triangle$78 where the TTG1 interaction domain (mapped in this study) was

deleted resulted in no influence on the TTG1:YFP localization (Figure 2.8G). In a reciprocal experiment a 78 amino acid aptamer from GL3 corresponding to the TTG1 interaction effectively competed with GL3 thereby hindering the nuclear trapping of TTG1 by GL3 when TTG1, GL3 and 78GL3 were co-expressed in onion epidermal cells (Figure 2.10). This observation further supported the specificty of TTG1 and GL3 interaction for nuclear trapping of TTG1 by GL3. Also GL3△NLS where the NLSs are missing failed to relocalize the bulk of the TTG1:YFP into the nucleus hence TTG1:YFP was in both cytoplasm and the nucleus (Figure 2.8I).

In a yeast based NTT assay I could show that TTG1 has no fucntional NLS. It is therefore always exported to the cytoplasm in this assay (Figure 2.7A). It is interesting to note that TTG1 is targeted to the nucleus in the presence of GL3 but not when the interaction between TTG1 and GL3 is inhibited by deleting the specific interaction domains in either or both proteins (Figure 2.7B). Similar observation was made by Sompornpailin *et al*., (2002) where they showed that nuclear amount of PFWD a TTG1 homologue from *Perilla frutescens* is much higher when co-expressed in onion epidermal cells with *MYC-RP* a bHLH gene similar to *GL3* compared to when it is expressed alone. This kind of co-localization phenomenon was also described earlier for AP3 and PI during the specification of floral organ identities. Nuclear localization of these transcription factors depends on their simultaneous expression which are otherwise localized in the cytoplasm when expressed alone (McGonigle *et al*., 2001). It is known that overexpression of *GL3* partially rescues the *ttg1* phenotype while overexpression of both *GL3* and *GL1* leads to complete rescue of the *ttg1* mutant phenotype (Payne *et al*., 1999). TTG1 seems to be necessary to regulate the stability of the bHLH and GL1 interaction at the promoters of the target genes by maintaining stable GL3-GL1 complex (Morohashi et al., 2007; Zhao et al., 2008). This genetic observation can be explained by the hypothesized stable trichome activator complex formation rate. Chances of GL3-GL1 complex formation are much higher under their

overexpression conditions due to increased abundance of both the activator protein molecules. On the other hand in wild type situations where both *GL3* and *GL1* are under control of their respective endogenous promoters there is limited amount of these molecules and so will be the GL3-GL1 complex formation rate. Although TTG1 is required for the expression of several trichome regulators that are common to GL3 and GL1, it has no NLS to enter into the nucleus nor does it has any known DNA binding or activation domain. Therefore it is conceivable that GL3 traps it in the nucleus in a complex together with GL1 and form a stable activator complex. Hence TTG1 transport into the trichome initials might be a mechanism adopted to maintain the stability of the GL3-GL1 complex thereby together regulating the expression of other trichome regulators. At the same time removal of the TTG1 protein from the neighboring cells could result in abolition/reduction of the expression of trichome regulators in them thereby effectivly inhibiting the neighboring cell from entering into trichome fate. Unlike in the proanthocyanidin biosynthesis pathway where the expression of a *GL3* homologue *TT8* is directly under the control of TTG1, in the trichome patterning TTG1 seems to have no role in the positive feed back loop of GL3 as *GL3* expression is not influenced by TTG1 (Zhao *et al*., 2008)

The other possible mechanism where TTG1 might be functioning is through its interaction with the *GLABRA2 EXPRESSION MODIFIER* (*GEM*). In *Arabidopsis* roots GEM represses the expression of *GL2* and *CPC* by maintaining the repressor histone H3K9 methylation status and also modulating cell division (Caro *et al*., 2007). Overexpression of *GEM* led to increased root hair and decreased trichome number indicating its role not only in root hair but also in trichome cell fate regulation. It was shown that TTG1 physically interacts with GEM (Caro *et al*., 2007). Here I could imagine that the increasing amount of TTG1 in trichome initials and its decrease in the pavement cells also has a similar opposite effect on the available GEM amounts to perform its function in these two cell types. TTG1 by

its interaction with GEM might keep GEM protein away from participating in the complex responsible for the repression of trichome regulatory genes in the trichome initials. On the other hand due to less TTG1 in the trichome surrounding cells more free available GEM keeps these genes repressed in the pavement cells. This effect could possibly be by spatial separation of GEM protein or by modification of structural and functional domains of GEM. Therefore GL3 mediated depletion of TTG1 could be one mechanism to render different effects on the GEM protein in different cell types thereby differentially regulating the function of the GEM protein.

3.3 EGL3 contributes to TTG1 nuclear localization

The bHLH factors invloved in TTG1 regulated cell fate determination pathways have partial functional redundancy. EGL3 and TT8 both interact with TTG1 and regulate some overlapping (anthocyanin production and development of seed coat epidermal cells) and some distinct (develoment of non root hair epidermal cells and trichome development by EGL3 and seed coat proanthocyanidin production by TT8) TTG1 regulated developmental pathways (Zhang *et al*., 2003; Baudry *et al*., 2006; Gonzalez *et al*., 2008, 2009; Nesi *et al*., 2000; Bernhardt *et al*., 2003, 2005).
A recent study also indicated a role of TT8 in the leaf marginal trichome development (Maes *et al*., 2008). Therefore it is highly likely that not only GL3 but also EGL3 and TT8 contribute to sequester TTG1 in the nucleus. By analysis of nuclear TTG1:YFP in wild type, *gl3*, *gl3 egl3*, and *gl3 egl3 tt8* mutant backgrounds I could show that GL3 has major influence followed by EGL3 on the nuclear trapping of TTG1:YFP. TT8 has no effect on retaining the TTG1:YFP in the nucleus (Figure 2.4). It is noteworthy that EGL3 has an additive effect on the retention of TTG1 in the nucleus in addition to GL3 while TT8 does not have the same effect. This observation is consistent with the previous genetic observations that among the bHLH

proteins GL3 and EGL3 are the sole regulators of trichome fate on the leaf lamina with GL3 playing a major role whereas TT8 mainly regulates the leaf margin/edge trichomes (Maes *et al*., 2008). Since *egl3* and *tt8* single mutants exhibit no obvious trichome phenotype on the leaf lamina, quantification of subcellular TTG1:YFP distribution in these mutants was not considered (Zhang *et al*., 2003; Maes *et al*., 2008). Considering the role of TT8 on the trichome development at the leaf margin its influence on the subcellular distribution of TTG1 in this region cannot be excluded but was not analysed here. Furthermore, TTG1△C26 does not interact with any of the bHLH proteins of TTG1 regulated developmental pathway (Figure 2.17) (Payne *et al*., 2000). Consistent with this TTG1△C26:YFP is cytoplasmic in contrast to TTG1:YFP in stable transformed plants (Figure 2.11). But these results are contradictory. While, the TTG1△C26:YFP, which does not interact with GL3, EGL3 and TT8 is exclusively cytoplasmic, almost 50% of the TTG:YFP is in the nucleus in *gl3 egl3 tt8* triple mutant in contrast to 69% in wild type (Figure 2.4Q). This is tempting to speculate that apart from GL3, EGL3 and TT8 there could be other interacting partners that are capable of retaining TTG1 in the nucleus as can be seen in *gl3 egl3 tt8* triple mutant. Hence, if there are no other partners to sequester TTG1 in the nucleus, TTG1 might simply keep shuttling in and out of the nucleus in the absence of GL3/EGL3. The latter scenario further prompts to speculate that C-terminal 26 amino acid region in TTG1 is necessary to maintain the ability for passive transport of TTG1 into the nucleus. However, it is not clear yet how exactly GL3/EGL3 target TTG1 into the nucleus. Whether GL3/EGL3-TTG1 is entering into the nucleus as a complex or TTG1 is passively transported into the nucleus and is then seqestered by GL3/EGL3 is not known.

Qualitative observation in the root also showed a similar tendency of bHLH proteins effect on the nuclear TTG1:YFP (Figure 2.5). The observation of TTG1:YFP in the roots of *gl3 egl3 tt8* was not included in this assay as *TT8* is not expressed in the roots (Baudry *et al*., 2006).

3.4 Is the nuclear import of TTG1 necessary for cell-to-cell transport ?

There is no general strict rule for the relationship between subcellular localization and protein mobility. While mutations or modifications in CPC, KN1 and SHR that reduce their nuclear localization led to decrease in their mobility between cells, nuclear targeting of GFP partially reduced its passive transport ability (Gallagher *et al*., 2004; Kim *et al*., 2005; Kurata *et al*., 2005; Lucas *et al*., 1995; Prochiantz and Joliat, 2003; Tassetto *et al*., 2005; Crawford and Zambryski 2000). However, a balance between nuclear import and export is also suggested to be essential for the mobility of SHR and LFY transcription factors (Gallagher and Benfey, 2009; Kim *et al*., 2002; Wu *et al*., 2003). Looking at the nuclear and cytoplasmic localization dynamics of TTG1:YFP, it is tempting to speculate that like SHR and LFY, nuclear and cytoplasmic localization of TTG1 is necessary for the mobility of TTG1 protein. However, expression of pRBC::NLS:TTG1:YFP in *ttg1-13* that results in exclusively nuclear TTG1:YFP fusion protein showed a complete rescue of the trichome phenotype. This observation points to non dependency on cytoplasmic localization of TTG1 for its mobility (Table 2.3). Also pTTG1::NLS:TTG1:YFP rescued as good as pTTG1::TTG1:YFP when expressed in the *ttg1-13* mutant. Recent report suggest that TTG1:YFP produces significantly higher cluster frequency than TTG1 without fusion due to increased protein size that might partially decrease its mobility (Bouyer *et al*., 2008; Bouyer D., 2004). I also confirmed this observation in this study (Table 2.5). It is known that in general increasing protein size leads to decrease in its mobility as was shown for different sized GFP fusions during *Arabidopsis* embryo development (Kim *et al*., 2005). Therefore if there is a difference in the mobility rate of NLS:TTG1:YFP and the TTG1:YFP proteins there should also be differences in the frequency of the clusters formed in lines expressing these proteins. However, the cluster frequency in pTTG1::TTG1:YFP,

pTTG1::NLS:TTG1:YFP and pRBC::NLS:TTG1:YFP was not significantly different from each other, which means these nuclear targeted and wild type distributed (nuclear and cytoplasmic) fusion proteins were not different from each other with respect to their intercellular transport rates (Table 2.3). Mechanistically how nuclear localization and intercellular mobility are related is still unclear. Prochiantz and Joliot (2003) have speculated that EN2, a homeodomain protein may gain competence to move after some specific modifications in the nucleus. Further they also suggested that nuclear localization may bring cargo proteins in close proximity with factors that facilitate their transport or they get access to the secretory pathway. Gallagher and Benfey, (2009) also considered these factors as possible explanation for the correlation they observed between SHR subcellular localization and its movement between cells. Similar mechanism might be responsible for the TTG1 mobility as well. However, before speculating similar thoughts for the TTG1 mobility it would be extremely important to compare how TTG1 targeted exclusively either to the nucleus or to the cytoplasm behave with respect to mobility. Detailed quantitative analysis of the TTG1:YFP depletion in lines expressing pTTG1::NLS:TTG1:YFP in comparison to lines expressing pTTG1::TTG1:YFP will put more light on the relationship between TTG1 nuclear localization and its depletion. Nevertheless, with the current data it can be postulated that targeting of TTG1:YFP exclusively to the nucleus has minimum or no negative influence on its mobility within as well as between the tissue layers in the leaves. It is likely that TTG1:YFP in the nucleus in wild type is already at a threshold level hence further increase in the nuclear TTG1:YFP amount is immaterial for its intercellular transport during the trichome development and pattern formation. Therefore the observation that the mobility of NLS:TTG1:YFP fusion protein, which is exclusively nuclear is as good as TTG1:YFP hints that nuclear targeting is necessary for TTG1 mobility during trichome pattern formation. Furthermore, depletion was not affected when TTG1:YFP was partially trapped in the cytoplasm by 78GL3 ap-

tamer (Figure 2.23A, A'). Hence, the cytoplasmic TTG1 protein appears to have no role in cell-to-cell transport of TTG1 protein and thereby does not contribute to the depletion. However, whether the cytoplasmic TTG1 is able to move or not need to be verified in future studies either by expressing under the *pRBC* promoter or by microinjection technique in the tobacco leaves.

Interestingly NLS:TTG1:YFP expressed under the *pRBC* promoter did not complement the seed coat color defect in contrast to TTG1:YFP expressed under the same promoter in *ttg1* mutant (Figure 2.16). To confirm that the NLS:TTG1:YFP fusion protein is functional in the seeds I tested the seed coat mucilage production, which is another seed phenotype controlled by TTG1. Seeds from the transgenic plants *ttg1*pRBC::NLS:TTG1:YFP, *ttg1*pRBC::TTG1:YFP, *ttg1*pTTG1::NLS:TTG1:YFP and *ttg1*pTTG1::TTG1:YFP showed no difference in mucilage production compared to wild type seeds (Figure 2.16). This observation suggested a defect specifically for proanthocyanadin (PA) biosynthesis in *ttg1*pRBC::NLS:TTG1:YFP. Furthermore rescue of seed coat color in *ttg1*pRBC::TTG1:YFP and *ttg1*pTTG1::NLS:TTG1:YFP lines excluded respectively the differences in spatial expression pattern and subcellular localizations as the cause of transparent testa phenotype in *ttg1*pRBC::NLS-:TTG1:YFP. It was previously demonstrated using yeast two-hybrid and three-hybrid analysis that TTG1, TT8 and a MYB protein TT2 encoded by *TRANSPARENT TESTA2* (*TT2*) can form a ternary complex (Baudry *et al*., 2004). Furthermore, TT2, TT8 and TTG1 can directly activate the *BANYULS* (*BAN*) gene expression and the activity of TT2-TT8 complex correlated with the expression levels of *TTG1* (Baudry *et al*., 2004). TTG1 is required for the expression of *TT8* promoter specifically in the inner (regions 1 and 2 defined by Debeaujon *et al*., 2003) and outer integument of the seed coat (Baudry *et al*., 2006). In the outer integument TTG1 together with EGL3/TT8 and MYB5/TT2 is involved in the differentiation and maintenance of epidermal cell layer where mucilage is synthesized (Penfield *et al*., 2001; Baudry *et al*., 2006; Gonzalez *et al*., 2009). Similarly in the inner integu-

ment TTG1 functions in the endothelial cell layer by controlling the expression of *TT8* which together with TTG1 and TT2/MYB5 regulate the expression of the *BAN* promoter that is necessary for the PA biosynthesis (Nesi *et al*., 2000, 2001; Baudry *et al*., 2004, 2006; Gonzalez *et al*., 2009). In future studies it is important to determine the differences in the localization of NLS:TTG1:YFP and TTG1:YFP in different cell types during the seed development when expressed under the *pRBC* promoter. Further at the molecular level it will be interesting to know the differences in the expression pattern of the TTG1 target genes such as *TT8*, *BAN* and *TTG2* in pRBC::TTG1:YFP and pRBC::NLS:TTG1:YFP expressing seeds. Under wild type situation these target genes are expressed in specific cells of the seed in a TTG1 dependent manner during seed development (Baudry *et al*., 2004, 2006; Gonzalez *et al*., 2009).

3.5 Mobility of TTG1:YFP is counteracted by GL3

Rescue efficiency of subepidermal expressed TTG1:YFP is reduced drastically from 80% in *ttg1* (Figure 2.12D) to 5% in *ttg1 gl3* (Figure 2.12F) strongly favoring the need of GL3 in the epidermis for the full function of subepidermal TTG1 (quantified by Daniel Bouyer). Moreover providing GL3 in the subepidermis together with TTG1:YFP in *ttg1 gl3* led to further loss of rescue efficiency of subepidermal TTG1:YFP (Figure 2.12M). This strongly favors the idea of TTG1:YFP being trapped in the subepidermis when co-expressed with GFP:GL3 consistent with my observations in quantification of the nuclear TTG1:YFP in the *gl3* mutant and *GL3* overexpression lines (Figure 2.3), NTT assay in yeast (Figure 2.7B), and transient expression assay in onion epidermal cells (Figure 2.8E). Moreover, in most of the lines tested the TTG1:YFP signal was restricted to the subepidermis when co-expressed with GFP:GL3 in the subepidermis and was colocalized with the GFP:GL3 (Figure 2.12N). Nevertheless, in some lines expressing both TTG1:YFP

and GFP:GL3 under the *pRBC* promoter, YFP fluorescence was observed in the epidermis as well. However there could be quantitative differences in amount of the TTG1 protein moving from the subepidermis to the epidermis when *TTG1* is expressed alone or when it is expressed together with *GL3* in the subepidermis. Drastic overproduction of trichomes was observed when GL3 was provided specifically in the epidermis under the *pAtML1* promoter in *ttg1 gl3*pRBC::TTG1:YFP line (Figure 2.12L). In this situation subepidermal TTG1:YFP that moves into the epidermis is trapped by the abundant GL3 present in the epidermis thereby most of the epidermal cells gain trichome fate, a phenotype reminiscent of p35S::GL3 in wildtype (Payne *et al*., 2000). As expected *ttg1 gl3* plants expressing *GL3* under the *pAtML1* promoter showed a partial rescue of trichomes resulting in a phenotype similar to p35S::GL3 in *ttg1* background (Payne *et al*., 2000).

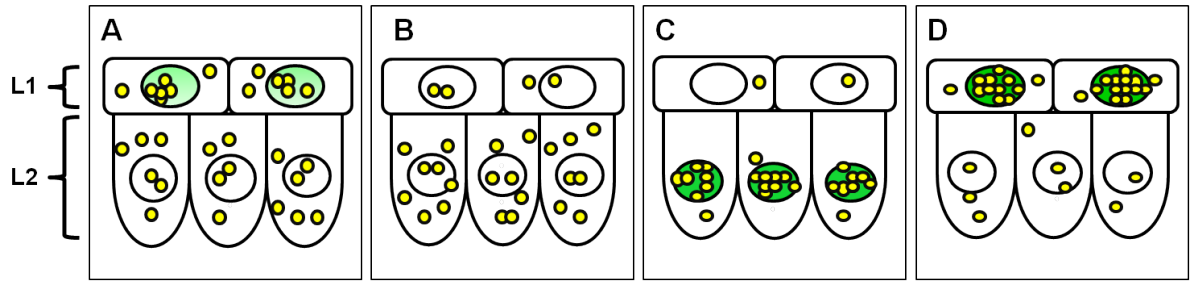

Figure 3.1: Schematic presentation of the effect of tissue specific *GL3* expression on the mobility of *TTG1* expressed in the subepidermal tissue. (A-D) TTG1:YFP is provided from subepidermis by expressing under *pRBC* promoter. (A) *ttg1*, TTG1:YFP is free to move into the epidermis. (B) *ttg1gl3*, there is no GL3 hence TTG1:YFP is not trapped although it moves into the epidermis resulting in drastic fall in trichome rescue efficiency. (C) *ttg1gl3*pRBC::GFP:GL3, even the small percentage of trichomes rescued in the situation like in (B) is lost as the subepidermal GL3 traps the bulk of the TTG1 protein in the subepidermis. (D) *ttg1gl3*pAtML1::GFP:GL3, here as a result of strong *GL3* expression in all the epidermal cells, the majority of the TTG1:YFP from the subepidermis is attracted and is trapped in the epidermis resulting in massive overproduction of trichomes. Yellow, depicts TTG1:YFP; Intensity of green, indicates amount of GL3; L1, epidermal layer; L2, subepidermal tissue.

I confirmed the observations of the rescue experiment explained above with another set of experiment using KikGR1, a photoconvertible marker. Using the pho-

toconvertible fluorescent marker KikGR1 as a C-terminal fusion to TTG1 I could show that the transport ability of TTG1 differs significantly in different epidermal cell types. TTG1:KikGR1(red) in trichome initials was less free to move compared to the TTG1:KikGR1(red) from other epidermal cells including the trichome neighboring cells and the epidermal cells away from the trichome initial (Table 2.2). What is more interesting is the difference in the gain of TTG1:KikGR1(red) in different epidermal cells. For this analysis the scenario where the TTG1:KikGR1(green) in the trichome neighboring cell is converted into TTG1:KikGR1(red) was used due to the presence of different types of cells as its neighbors. A Large proportion of the lost TTG1:KikGR1(red) from trichome neighboring cell was accounted in the trichome initial while gain in other immediate neighbors of the photoconverted cell was uniform and much less than the gain in the trichome initial (Figure 2.14B) (Table 2.2). Considering no directional movement of TTG1 into trichomes (Bouyer *et al*., 2008), it can be postulated that GL3 in the trichome simply traps/sequesters all the TTG1 entering in a trichome cell. On the other hand due to a much reduced level of GL3 in other epidermal cells TTG1:KikGR1(red) is free to move further into the next cell. These observations are consistent with the *GL3* expression and protein accumulation pattern (Zhang *et al*., 2003; Zhao *et al*., 2008).

3.6 Paradoxical phenotype of the *ttg1* weak alleles - Does depletion has a role to play ?

The weak alleles of *ttg1* are not completely glabrous, instead they produce trichomes though reduced in number. Trichomes in these weak alleles are underbranched and form frequent clusters whereas the strong alleles are completely glabrous (Koornneef, 1981; Larkin *et al*., 1994, 1999). This long standing paradoxical phenotype was recently explained with mathematical modeling of the GL3 dependent TTG1 depletion during pattern formation (Bouyer *et al*., 2008). I anal-

ysed these allelic forms of TTG1 with respect to their molecular interaction with GL3. With several experiments it is confirmed in this study that TTG1 is trapped in the nucleus of the high *GL3* expressing cells. Similarly I asked the question how do the weak allelic forms of TTG1 behave in their relation with GL3. Interestingly allelic forms of TTG1 either failed to interact or showed very weak interaction with known bHLH proteins of the TTG1 regulated pathway (*ttg1-10* was not tested) (Figure 2.17). Moreover GL3 failed to trap these allelic forms of TTG1 in the yeast NTT assay (Figure 2.18). It was shown in previous studies by RNA gel blot analysis that *TTG1* expression in these alleles is not affected (Larkin *et al*., 1999; Walker *et al*., 1999). Formation of trichomes in these alleles suggests that the function of the mutant TTG1 protein is not completely abolished. Loss of the *TRY* expression in *ttg1* mutant as the cause of cluster formation in weak *ttg1* alleles is excluded as cluster phenotype in *try* is accompanied with a overbranching phenotype. This is contrary to the reduced branching in weak *ttg1* alleles (Hülskamp *et al*., 1994; Schellmann *et al*., 2002). Therefore with the available results, I hypothesize that loss of strong and stable interaction with GL3/EGL3 results in a loss of TTG1 depletion from the epidermal cells surrounding an emerging trichome. Because of the loss of depletion of TTG1 sufficient amount of the activator (TTG1) in this adjacent cell triggers this cell also to develop into a trichome thereby resulting in cluster formation in the *ttg1* weak alleles. However, only detailed analysis of the cellular distribution of different weak allelic forms of TTG1 will bring a clear picture on the relationship of TTG1 depletion and trichome patterning.

Weak interaction or no interaction of TTG1 with GL3/EGL3 means reduction in the nuclear TTG1 amount as discussed earlier (Figure 2.3 and 2.4). Hence the obvious question comes up whether reduction in the nuclear concentration of TTG1 below certain threshold results in cluster formation. This was tested with two independent approaches.

In the first experiment CFP:GL3, CFP:GL3△78 and CFP:GL3△NLS were expressed

under the *p35S* promoter in the *ttg1*pTTG1::TTG1:YFP line. While the nuclear TTG1:YFP was increased in the lines expressing p35S::CFP:GL3, it was reduced in the lines expressing p35S::CFP:GL3△NLS (Table 2.6). p35S::CFP:GL3△78 lacking the TTG1 interaction domain had no effect on the TTG1:YFP localization consistent with the transient assay in onion epidermal cells (Table 2.6) (Figure 2.8). As expected trichome number was significantly increased in the p35S::CFP:GL3 expressing lines consistent with the previous report by Payne *et al*., (2000) (Table 2.7). It is known that *GL3* overexpression in *ttg1* mutant results in only partial rescue of *ttg1* trichome phenotype (Payne *et al*., 2000). This indicates that although trichomes are formed in *ttg1*p35S::GL3 independent of TTG1 it is less efficient compared to TTG1 dependent trichome formation. Hence CFP:GL3△78 that specifically lacks the TTG1 interaction ability when overexpressed under *p35S* promoter in wild type should participate in this TTG1 independent trichome formation pathway. Because of the partial rescue in p35S::GL3 TTG1 independent pathway the trichome number in wild type plants expressing p35S::CFP:GL3△78 would be expected to be less than the trichome number in the wild type plants expressing p35S::CFP:GL3. However, this was not the case as p35S::CFP:GL3△78 and p35S::CFP:GL3 had same effect on the trichome number and cluster formation when expressed in wild type plants (Table 2.7). I could envisage that the differences in the rescue ability could be seen when CFP:GL3 and CFP:GL3△78 are expressed in *gl3 egl3* double mutant background lacking the trichome regulating bHLH factors instead of wild type plants. It was indeed observed in a reciprocal experiment by Martina Pesch where she observed that the overexpression of GL3△78 in *gl3 egl3* resulted in a trichome phenotype that was reminiscent of *GL3* overexpression in the *ttg1* mutant (Payne *et al*., 2000). Here both, trichome number and morphology was affected. Trichome number was fewer than wild type and were underbranched with bloated appearance. The possibility of absence of EGL3 as the cause of the abnormal trichome development in the *gl3 egl3*p35S::CFP:GL3△78

was excluded as *gl3 egl3*p35S::CFP:GL3 resulted in a significantly higher trichome number with normal morphology. Descrepancy between the behaviour in wild type and *gl3 egl3* can be explained by the fact that GL3△78 only lacks TTG1 interaction domain but can still interact with wild type GL3 (tested by Martina Pesch). Hence it is conceivable that in wild type plants expressing p35S::CFP:GL3△78, CFP:GL3△78 can form a dimer with the endogenous GL3 in the trichome activator complex. Although TTG1 can not interact with GL3△78 it could still bind to GL3 in the GL3-GL3△78 dimer and render its fucntion of stabilizing the activator complex.

Surprisingly cluster frequency was found to be similar in CFP:GL3, CFP:GL3△78 and CFP:GL3△NLS (Table 2.7). This phenotype can be explained by the negative effect of GL3 variants on the mobility of inhibitors. All three GL3 variants GL3, GL3△78 and GL3△NLS are capable of interacting with the inhibitors (Table 2.1). Recent data have shown that *GL3* overexpression indeed has a negative effect on the mobility of inhibitors (Wester *et al*., 2008). These authors demonstrated that inhibitors interfere with the GL3-GL1 dimerization in a hierarchial manner with CPC being most potent followed by ETC1, TRY, ETC3 and ETC2. Finally they demonstrate that higher binding affinity of CPC makes it less mobile in *GL3* overexpressing line. Similar effect with varying degree is expected for the other inhibitors too. In an other theoratical possibility, trapping of TTG1 by GL3 in all the epidermal cells in p35S::GL3 expressing lines drastically reduce the TTG1 mobility should also lead to cluster formation. It could as well be a combination of both, reduction in the mobility of the inhibitors and TTG1 in the epidermal cells by overexpressing *GL3*. But one discrepancy for considering both the reasons as cause of cluster formation lies in the fact that CFP:GL3△78, which does not interact with TTG1 and the CFP:GL3△NLS which is in the cytoplasm show same amount of cluster formation as CFP:GL3 overexpressing lines (Table 2.7). Therefore cluster formation in the lines expressing *GL3* variants can be most probably

explained due to their negative influence on the mobility of the inhibitors. Nevertheless, the cluster phenotype caused by non mobility of inhibitors may simply be epistatic to the phenotype caused due to the non mobility of TTG1 because of the severe effect of the former and subtle effect of the latter phenomenon.

In order to test this with another approach an aptamer 78GL3 was used to effectively interfere with the interaction of GL3 and TTG1. 78GL3 is a 78 amino acid fragment from GL3 that is specific for TTG1 interaction.When p35S::78GL3:GUS is expressed 78GL3:GUS competitively binds to TTG1 thereby reducing the pool of available TTG1 for the formation of TTG1-GL3 complex. Since 78GL3:GUS fusion is cytoplasmic it also partially retains TTG1 in the cytoplasm (Figure 2.10). Qualitative analysis of the subcellular localization of TTG:YFP in *ttg1*pTTG1::TTG1:YFP lines expressing p35S::78GL3:GUS indeed showed that TTG1:YFP was partially shifted to cytoplasm compared to the control line *ttg1-13*pTTG1::TTG1:YFP (Figure 2.23). Although there was a shift of considerable amount of TTG1:YFP to the cytoplasm, no obvious trichome patterning defect was observed. This suggested that partial relocalization of TTG1 to the cytoplasm does not affect the trichome patterning. However, it was interesting to note that although TTG1:YFP was partially trapped in the cytoplasm in the *ttg1*pTTG1::TTG1:YFP lines transformed with p35S::78GL3:GUS TTG1:YFP depletion was not affected suggesting that it is the nuclear fraction of TTG1 that moves between the cells. Possibly because of the depletion process that is going on in these lines no trichome clusters were observed inspite of the fact that nuclear to cytoplasmic ratio of TTG1:YFP is affected due to the cytoplasmic trapping of TTG1:YFP by 78GL3:GUS aptamer.

The other prominant phenotype observed in p35S::CFP:GL3△NLS expressing lines is the underbranched trichome phenotype (Table 2.7). CFP:GL3△NLS is not affected in the dimerization domain therefore the chances that it interacts with GL3 are very high. p35S::CFP:GL3△NLS also interacts with TTG1 (Figure 2.8A). Hence CFP:GL3△NLS could participate in two possibile mechanisms that may

results in the observed trichome phenotype in the lines overexpressing it. In the first possible mechanism CFP:GL3△NLS efficiently or partially retains endogenous GL3 in the cytoplasm. It is known that GL3 controls endoreduplication and trichome branching (Hülskamp *et al*., 1994). Hence due to insufficient nuclear GL3 in the trichome endoreduplication and the branching is affected in the wild type plants expressing p35S::CFP:GL3△NLS. In the second mechanism CFP:GL3△NLS traps TTG1 in the cytoplasm which was confirmed by the quantification of subcellular distribution of TTG1:YFP by CLSM. (Table 2.6). The latter option seems to be true as the aptamer experiment result also support it. The aptamer overexpressing lines where significant amount of TTG1:YFP was shifted to cytoplasm compared to the control line *ttg1-13*pTTG1::TTG1:YFP (Figure 2.23) resulted in underbranched trichome phenotype suggesting that certain threshold levels of TTG1 in the nucleus is necessary for the normal development of trichomes branching.

One possible explanation for the underbranching phenotype is the reduced activity of *MYB23* gene as the *myb23* mutant shows an underbranched phenotype (Kirik *et al*., 2005). Based on the spatial and temporal expression pattern and genetic analysis in different trichome mutants it was proposed that similar to the trichome activator complex TTG1-GL3-GL1, TTG1-GL3 may form a complex together with MYB23 to act as a branch promoting complex (Kirik *et al*., 2005). Moreover, *MYB23* is not expressed in the undifferentiated epidermal cells but is expressed in a trichome specific manner and needs TTG1 for the expression (Kirik *et al*., 2005). TTG1 might regulate the expression of *MYB23* together with GL3/EGL3. Although *MYB23* expression is not affected in *gl3* mutant leaves its expression is completely abolished in roots of *gl3 egl3* double mutant (Kirik *et al*., 2005; Kang *et al*., 2009). So the presence of EGL3 may compensate for the loss of GL3 in the *gl3* mutant leaves for the expression of *MYB23* together with TTG1. These data suggested that TTG1-GL3/EGL3 complex formation is necessary for the *MYB23*

gene expression, which is not possible or is at a reduced rate in *ttg1* weak alleles as these allelic forms of TTG1 either do not interact or show a very weak interaction with GL3 and EGL3 (Figure 2.17). Similarly in *ttg1*pTTG1::TTG1:YFP lines transformed with p35S::CFP:GL3△NLS/p35S::78GL3:GUS a reduction in the nuclear concentration of TTG1:YFP below a certain threshold level may result in adverse effect on the TTG1-GL3/EGL3-MYB23 branch promoting complex thereby resulting in an underbranched phenotype.

Taken together it is conceivable that TTG1 is required in the trichome cells throughout the whole trichome development. At the early stage it is important for the trichome pattern formation by means of GL3 dependent depletion/trapping mechanism (Bouyer *et al*., 2008) and at a later stage it is required for promoting proper trichome branching by forming a TTG1-GL3/EGL3-MYB23 branch promoting complex (Kirik *et al*., 2005). Most of these speculations can be tested only with a non mobile form of TTG1 that does not have severe secondary effects. Attempts to make it immobile by targeting it to the nucleus failed as the nuclear targeted TTG1 protein is completely mobile (Table 2.3).

3.7 Mapping the TTG1 mobility domain

Since the discovery of the maize homeodomain protein KNOTTED1 (KN1) as the first plant protein able to traffic from cell-to-cell several other proteins were reported to function in a non cell-autonomous manner (Kim *et al*., 2003; Perbal *et al*., 1996; Wada *et al*., 2003; Sessions *et al*., 2000; Nakajima *et al*., 2001). Recent studies have focussed also on the identification of specific signal domains in a protein that are necessary for the intercellular trafficking of proteins during developmental processess (Kim *et al*., 2005).

Interestingly plasmodesmata and nuclear pore complex (NPC) exhibit parallel structural and functional features in terms of selective and nonselective macromolecular

trafficking (Lee *et al*., 2000). However, unlike the mechanism of translocation into the nucleus which involves the well characterized signal domains NLS on the cargo proteins, no conserved signal domains in NCAPs has yet been identified (Pemberton *et al*., 1998; Cokol *et al*., 2000; Macara, 2001; Madrid and Weis, 2006; Lucas *et al*., 1995; Aoki *et al*., 2002; Kurata *et al*., 2005; Trutnyeva *et al*., 2005; Sasaki *et al*., 2006). TTG1 has no obvious specific domains others than four WD40 repeat domains that are spread over the entire protein (Walker *et al*., 1999). *AN11* from *Petunia hybrida* an orthologue of *TTG1* rescued *ttg1* trichome phenotype when expressed under the *p35S* promoter (Table 2.8) consistent with the previous report by Payne *et al*., (2000); the information about the promoter was not given though. Interestingly expression under the subepidermal specific *pRBC* promoter hinted at the differences between TTG1 and AN11 as latter failed to rescue trichomes when provided in the subepidermis of the *ttg1* mutant (Table 2.8). Similar observation was made in KNOX class of proteins where homeodomain (HD) trafficking signal is conserved in closely related class I KNOX HD proteins (STM and KNAT1 in *Arabidopsis* and LeT6 in tomato) but not in less closely related class I KNOX proteins such as KNAT2 and KNAT6 or class II HD protein KNAT3 (Kim *et al*., 2005). Similarly a short motif of 20 amino acids on Cm-Hsc70-1 and Cm-Hsc70-2 made these proteins to function as NCAP but had no such effect on the closely related Cm-Hsc70-3 (Aoki *et al*., 2002). Moreover when this motif from Cm-Hsc70-1 was transferred to most closely related human Hsp 70 chaperone, it resulted in the gain of function of intercellular transport ability. However, the same motif when fused to the C-terminus of GFP did not result in conferring the movement ability to GFP. These data suggested that the mobility motifs/domains in certain protein do not function as a simple targeting signals rather they are specific to certain class of proteins (Taoka *et al*., 2007). Therefore in spite of high percentage of homology between TTG1 and AN11, the difference in their mobility property was not surprising. Interestingly TTG1 and AN11 had clear differences in their

N-terminus. Taking advantage of these differences I did a gain of function experiment by swapping non homologous domains within the N-terminus of TTG1 and AN11 and expressing them in the subepidermal tissue (Figure 2.25). AN11 with three small domains swapped from TTG1 could partially rescue trichomes when provided in the subepidermis. On the other hand rescue efficiency of TTG1 with domains swapped from AN11 was reduced when provided in the subepidermis (Table 2.8). Swapping of entire N-terminal 62 amino acids between TTG1 and AN11 led to efficient rescue of trichomes by N-TTG:C-AN11 fusion protein from the subepidermis while N-AN11:C-TTG1 lost its ability to rescue from the subepidermis (Daniel Bouyer, personal communication). Comparing both data I could visualise that TTG1 mobility is partly controlled by the sequences in the swapped domains while other differences in the N-terminus could contribute to the efficient transport of TTG1. Infact in an independent study Daniel Bouyer could efficiently rescue the *ttg1* trichomes by expressing pRBC::AN11 where putative phosphorylation sites were exchanged from TTG1, while the reciprocal experiment did not have major effect (Daniel Bouyer, unpublished data). Kim *et al*., (2005) could show using similar gain of fucntion approach that the homeodomain of KN1 is necessary and sufficient to retain the mobility of the KN1 protein. In this approach they fused different fragments of KN1 to the cell autonomous trichome regulator GL1 and provided it in the meshophyll tissue and observed the rescue of trichome in the *gl1* mutant in contrast to the wild type GL1. It is interesting to note that although AN11 and TTG1 show high degree of similarities they do have fundamnetal differences. AN11 controls only anthocyanin in petals and mutations at this locus do not affect trichomes or anthocyanins in the rest of the plant whereas TTG1 controls multitude of phenotypes in *Arabidopsis* (Koornneef *et al*., 1981; de Vetten *et al*., 1997; Walker *et al*., 1999; Zhang *et al*., 2003; Schiefelbein *et al*., 2003; Haughn and Chaudhary 2005; Baudry *et al*., 2006). Interestingly, AN11 also interacts with GL3 in yeast two-hybrid assay (Figure 2.24A) and similar to TTG1 it is trapped

in the nucleus by GL3 in NTT assay (Figure 2.24D). An *In planta* experiment to study the patterning defects and depletion similar to TTG1 was not possible for AN11 as AN11 showed almost no rescue of the *ttg1* trichome phenotype under the *TTG1* promoter and the *p35S* promoter would not be appropriate for this kind of sensitive experiment. From the evolutionary point of view it is very interesting to note how highly conserved proteins such as WD40 repeat proteins can undergo modifications in order to fulfill additional roles adopted by the species during the course of evolution.

3.8 Isolation of TTG1 transport inhibitor mutants

Microinjection studies in tobacco mesophyll cells suggested that TTG1 in *Arabidopsis* is most likely transported in a regulated manner through PD (Bouyer *et al*., 2008). Based on this it was postulated that *TTG1* expressed in mesophyll cells moves to the epidermis in a regulated manner through PDs and rescues the trichome phenotype of *ttg1* mutant. This regulated transport of TTG1 means that TTG1 is interacting with the PD components to dilate the PD aperture for its transit between the cells. Any defect in the mobility of TTG1 from the subepidermis to the epidermis should result in the loss of trichome initiation in the *ttg1*pRBC::TTG1 background. In the EMS mutagenesis screen the *tti* mutant was isolated as a potential candidate for the mutation in the locus regulating the TTG1 mobility via PD.

The putative *tti* mutant showed defects in differentiation of two types of epidermal cells that depend on the presence of TTG1. Loss of leaf trichomes as well as the loss of mucilage production by the seed epidermal cells suggested that the TTG1 transport from the subepidermis to the epidermis is blocked in leaf as well as in seeds of the *tti* mutant (Figure 2.26A, C). It can be noted that mutations in TTG1 affects all phenotypes controlled by TTG1 and so far no *ttg1* allele, which shows a defect in

only one of the *TTG1* controlled phenotypes is isolated (Koornneef 1982; Larkin *et al*., 1999; Walker *et al*., 2000). Hence proanthocyanidin synthesis that gives brown color to seeds in *tti* mutant indicates that the transgene *TTG1* expressed under the *pRBC* promoter is fully functional (Figure 2.26E). Further F1 from the cross between the *tti* mutant and *ttg1* mutant completely rescued the *ttg1* trichome phenotype and showed a wild type trichome distribution (Figure 2.26J). This shows that mutation in *tti* mutant is recessive because the *tti* mutant phenotype was masked in the heterozygous condition and also further supports that the *TTG1* transgene is fully functional. Complementation experiments with *ttg1*, *gl1* and *gl3* mutants showed that mutation in the *tti* mutant is at a different locus than the *TTG1*, *GL1* and *GL3* loci (Figure 2.26H-J). Furthermore, restriction of YFP specific fluorescence to the subepidermal tissue in *tti*pRBC::TTG1:YFP demonstrates that specific transport of TTG1 from the subepidermis to the epidermis is affected in the *tti* mutant (Figure 2.26O-R). However, it is hard to predict whether this mutation renders the same effect on the mobility of TTG1 through cytoplasmic connections within the same tissue layer because symplasmic connections within the same tissue is different from the connections between the two adjacent tissue layers. The cells within a layer are connected mainly via primary PDs while the two adjacent layers are connected mostly via secondary PDs (Ding, 1998). The likelihood that the PD mutants will result in lethality is very high as a result the understanding about the molecular structure and mechanism of transport through PD is very poor. Indeed several seedling lethal mutants were observed in my screening as well but were not isolated as they died before opening the rosette leaves where the loss of trichome formation was the criteria for the selection of mutant.

Protein-protein interactions seems to play an important role in conferring the specificity in the selective trafficking of NCAPs across the plasmodesmata (Crawford and Zambryski, 2000; Haywood *et al*., 2002; Lucas and Lee, 2004; Zambryski, 2004). Cell-to-cell transport is controlled by modification of PD structure or oc-

clusion by callose. Callose deposition at the neck of PD leads to constriction of PD hence plants deficient in beta-1,3-glucanase enzymes required to degrade callose shows reduced PD SEL (Iglesias and Meins 2000; Levy *et al*., 2007). Benitez-Alfonso *et al*., (2009) showed that *gat1* (GFP arrested trafficking 1) mutants show induction of callose and structural modification of PD thereby reducing the trafficking of GFP between the cells. But unlike *tti* mutants the *gat1* seedlings arrested soon after the germination thereby excluding the possibility of mutation at the same locus in the *tti* mutant (Benitez-Alfonso *et al*., 2009).

Recently, a novel family of eight proteins, called PD-located protein 1 (PDLP1), which span the plasma membrane within PDs have been reported (Thomas *et al*., 2008). These proteins have the features of type I membrane receptor-like proteins and most likely form a part of the signal transduction machinary that perceives external signals to regulate molecular trafficking between cells (Bayer *et al*., 2008). The results so far suggest that the specific transport of TTG1 from subepidermis to epidermis is affected. However, relatively small size of the *tti* mutant plants indicate some general defect as well. Using other mobile proteins as markers it would be nice to know whether the mutant is affected specifically in TTG1 transport or the mobility of proteins in general is affected. Furthermore the question, is the mobility of TTG1 affected within the same tissue will be addressed in future as this is more relevant during the trichome patterning. Physical mapping and cloning of the gene will be done in future and this could be a big step towards the understanding of the mechanism of protein transport in general and in trichome patterning in particular across the PD.

3.9 Model for the GL3 dependent TTG1 depletion during the trichome pattern formation

The observation of the TTG1 depletion led to looking at the trichome patterning from a new perspective. The behaviour of the components of trichome patterning machinary and their corresponding mutant phenotypes could be nicely explained by the activator-inhibitor mechanism. However, different phenotypes of the strong and weak alleles of *ttg1* mutants was a paradox for a long time. The new findings where the TTG1 protein was shown to be depleted in the trichome neighboring cells strongly suggested a role of the activator depletion mechanism during trichome patterning. This mechanism fits well to support the phenotype of the *ttg1* weak allels. In this study I show how mechanistically the TTG1 depletion is taking place. I confirm with several experiments that TTG1 is trapped in high *GL3* expressing cells. TTG1 depletion is completely abolished in the *gl3* mutant strongly suggesting the role of GL3 dependent nuclear trapping of TTG1 for the depletion. In the following model (Figure 3.2) I present schematically the mechanism of GL3 dependent TTG1 depletion during the trichome patterning in *Arabidopsis thaliana.*

All epidermal cells are uniform in the beginning and are equally potent to develop into a trichome. Because *GL3* is uniformly expressed in all epidermal cells of this stage TTG1 protein is also uniformy distributed in these cells. However, a non directional transport of the TTG1 protein is going on between the epidermal cells. Due to small fluctuations in the concentration of the activators because of an postulated (but so far unknown) autocatalytic positive feed back of the activators some cells transit into the trichome pathway. As soon as a cell enters the trichome fate the *GL3* expression in the surrounding cells goes down significantly and its expression in the trichome cell is enhanced. At this stage while in the trichome surrounding cells TTG1 is shuttling in and out of the nucleus, in the trichome

initial TTG1 is sequesterd in the nucleus as a result of strong binding to the GL3. This means that less TTG1 is entering into the immediate neighbor of the trichome as no or very little TTG1 is going out from the trichome initial. On the other hand the cells being second or third neighbor get TTG1 coming from all their neighbors. As a result the immediate neighbor to the trichome has the least amount of TTG1. It is at this stage when the TTG1 depletion is visible.

With the advancement of the trichome development the *GL3* expression in the trichome surrounding cells is almost completely ceased while it continues to be expressed in the trichome thereby leading to GL3 protein accumulation as a result also to the accumulation of TTG1 due to the nuclear trapping by GL3.

Accumulation of TTG1 in the trichome initials results in the formation of a higher concentration of the activator complex and helps in the positive feedback loop of the activators that in turn leads to the increased production of the inhibitors, which diffuse into the neighboring cells. On the other hand the neighboring cells are inhibited from entering into the trichome fate through two processes, the removal of the activator TTG1 as well as due to the increased influx of the inhibitors from the trichome cells.

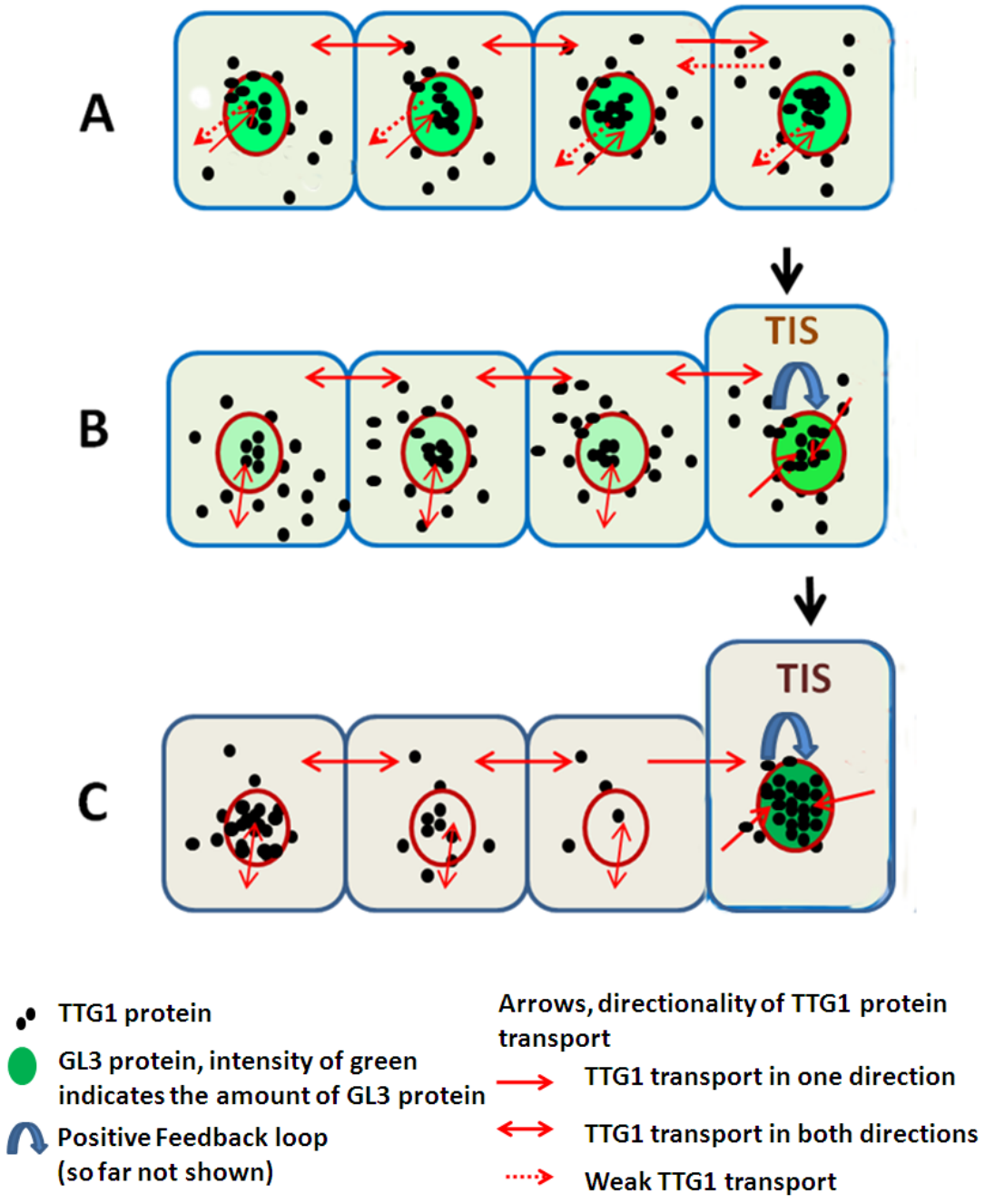

Figure 3.2: Gl3 dependent TTG1 depletion model during trichome pattern formation (A) Epidermal cells with equal potential to develop into a trichome. Here both TTG1 (nuclear and cytoplasmic) and GL3 (nuclear) are uniformly distributed in all cells. (B) Due to an autocatalytic positive feedback of the activators a slight fluctuation in the relative concentration of the activators in the epidermal cells results in a cell entering into trichome pathway (TIS). *GL3* expression goes slightly higher in the TIS but is reduced in the neighboring cells hence TTG1 protein is relatively more free to move in the neighboring cells compared to TIS where it is sequestered in the nucleus by GL3. (C) *GL3* continue to be expressed in the TIS but expression is completely ceased in the neighboring cells. Therefore TTG1 shuttles in and out of the nucleus in the neighboring cells and is also freely transported into the other cells but more and more TTG1 is trapped in the TIS thus creating a gradient of TTG1 concentration around the TIS.

4 Materials and Methods

4.1 Chemicals and antibiotics

All chemicals and antibiotics used were of analytical quality and were obtained from Sigma-Aldrich (Muenchen, Steinheim), Roth (Karlsruhe), Merck (Darmstadt), and Duchefa (Haarlem, Netherlands).

4.2 Enzymes, Kits, Primers and Molecular biological materials

Restriction enzymes were used from MBI-fermentas (St.Leon-Rot), New England Biolabs (Frankfurt/Main) and Roche (Mannheim). Taq polymerase was from MBI-Fermentas (St.Leon-Rot) and Bioline and Phusion high fidelity polymerase was from Finzymes, T4 ligase Invitrogen (Karlsruhe), Kits were supplied from QIAGEN (Hilden), Fermentas (St.Leon-Rot), peqlab (Erlangen), Roche (Mannheim) and Invitrogen (Karlsruhe). All primers were obtained from either Invitrogen (Karlsruhe) or Sigma (Muenchen, Steinheim).

4.3 Bacterial strains and Yeast strains

For standard clonings the *Escherichia coli* (*E.coli*) strain DH5 α was used. For gateway cloning of destination vectors the DB3.1 strains were used which are

resistant to the *ccdB* gene. For plant transformation *Agrobacterium tumefaciens* strains GV3101 were used. The gateway cloning required the usage of a modified strained of GV3101-pMP90RK. Yeast strain *Saccharomyces serevisiae* strain AH109 was used for yeast two-hybrid experiments. Yeast strain EGY48 was used for the nuclear transportation trap (NTT).

4.4 Plant lines

In this study Landsberg *erecta* (L*er*), Columbia (Col), Wassilewskaja (WS-O) and RLD ecotypes were used. The mutant alleles *ttg1-1* is in L*er* (Koornneef 1981), *ttg1-9*, *ttg1-10*, *ttg1-11* and *ttg1-12* in Col (Larkin*et al*.,1994a; 1994b; 1999), *ttg1-13* in RLD (Walker *et al*., 1999). *gl1-1*, *gl3-1* and *gl3-1 egl3-1* double and *gl3-1 egl3-1 tt8-1* -1tripple mutant are in L*er* (Oppenheimer *et al*., 1991; Hülskamp *et al*., 1994; Zhang*et al*., 2003), *gl3-1 ttg1-1*.

4.5 Vectors, Constructs and Transgenic lines

Table 4.1: List of basic vectors used in this study

Vector	Company	Application
pBluescript (pBSK)	Stratagene	Standard clonings and PCR-product clonings
pENTR1a(pEN1a)	Invitrogen	Used as a donor in gateway based clonings.
pAMPAT	GenBank accession AY027531	Binary gateway target vector containing a CaMV 35S promoter cassette and BASTA resistance

Table 4.2: List of pENTRY/donor vectors used in gateway cloning

Construct	Vector	Created by
TTG1	pEN1a	Daniel Bouyer
TTG:YFP	pEN1a	Daniel Bouyer
AN11	pEN1a	Rachappa S.B/Daniel Bouyer
AN11:YFP	pEN1a	Rachappa S.B
78GL3:GUS	pEN1a	Rachappa S.B
GUS	pEN1a	Rachappa S.B
TTG1:YFP(Swap)	pEN1a	Rachappa S.B
AN11:YFP(Swap)	pEN1a	Rachappa S.B
TTG1△C26:YFP	pEN1a	Rachappa S.B
TTG1(S282F):YFP	pEN1a	Rachappa S.B
TTG1(G43R):YFP	pEN1a	Rachappa S.B
TTG1(G149R):YFP	pEN1a	Rachappa S.B
CFP:GL3	pEN1a	Rachappa S.B
CFP:GL3△78	pEN1a	Rachappa S.B
CFP:GL3△NLS	pEN1a	Rachappa S.B
NLS:TTG1:YFP	pEN1a	Rachappa S.B
NLS:TTG1:YFP	pEN1a	Rachappa S.B

Table 4.3: List of yeast vectors/constructs used in this study

Construct	**Vector**	**Created by**
-	pc-ACT2	Invitrogen
-	pAS2	Invitrogen
AD:GL3	pc-ACT2	Rachappa S.B
AD:GL3△78	pc-ACT2	Rachappa S.B
AD:GL3△NLS	pc-ACT2	Rachappa S.B
AD:CFP:GL3	pc-ACT2	Rachappa S.B

Construct	Vector	Created by
AD:CFP:GL3△78	pc-ACT2	Rachappa S.B
AD:CFP:GL3△NLS	pc-ACT2	Rachappa S.B
AD:EGL3	pc-ACT2	Martina Pesch
AD:TT8	pc-ACT2	Martina Pesch
AD:78GL3:GUS	pc-ACT2	Rachappa S.B
AD:41GL3:GUS	pc-ACT2	Rachappa S.B
AD:GUS	pc-ACT2	Rachappa S.B
BD:78GL3:GUS	pAS2	Rachappa S.B
BD:41GL3:GUS	pAS2	Rachappa S.B
BD:TTG1	pAS2	Martina Pesch
BD:TTG1△C26	pAS2	Rachappa S.B
BD:TTG1(S282F)	pAS2	Rachappa S.B
BD:TTG1(G43R)	pAS2	Rachappa S.B
BD:TTG1(G149R)	pAS2	Rachappa S.B
BD:AN11	pAS2	Rachappa S.B
NES:LexAD	pNH2	Ueki *et al*., 1998
NES:LexAD:NLS	pNH3	Ueki *et al*., 1998
NES:LexAD with modified MCS	modified pNH2	Ueki *et al*., 1998
NES:LexAD:TTG1	pNS	Rachappa S.B
NES:LexAD:TTG1△C26	pNS	Rachappa S.B
NES:LexAD:TTG1(S282F)	pNS	Rachappa S.B
NES:LexAD:TTG1(G43R)	pNS	Rachappa S.B
NES:LexAD:TTG1(G149R)	pNS	Rachappa S.B
NES:LexAD:AN11	pNS	Rachappa S.B
NES:LexAD:GL3	pNS	Rachappa S.B
NES:LexAD:GL3△78	pNS	Rachappa S.B
NES:LexAD:AN14	pNS	Rachappa S.B

Construct	Vector	Created by
NES:LexAD:AN15	pNS	Rachappa S.B
pVTU	pVTU	Joahim Uhrig
GL3	pVTU	Rachappa S.B
GL3△78	pVTU	Rachappa S.B

Table 4.4: List of destination vectors/constructs used in this study

Construct	Vector	Created by
p35S::pAMPAT-GW	pAMPAT	Genebank Accession AY027531
pRBC::pAM PAT-GW	pAM PAT	Daniel Bouyer
pTTG1::pAM PAT-GW	pAM PAT	Daniel Bouyer
pTTG1::TTG1:YFP	pAMPAT	Rachappa S.B/Daniel Bouyer
pRBC::TTG1:YFP	pAMPAT	Rachappa S.B
p35S::TTG1:YFP	pAMPAT	Rachappa S.B
pTTG1::TTG1	pAMPAT	Rachappa S.B
pRBC::TTG1	pAMPAT	Rachappa S.B
p35S::TTG1	pAMPAT	Rachappa S.B
pTTG1::AN11:YFP	pAMPAT	Rachappa S.B
pRBC::AN11:YFP	pAMPAT	Rachappa S.B
p35S::AN11:YFP	pAMPAT	Rachappa S.B
pTTG1::AN11	pAMPAT	Rachappa S.B
pRBC::AN11	pAMPAT	Rachappa S.B
p35S::AN11	pAMPAT	Rachappa S.B
p35S::CFP:GL3	pAMPAT	Rachappa S.B
p35S::CFP:GL3△78	pAMPAT	Rachappa S.B
p35S::CFP:GL3△NLS	pAMPAT	Rachappa S.B
p35S::CFP:GL3	pMDC32	Rachappa S.B
p35S::CFP:GL3△78	pMDC32	Rachappa S.B

Construct	Vector	Created by
p35S::CFP:GL3△NLS	pMDC32	Rachappa S.B
pTTG1::TTG1△C26:YFP	pAMPAT	Rachappa S.B
p35S::TTG1△C26:YFP	pAMPAT	Rachappa S.B
pTTG1::TTG1(S282F):YFP	pAMPAT	Rachappa S.B
p35S::TTG1(S282F):YFP	pAMPAT	Rachappa S.B
pTTG1::TTG1(G43R):YFP	pAMPAT	Rachappa S.B
p35S::TTG1(G43R):YFP	pAMPAT	Rachappa S.B
pTTG1::TTG1(G149R):YFP	pAMPAT	Rachappa S.B
p35S::TTG1(G149R):YFP	pAMPAT	Rachappa S.B
pTTG1::TTG1:KikGR1	pAMPAT	Rachappa S.B
p35S::78GL3:GUS	pGWB2	Rachappa S.B
p35S::mRFP	pBattL	Andrea Schrader
p35S::RFP:78GL3:GUS	pBattL	Rachappa S.B
p35S::RFP:GUS	pBattL	Rachappa S.B
pTTG1::NLS:TTG1:YFP	pAMPAT	Rachappa S.B
pRBC::NLS:TTG1:YFP	pAMPAT	Rachappa S.B

Table 4.5: List of transgenic plants used in this study

Transgenic line	Selection	Generated by
*ttg1-1*p35S::TTG1	BASTA	Rachappa S.B
*ttg1-1*p35S::TTG1:YFP	BASTA	Rachappa S.B
*ttg1-9*p35S::TTG1	BASTA	Rachappa S.B
*ttg1-9*p35S::TTG1:YFP	BASTA	Rachappa S.B
*ttg1-10*p35S::TTG1	BASTA	Rachappa S.B
*ttg1-10*p35S::TTG1:YFP	BASTA	Rachappa S.B
*ttg1-11*p35S::TTG1	BASTA	Rachappa S.B
*ttg1-11*p35S::TTG1:YFP	BASTA	Rachappa S.B

Transgenic line	**Selection**	**Generated by**
*ttg1-12*p35S::TTG1	BASTA	Rachappa S.B
*ttg1-12*p35S::TTG1:YFP	BASTA	Rachappa S.B
*ttg1-13*p35S::TTG1	BASTA	Rachappa S.B
*ttg1-13*p35S::TTG1:YFP	BASTA	Rachappa S.B
*ttg1-12*pTTG1::TTG1:YFP	BASTA	Rachappa S.B
*ttg1-12*pTTG1::TTG1△C26:YFP	BASTA	Rachappa S.B
*Col*p35S::TTG1:YFP	BASTA	Rachappa S.B
*Col*p35S::TTG1△C26:YFP	BASTA	Rachappa S.B
*Col*p35S::TTG1(S282F):YFP	BASTA	Rachappa S.B
*Col*p35S::TTG1(G43R):YFP	BASTA	Rachappa S.B
*Col*p35S::TTG1(G149R):YFP	BASTA	Rachappa S.B
*gl3 egl3*pTTG1::TTG1:YFP	BASTA	Rachappa S.B
*gl3 egl3 tt8*pTTG1::TTG1:YFP	BASTA	Rachappa S.B
*ttg1-13*pTTG1::TTG1:YFPp35S::CFP:GL3	BASTA+HygR	Rachappa S.B
*ttg1-13*pTTG1::TTG1:YFPp35S::CFP:GL3△78	BASTA+HygR	Rachappa S.B
*ttg1-13*pTTG1::TTG1:YFPp35S::CFP:GL3△NLS	BASTA+HygR	Rachappa S.B
*ttg1-13*pTTG1::TTG1:YFPp35S::78GL3:GUS	BASTA+KanR	Rachappa S.B
*ttg1 gl3*pRBC::TTG1:YFPpRBC::GFP:GL3	BASTA	Rachappa S.B
*ttg1 gl3*pRBC::TTG1:YFPpAtML1::GFP:GL3	BASTA	Rachappa S.B
*ttg1-13*pTTG1::TTG1:KikGR1	BASTA	Rachappa S.B
*ttg1-13*pTTG1::NLS:TTG1:YFP	BASTA	Rachappa S.B
*ttg1-13*pRBC::NLS:TTG1:YFP	BASTA	Rachappa S.B
*ttg1-1*pRBC::TTG1:YFP	BASTA	Daniel Bouyer
*ttg1 gl3*pRBC::TTG1:YFP	BASTA	Daniel Bouyer
*ttg1 gl3*pRBC::GFP:GL3	BASTA	Daniel Bouyer
*ttg1 gl3*pAtML1::GFP:GL3	BASTA	Daniel Bouyer
*ttg1-13*pTTG1::TTG1:YFP	BASTA	Daniel Bouyer

Transgenic line	Selection	Generated by
*gl3*pTTG1::TTG1:YFP	BASTA	Daniel Bouyer
p35S::GL3pTTG1::TTG1:YFP	BASTA	Daniel Bouyer
*gl3.2*pGL3::GL3:YFP	KanR	Bernhardt *et al*., 2005

4.6 Creation of pENTRY vectors

pEN1a:TTG1:YFP was described in Bouyer *et.al*., (2008). pEN1a:TTG1△C26:YFP, pEN1a:TTG1(S282F):YFP, pEN1a:TTG1(G43R):YFP and pEN1a:TTG1(G149R):YFP were created by inverse PCR using specific primers with mutations or primers flanking the deletion regions with pEN1a:TTG1:YFP as a template. Similarly, these TTG1 versions without YFP fusion were created with the same primers using pEN1a:TTG1 as a template. NLS versions of the pEN1a:TTG1:YFP and TTG1 mutant versions were created using respective pENTRY vectors as PCR template. Here TTG1 forward primer with NLS attachment on to 5' of the primer and reverse primer within vector backbone at position (-1) with respect to TTG1 start codon in pEN1a:TTG1:YFP were used. pEN1a:AN11:YFP was created by replacing the TTG1 in pEN1a:TTG1:YFP.

To create pEN1a:TTG1:KikGR1, KikGR1 (Accession No.AB193293) was amplified from the pKikGR1-MN1 (MBL) with forward and reverse primers attached with SalI and XhoI restriction sites respectively. This PCR product was cloned in pBSK and was sequenced. Then SalI/XhoI fragment from pBS:SalI-KikGR1-XhoI was cloned in pEN1a digested with same enzymes. TTG1 was amplified from pEN1a:TTG1 and was fused 5'to KikGR1 at XmnI site as a blunt end ligation. pEN1a:TTG1:KikGR1 was then used as a template for PCR with KikGR1 forward and TTG1 reverse primer without STOP codon. TTG1 reverse primer without STOP codon was also

attached with a linker which was also used in pEN1a:TTG1:YFP.

To create pEN1a:CFP:GL3, full length GL3 cDNA was amplified by PCR using pGMT:GL3 as a template with forward and reverse primers having SalI as 5'attachment on both the primers. The PCR product was cloned in pBSK vector to get pBSK:GL3. SalI fragment was then cloned into pEN1a at SalI/XhoI site. CFP was then cloned at the XmnI site 5' to GL3 cDNA to create pEN1a:CFP:GL3. pEN1a:CFP:GL3△78 and pEN1a:CFP:GL3△NLS were created by deletion PCR using pEN1a:CFP:GL3 as a template and primers flanking the deletion region. Internal 78 aa fragment (aa360-437) and 41aa fragment (aa360-400) from GL3 were amplified by PCR and cloned as a fusion to 5'GUS at NcoI restriction site in pEN:GUS (Invitrogen) to get pEN:78GL3:GUS and pEN:41GL3:GUS respectively. The constructed created by PCR were sequenced.

4.7 Creation destination vectors

All destination vectors for plant expression and yeast studies were created by gateway LR reaction system as described by the user's manual (Invitrogen).

4.8 Yeast two-hybrid

Saccharomyces cerevisiae strain AH109 was used for the yeast two-hybrid assay. Yeast transformation was performed as described before (Gietz and Schiestl, 1995). pCACT2/pACT2 and pAS2/pCD2 plasmids (Clontech) were used for the fusion with GAL4 activation domain and GAL4 DNA binding domain respectively. GL3, GL3△78, GL3△NLS, GUS and 78GL3:GUS were fused to activation domain and TTG1, TTG1△C26, TTG1(S282F), TTG1(G43R), TTG1(G149R), AN11 and 78GL3:GUS were fused to DNA binding domain by the gateway LR reaction system as described by the user's manual (Invitrogen). Yeast was grown on synthetic

media lacking leucine and tryptophan for the selection of transformed yeast. For the positive interaction analysis the transformed yeast was plated on the synthetic yeast media lacking leucine, tryptophan and histidine supplemented with 5mM 3-amino-1, 2, 4-triazole (3AT). All the constructs fused to DNA binding domain were tested for the auto-activation by transforming them in yeast and selecting on medium lacking tryptophan and histidine supplemented with 5mM 3AT. None of the constructs showed any auto-activation.

4.9 Nuclear Transportation Trap (NTT) assay (Modified from Ueki *et al*., 1998)

Plasmid vectors pNH2, pNH3 that carry the expression cassette NES:LexAD and NES:LexAD:NLS respectively and plasmid pNS (modified pNH2) have been described Ueki *et.al*., (1998). pNS:NES:LexAD:TTG1 and pNS:NES:LexAD:TTG1△C26 were constructed by cloning the salI/XhoI fragments of TTG1/TTG1 △C26 into the SalI site within the MCS in pNS. pNS:NES:LexAD:GL3 and pNS:NES:LexAD:GL3 △78were constructed by cloning salI GL3 and GL3△78 inserts into the SalI site in pNS. SalI/EclI36I and SalI/PvuII fragments of GL3 and GL3 △78 respectively were cloned at the XhoI/PvuII digested pVTU vector to get pVTU:GL3 and pVTU:GL3△78. Transformation was performed as described by (Gietz and Schiestl, 1995) using the yeast strain EGY48 (Clontech). Plasmids vectors carrying the expression cassettes NES:LexAD [pNH2] as a negative control, NES:LexAD:NLS [pNH3] as a positive control, NES:LexAD:TTG1 [pNS:TTG1], NES:LexAD:TTG1△C26 [pNS:TTG1△C26], NES:LexAD:GL3 [pNS:GL3], NES:LexAD:GL3△78 [pNS:GL3△78], NES:LexAD:-TTG1(S282F) [pNS:TTG1(S282F)], NES:LexAD:TTG1(G43R) [pNS:TTG1(G43R)], NES:LexAD:TTG1(G149R) [pNS:TTG1(G149R)] and NES:LexAD:AN11 [pNS:AN11] were transformed individually and were grown on synthetic dropout media lacking

leucine and histdine for 4-7 days at 30 ^{0}C to detect the expression of *LEUCINE2* (*LEU2*) reporter gene expression for the transport of fusion protein into the nucleus. Similarly to study the influence of GL3 on the nuclear transport of protein of interest the vector carrying the gene of interest in pNS vector was co-transformed with either GL3 or GL3△78 cloned in pVTU vector. In co-transformation assay yeast was selected on synthetic dropout media lacking histidine (pNS vector selection), uracil (pVTU vector selection) and leucine (selection for nuclear transport).

4.10 Microscopy and quantification of YFP Fluorescence

Fluorescent pictures were made using the Leica TCS-SP2 confocal microscope equipped with the LCS software. Images were made using 40x water immersion objectives. The Z-stack images were obtained and were then merged to one plane. Raw images were used for quantifying the YFP fluorescence using the histogram quantification software of the LCS software. Young rosette leaves were stained with 5µg/ml of propidium iodide (PI) for 1-2 minutes to mark the cell walls. Fluorescent pictures in the onion epidermal cells in the transient assay experiment were captured using the LEICA-DMRE microscope equipped with a high-resolution KY-F70 3-CCD JVC camera and DISKUS software. Images were processed with Adobe Photoshop CS2.

4.11 Transient expression

A. Particle bombardment in onion epidermal cells

Biolistic PDS -1000/ He system (Bio- Rad) was used for the transient expression studies. Gold particles (1.0 µm) were coated with 300ng of each DNA and were co-bombarded in the onion epidermal cells with 900-psi rupture discs under a vacuum

of 26 inches of Hg. Fluorescence was analysed 12-15 hours after the bombardment.

B. Agro-infiltration in tobacco leaves

For localization studies of TTG1 allelic forms they were fused N-terminal to YFP and cloned under *p35S* promoter in pAMPAT binary vector. The constructs were infiltrated into *Nicotiana benthamiana* plants. *Agrobacterium tumefaciens* strain GV3101-pMP90RK was grown to mid exponential phase, centrifuged and resuspended to an OD600 of 0.8 with the infiltration medium (10 mM MES, pH 5.6, 10 mM MgCl2, 200 mM acetosyringone). YFP fluorescence was detectable 3-5 days after infiltration. Intracellular localization was analyzed using Leica SP2 confocal laser scanning microscope.

4.12 Plant growth conditions

Seeds were sown on humid freshly prepared *Arabidopsis* culture soil, covered with a plastic lid and stored for three to seven days at 4^0C. Plants were grown at constant 16hours light and 8hours dark condition at constant temperatures of either 18^0C or 23^0C and the lid was removed after three to four days.

4.13 Crossing of plants

Using fine-tweezers the anthers of flowers at a stage when the petals grew out of the sepals were removed. All remaining older and younger flowers were removed and the prepared flower was fixed on a wooden stick. After two days the stigma of the carpels were pollinated.

4.14 Plant transformation

Plants were transformed according to the "floral dip" method (Clough and Bent 1998). To gain strong plants, these were allowed to grow at 18^0C and till the first flowers appeared at stalks of approximately 10 cm in length. Four days before plant transformation a 5 ml preculture in YEB medium of the Agrobacterial clone was incubated for two days at 28^0C and 1 ml of this preculture was used to inoculate the final 200 ml culture. This culture was incubated again for two days at 28^0C and afterwards precipitated at 6800 rpm for 10 minutes. The pellet was resuspended in a 5% Sucrose solution containing 0.05% silwett L-77. Plants were dipped for approximately 15-20 seconds and afterwards covered with a lid. The lid was removed after two days and after that plants were treated as usual.

4.15 Seed sterilisation

Before placing seeds on MS-agar-plates (1% Murashige-Skoog salts, 1% sucrose, 0.7% agaragar, pH5.7, eventually with kanamycin (50 µg/ml) or hygromycin (25µg/ml)) they were incubated for five minutes in 95% Ethanol (Rotisol) and afterwards incubated for 15 minutes in a 3% NaOCl solution containing 0.1% triton X-100. Seeds were then washed two to three times with sterile water

4.16 Seed coat mucilage staining

Mucilage synthesis by seed epidermal cells was studied by staining with ruthenium red. Seeds were imbibed with water by placing them on wet filter papers for about 10-15 minutes. Then the seeds were immersed in 0.01% ruthenium red solution directly on the filter paper to see the pink layer around the seeds. (Western *et al*., 2000)

Bibliography

Aoki, K., Kragler, F., Xoconostle-Czares, B. & Lucas, W. J. (2002), 'A subclass of plant heat shock cognate 70 chaperones carries a motif that facilitates trafficking through plasmodesmata', *Proceedings of the National Academy of Sciences* **99**(25), 16342–16347.

Bai, Y., Falk, S., Schnittger, A., Jakoby, M. J. & Hülskamp, M. (2009), 'Tissue layer specific regulation of leaf length and width in *Arabidopsis* as revealed by the cell autonomous action of ANGUSTIFOLIA', *The Plant Journal* **61**(2), 191–199.

Baudry, A., Caboche, M. & Lepiniec, L. (2006), '*TT8* controls its own expression in a feedback regulation involving TTG1 and homologous MYB and bHLH factors, allowing a strong and cell-specific accumulation of flavonoids in *Arabidopsis thaliana*', *The Plant Journal* **46**(5), 768–779.

Baudry, A., Heim, M. A., Dubreucq, B., Caboche, M., Weisshaar, B. & Lepiniec, L. (2004), 'TT2, TT8, and TTG1 synergistically specify the expression of *BANYULS* and proanthocyanidin biosynthesis in *Arabidopsis thaliana*', *The Plant Journal* **39**(3), 366–380.

Bayer, E., Thomas, C. L. & Maule, A. J. (2004), 'Plasmodesmata in *Arabidopsis thaliana* suspension cells', *Protoplasma* **223**(2-4), 93–102.

Bayer, E., Thomas, C. L. & Maule, A. J. (2008), 'Symplastic domains in the *Arabidopsis* shoot apical meristem correlate with *PDLP1* expression patterns', *Plant Signaling and Behaviour* **3**(10), 853–855.

Benitez-Alfonso, Y., Cilia, M., Roman, A. S., Thomas, C., Maule, A., Hearn, S. & Jackson, D. (2009), 'Control of *Arabidopsis* meristem development by thioredoxin-dependent regulation of intercellular transport', *Proceedings of the National Academy of Sciences* **106**(9), 3615–3620.

Benitez, M., Espinosa-Soto, C., Padilla-Longoria, P. & Alvarez-Buylla, E. R. (2008), 'Interlinked nonlinear subnetworks underlie the formation of robust cellular patterns in *Arabidopsis* epidermis: a dynamic spatial model', *BMC Systems Biology* **2**(1), 98.

Berger, F., Haseloff, J., Schiefelbein, J. & Dolan, L. (1998), 'Positional information in root epidermis is defined during embryogenesis and acts in domains with strict boundaries', *Current Biology* **8**(8), 421–430.

Bernhardt, C., Lee, M. M., Gonzalez, A., Zhang, F., Lloyd, A. & Schiefelbein, J. (2003), 'The bHLH genes *GLABRA3 (GL3)* and *ENHANCER OF GLABRA3 (EGL3)* specify epidermal cell fate in the *Arabidopsis* root', *Development* **130**(26), 6431–6439.

Bernhardt, C., Zhao, M., Gonzalez, A., Lloyd, A. & Schiefelbein, J. (2005), 'The bHLH genes *GL3* and *EGL3* participate in an intercellular regulatory circuit that controls cell patterning in the *Arabidopsis* root epidermis', *Development* **132**(2), 291–298.

Bouyer, D. (2004), 'Analysis of trichome differentiation in *Arabidopsis thaliana*: From cell fate initiation to cell death', *Ph.D Thesis* .

Bouyer, D., Geier, F., Kragler, F., Schnittger, A., Pesch, M., Wester, K., Balkunde, R., Timmer, J., Fleck, C. & Hülskamp, M. (2008), 'Two-Dimensional patterning by a Trapping/Depletion mechanism: The role of TTG1 and GL3 in *Arabidopsis* trichome formation', *PLoS Biology* **6**(6), e141.

Caro, E., Castellano, M. M. & Gutierrez, C. (2007), 'A chromatin link that couples cell division to root epidermis patterning in *Arabidopsis*', *Nature* **447**(10), 213–217.

Chytilova, E., Macas, J., Sliwinska, E., Rafelski, S. M., Lambert, G. M. & Galbraith, D. W. (2000), 'Nuclear dynamics in *Arabidopsis thaliana*', *Molecular Biology of the Cell* **11**(8), 2733–2741.

Clough, S. J. & Bent., A. F. (1998), 'Floral dip: a simplified method for *Agrobacterium* -mediated transformation of *Arabidopsis thaliana*', *The Plant Journal* **16**(6), 735–743.

Cokol, M., Nair, R. & Rost, B. (2000), 'Finding nuclear localization signals', *EMBO Reports* **1**(5), 411–415.

Crawford, K. M. & Zambryski, P. C. (2000), 'Subcellular localization determines the availability of non-targeted proteins to plasmodesmatal transport', *Current Biology* **10**(17), 1032–1040.

Crawford, K. M. & Zambryski, P. C. (2001), 'Non-targeted and targeted protein movement through plasmodesmata in leaves in different developmental and physiological states', *Plant physiology* **125**(4), 1802–1812.

Cristina, M. D., Sessa, G., Dolan, L., Linstead, P., Baima, S., Ruberti, I. & Morelli1, G. (1996), 'The *Arabidopsis* athb-10 (glabra2) is an hd-zip protein required for regulation of root hair development.', *Plant Journal* **10**(3), 393–402.

Cui, H., Levesque, M. P., Vernoux, T., Jung, J. W., Paquette, A. J., Gallagher, K. L., Wang, J. Y., Blilou, I., Scheres, B. & Benfey, P. N. (2007), 'An evolutionarily conserved mechanism delimiting SHR movement defines a single layer of endodermis in plants', *Science* **316**(5823), 421–425.

de Vetten, N., Quattrocchio, F., Mol, J. & Koes, R. (1997), 'The *an11* locus controlling flower pigmentation in *Petunia* encodes a novel WD-repeat protein conserved in yeast, plants, and animals.', *Genes & Development* **11**(11), 1422–1434.

Debeaujon, I., Nesi, N., Perez, P., Devic, M., Grandjean, O., Caboche, M. & Lepiniec, L. (2003), 'Proanthocyanidin-accumulating cells in *Arabidopsis* testa: regulation of differentiation and role in seed development', *The Plant Cell* **15**(11), 2514–2531.

Digiuni, S. (2008), 'Trichome patterning in *Arabidopsis*: Role of activators and inhibitors', *Ph.D Thesis* .

Digiuni, S., Schellmann, S., Geier, F., Greese, B., Pesch, M., Wester, K., Dartan, B., Mach, V., Srinivas, B. P., Timmer, J., Fleck, C. & Hülskamp, M. (2008), 'A competitive complex formation mechanism underlies trichome patterning on *Arabidopsis* leaves', *Molecular Systems Biology* **4**.

Ding, B. (1998), 'Intercellular protein trafficking through plasmodesmata', *Plant molecular biology* **38**(1), 279–310.

Ding, B., Haudenshield, J. S., Hull, R. J., Wolf, S., Beachy, R. N. & Lucas, W. J. (1992), 'Secondary plasmodesmata are specific sites of localization of the tobacco mosaic virus movement protein in transgenic tobacco plants', *The Plant Cell* **4**(8), 915–928.

Dolan, L., Duckett, C. M., Grierson, C., Linstead, P., Schneider, K., Lawson, E., Dean, C., Poethig, S. & Roberts, K. (1994), 'Clonal relationships and cell patterning in the root epidermis of *Arabidopsis*.', *Development* **120**, 2465–2474.

Egea-Cortines, M., Saedler, H. & Sommer, H. (1999), 'Ternary complex formation between the MADS-box proteins SQUAMOSA, DEFICIENS and GLOBOSA is involved in the control of floral architecture in *Antirrhinum majus*', *The EMBO Journal* **18**(19), 5370–5379.

Esch, J. J., Chen, M., Sanders, M., Hillestad, M., Ndkium, S., Idelkope, B., Neizer, J. & Marks, M. D. (2003), 'A contradictory *GLABRA3* allele helps define gene interactions controlling trichome development in *Arabidopsis*', *Development* **130**(24), 5885–5895.

Feller, A. (2006), 'An ACT-like domain participates in the dimerization of several plant basic-helix-loop-helix transcription factors', *Journal of Biological Chemistry* **281**(39), 28964–28974.

Gallagher, K. L. & Benfey, P. N. (2005), 'Not just another hole in the wall: understanding intercellular protein trafficking', *Genes & Development* **19**(2), 189–195.

Gallagher, K. L. & Benfey, P. N. (2009), 'Both the conserved GRAS domain and nuclear localization are required for SHORT-ROOT movement', *The Plant Journal* **57**(5), 785–797.

Gallagher, K. L., Paquette, A. J., Nakajima, K. & Benfey, P. N. (2004), 'Mechanisms regulating SHORT-ROOT intercellular movement', *Current Biology* **14**(20), 1847–1851.

Galway, M. E., Masucci, J. D., Lloyd, A. M., Walbot, V., Davis, R. W. & Schiefelbein, J. W. (1994), 'The *TTG* gene is required to specify epidermal cell fate and cell patterning in the *Arabidopsis* root.', *Developmental Biology* **166**(2), 740–754.

Gao, Y., Gong, X., Cao, W., Zhao, J., Fu, L., Wang, X., Schumaker, K. S. & Guo, Y. (2008), '*SAD2* in *Arabidopsis* functions in trichome initiation through mediating GL3 function and regulating *GL1*, *TTG1* and *GL2* expression', *Journal of Integrative Plant Biology* **50**(7), 906–917.

Gonzalez, A., Mendenhall, J., Huo, Y. & Lloyd, A. (2009), 'TTG1 complex MYBs, MYB5 and TT2, control outer seed coat differentiation', *Developmental biology* **325**(2), 412–421.

Gonzalez, A., Zhao, M., Leavitt, J. M. & Lloyd, A. M. (2008), 'Regulation of the anthocyanin biosynthetic pathway by the TTG1/bHLH/Myb transcriptional complex in *Arabidopsis* seedlings', *The Plant Journal* **53**(5), 814–827.

Haughn, G. & Chaudhury, A. (2005), 'Genetic analysis of seed coat development in *Arabidopsis*', *Trends in Plant Science* **10**(10), 472–477.

Haywood, V., Kragler, F. & Lucas, W. J. (2002), 'Plasmodesmata: pathways for protein and ribonucleoprotein signaling', *The Plant Cell* **14**, S303–S325.

Honma, T. & Goto, K. (2001), 'Complexes of mads-box proteins are suficient to convert leaves into floral organs', *Nature* **409**, 525–529.

Hung, C. Y., Lin, Y., Zhang, M., Pollock, S., Marks, M. D. & Schiefelbein, J. (1998), 'A common position-dependent mechanism controls cell-type patterning and *GLABRA2* regulation in the root and hypocotyl epidermis of *Arabidopsis*', *Plant physiology* **117**(1), 73–84.

Iglesias, V. A. & Jr, F. M. (2000), 'Movement of plant viruses is delayed in a beta-1, 3-glucanase-deficient mutant showing a reduced plasmodesmatal size exclusion limit and enhanced callose deposition', *The Plant Journal* **21**(2), 157–166.

Ishida, T., Hattori, S., Sano, R., Inoue, K., Shirano, Y., Hayashi, H., Shibata, D., Sato, S., Kato, T., Tabata, S., Tabata, S., Okada, K. & Wada, T. (2007a), '*Arabidopsis TRANSPARENT TESTA GLABRA2* is directly regulated by R2R3 MYB transcription factors and is involved in regulation of *GLABRA2* transcription in epidermal differentiation', *The Plant Cell* **19**(8), 2531–2543.

Ishida, T., Kurata, T., Okada, K. & Wada, T. (2007b), 'A genetic regulatory network in the development of trichomes and root hairs', *Annual Review of Plant Biology* **59**, 365–386.

Johnson, C. S., Kolevski, B. & Smyth, D. R. (2002), '*TRANSPARENT TESTA GLABRA2,* a trichome and seed coat development gene of *Arabidopsis*, encodes a WRKY transcription factor', *The Plant Cell* **14**(6), 1359–1375.

Kang, Y. H., Kirik, V., Hülskamp, M., Nam, K. H., Hagely, K., Lee, M. M. & Schiefelbein, J. (2009), 'The *MYB23* gene provides a positive feedback loop for cell fate specification in the *Arabidopsis* root epidermis', *The Plant Cell* **21**(4), 1080–1094.

Kim, I., Cho, E., Crawford, K., Hempel, F. D. & Zambryski, P. C. (2005), 'Cell-to-cell movement of GFP during embryogenesis and early seedling development in *Arabidopsis*', *Proceedings of the National Academy of Sciences* **102**(6), 2227–2231.

Kim, I., Kobayashi, K., Cho, E. & Zambryski, P. C. (2005), 'Subdomains for transport via plasmodesmata corresponding to the apical-basal axis are established during *Arabidopsis* embryogenesis', *Proceedings of the National Academy of Sciences of the United States of America* **102**(33), 11945–11950.

Kim, J., Rim, Y., Wang, J. & Jackson, D. (2005), 'A novel cell-to-cell trafficking assay indicates that the KNOX homeodomain is necessary and sufficient for intercellular protein and mRNA trafficking', *Genes & Development* **19**(7), 788–793.

Kim, J. Y., Yuan, Z., Cilia, M., Khalfan-Jagani, Z. & Jackson, D. (2002), 'Intercellular trafficking of a KNOTTED1 green fluorescent protein fusion in the leaf and shoot meristem of *Arabidopsis*', *Proceedings of the National Academy of Sciences of the United States of America* **99**(6), 4103–4108.

Kim, J. Y., Yuan, Z. & Jackson, D. (2003), 'Developmental regulation and significance of KNOX protein trafficking in *Arabidopsis*', *Development* **130**(18), 4351–4362.

Kirik, V., Lee, M. M., Wester, K., Herrmann, U., Zheng, Z., Oppenheimer, D., Schiefelbein, J. & Hülskamp, M. (2005), 'Functional diversification of *MYB23* and *GL1* genes in trichome morphogenesis and initiation', *Development* **132**(7), 1477–1485.

Kirik, V., Schnittger, A., Radchuk, V., Adler, K., Hülskamp, M. & Baeumlein, H. (2001), 'Ectopic expression of the *Arabidopsis AtMYB23* gene induces differentiation of trichome cells', *Developmental Biology* **235**(2), 366–377.

Kirik, V., Simon, M., Hülskamp, M. & Schiefelbein, J. (2004a), 'The *ENHANCER OF TRY and CPC1* gene acts redundantly with *TRIPTYCHON* and *CAPRICE*

in trichome and root hair cell patterning in *Arabidopsis*', *Developmental biology* **268**(2), 506–513.

Kirik, V., Simon, M., Wester, K., Schiefelbein, J. & Hülskamp, M. (2004b), '*ENHANCER of TRY and CPC 2 (ETC2)* reveals redundancy in the region-specific control of trichome development of *Arabidopsis*', *Plant molecular biology* **55**(3), 389–398.

Koch, A. J. & Meinhardt., H. (1994), 'Biological pattern formation- from basic mechanism to complex structres', *Reviews of Modern Physics* **66**(4), 1481–1507.

Koornneef, M. (1981), 'The complex syndrome of *ttg* mutants', *ArabidopsisInformation Service* **18**, 45–51.

Koornneef, M., Dellaert, L. W. & van der Veen JH. (1982), 'Ems-and radiation-induced mutation frequencies at individual loci in *Arabidopsis thaliana*', *Mutation research* **93**, 109–123.

Kurata, T., Ishida, T., Kawabata-Awai, C., Noguchi, M., Hattori, S., Sano, R., Nagasaka, R., Tominaga, R., Koshino-Kimura, Y., Kato, T. et al. (2005), 'Cell-to-cell movement of the CAPRICE protein in *Arabidopsis* root epidermal cell differentiation', *Development* **132**(24), 5387–5398.

Larkin, J. C. (2009), 'Morphological evolution: By any means necessary?', *Current Biology* **19**(20), R953–R954.

Larkin, J. C., Oppenheimer, D. G., Lloyd, A. M., Paparozzi, E. T. & Marks, M. D. (1994), 'Roles of the *GLABROUS1* and *TRANSPARENT TESTA GLABRA* genes in *Arabidopsis* trichome development', *The Plant Cell* **6**(8), 1065–1076.

Larkin, J. C., Walker, J. D., Bolognesi-Winfield, A. C., Gray, J. C. & Walker, A. R. (1999), 'Allele-specific interactions between *ttg1* and *gl1* during trichome development in *Arabidopsis thaliana*', *Genetics* **151**(4), 1591–1604.

Larkin, J. C., Young, N., Prigge, M. & Marks, M. D. (1996), 'The control of trichome spacing and number in *Arabidopsis*', *Development* **122**(3), 997–1005.

Lee, J.-Y., Yoo, B.-C., Rojas, M. R., Gomez-Ospina, N., Staehelin, L. A. & Lucas, W. J. (2003), 'Selective trafficking of non-cell-autonomous proteins mediated by NtNCAPP1', *Science* **299**(5606), 392–396.

Levy, A., Erlanger, M., Rosenthal, M. & Epel, B. L. (2007), 'A plasmodesmata-associated beta-1, 3-glucanase in *Arabidopsis*', *The Plant Journal* **49**(4), 669–682.

Lu, B., Roegiers, F., Jan, L. Y. & Jan, Y. N. (2001), 'Adherens junctions inhibit asymmetric division in the *Drosophila* epithelium', *Nature* **409**(6819), 522–525.

Lucas, W. J., Bouche-Pillon, S., Jackson, D. P., Nguyen, L., Baker, L., Ding, B. & Hake, S. (1995), 'Selective trafficking of KNOTTED1 homeodomain protein and its mRNA through plasmodesmata', *Science* **270**(5244), 1980–1983.

Lucas, W. J. & Lee, J. Y. (2004), 'Plasmodesmata as a supracellular control network in plants', *Nature Reviews Molecular Cell Biology* **5**, 712–726.

Macara, I. G. (2001), 'Transport into and out of the nucleus', *Microbiology and molecular biology reviews* **65**(4), 570–594.

Madrid, A. S. & Weis, K. (2006), 'Nuclear transport is becoming crystal clear', *Chromosoma* **115**(2), 98–109.

Maes, L., Inze, D. & Goossens, A. (2008), 'Functional specialization of the *TRANSPARENT TESTA GLABRA1* network allows differential hormonal control of laminal and marginal trichome initiation in *Arabidopsis* rosette leaves', *Plant physiology* **148**(3), 1453–1464.

Marks, M. D., Gilding, E. & Wenger, J. P. (2007), 'Genetic interaction between *glabra3-shapeshifter* and *siamese* in *Arabidopsis thaliana* converts trichome precursors into cells with meristematic activity', *The Plant Journal* **52**(2), 352–361.

Marks, M. D., Wenger, J. P., Gilding, E., Jilk, R. & Dixon, R. A. (2009), 'Transcriptome analysis of *Arabidopsis* wild-type and *gl3-sst sim* trichomes identifies four additional genes required for trichome development', *Molecular plant* **2**(4), 803–822.

Masucci, J. D., Rerie, W. G., Foreman, D. R., Zhang, M., Galway, M. E., Marks, M. D. & Schiefelbein, J. W. (1996), 'The homeobox gene *GLABRA 2* is required for position-dependent cell differentiation in the root epidermis of *Arabidopsis thaliana*', *Development* **122**, 1253–1260.

Matsubayashi, Y., Yang, H. & Sakagami, Y. (2001), 'Peptide signals and their receptors in higher plants', *Trends in Plant Science* **6**(12), 573–577.

McGonigle, B., Bouhidel, K. & Irish, V. F. (1996), 'Nuclear localization of the *Arabidopsis APETALA3* and *PISTILLATA* homeotic gene products depends on their simultaneous expression.', *Genes & Development* **10**(14), 1812–1821.

Meinhardt, H. & Gierer, A. (1974), 'Applications of a theory of biological pattern formation based on lateral inhibition', *Journal of cell science* **15**(2), 321–346.

Meinhardt, H. & Gierer, A. (2000), 'Pattern formation by local self-activation and lateral inhibition', *Bioessays* **22**(8), 753–760.

Miura, T. & Shiota, K. (2002), 'Depletion of FGF acts as a lateral inhibitory factor in lung branching morphogenesis in vitro', *Mechanisms of development* **116**(1-2), 29–38.

Morohashi, K. & Grotewold, E. (2009), 'A systems approach reveals regulatory circuitry for *Arabidopsis* trichome initiation by the *GL3* and *GL1* selectors', *PLoS Genetics* **5**(2), e1000396.

Morohashi, K., Zhao, M., Yang, M., Read, B., Lloyd, A., Lamb, R. & Grotewold, E. (2007), 'Participation of the *Arabidopsis* bHLH factor *GL3* in trichome initiation regulatory events', *Plant physiology* **145**(3), 736–746.

Nakajima, K., Sena, G., Nawy, T. & Benfey., P. N. (2001), 'Intercellular movement of the putative transcription factor shr in root patterning', *Nature* **413**, 307–311.

Nesi, N., Debeaujon, I., Jond, C., Pelletier, G., Caboche, M. & Lepiniec, L. (2000), 'The *TT8* gene encodes a basic helix-loop-helix domain protein required for expression of *DFR* and *BAN* genes in *Arabidopsis* siliques', *The Plant Cell* **12**(10), 1863–1878.

Nesi, N., Jond, C., Debeaujon, I., Caboche, M. & Lepiniec, L. (2001), 'The *Arabidopsis TT2* gene encodes an R2R3 MYB domain protein that acts as a key determinant for proanthocyanidin accumulation in developing seed', *The Plant Cell* **13**(9), 2099–2114.

Ohashi, Y., Oka, A., Ruberti, I., Morelli, G. & Aoyama, T. (2002), 'Entopically additive expression of *GLABRA2* alters the frequency and spacing of trichome initiation', *The Plant Journal* **29**(3), 359–369.

Olesen, P. (1979), 'The neck constriction in plasmodesmata', *Planta* **144**(4), 349–358.

Oparka, K. J., Roberts, A. G., Boevink, P., Cruz, S. S., Roberts, I., Pradel, K. S., Imlau, A., Kotlizky, G., Sauer, N. & Epel, B. (1999), 'Simple, but not branched, plasmodesmata allow the nonspecific trafficking of proteins in developing tobacco leaves', *Cell* **97**(6), 743–754.

Oppenheimer, D. G., Herman, P. L., Sivakumaran, S., Esch, J. & Marks, M. D. (1991), 'A myb gene required for leaf trichome differentiation in *Arabidopsis* is expressed in stipules', *Cell* **67**(3), 483–493.

Payne, C. T., Zhang, F. & Lloyd, A. M. (2000), '*GL3* encodes a bHLH protein that regulates trichome development in *Arabidopsis* through interaction with GL1 and TTG1', *Genetics* **156**(3), 1349–1362.

Penfield, S., Meissner, R. C., Shoue, D. A., Carpita, N. C. & Bevan, M. W. (2001), 'MYB61 is required for mucilage deposition and extrusion in the *Arabidopsis* seed coat', *The Plant Cell* **13**, 2777–2791.

Perbal, M.-C., Haughn, G., Saedler, H. & Schwarz-Sommer, Z. (1996), 'Non-cell-autonomous function of the *Antirrhinum* floral homeotic proteins DEFICIENS and GLOBOSA is exerted by their polar cell-to-cell trafficking', *Development* **122**, 3433–3441.

Pesch, M. & Hülskamp, M. (2004), 'Creating a two-dimensional pattern de novo during *Arabidopsis* trichome and root hair initiation', *Current Opinion in Genetics & Development* **14**(4), 422–427.

Pesch, M. & Hülskamp, M. (2009), 'One, two, three: models for trichome patterning in *Arabidopsis* ?', *Current Opinion in Plant Biology* **12**(5), 587–592.

Prochiantz, A. & Joliat., A. (2003), 'Can transcription factors function as cell-cell signalling molecules', *Nature Review Molecular Cell Biology* **4**(10), 814–819.

Reinhardt, D. (2003), 'Vascular patterning: More than just auxin ?', *Current Biology* **13**(12), R485–R487.

Rerie, W. G., Feldmann, K. A. & Marks, M. D. (1994), 'The *GLABRA2* gene encodes a homeo domain protein required for normal trichome development in *Arabidopsis*.', *Genes & Development* **8**(12), 1388–1399.

Riechmann, J. L., Krizek, B. A. & Meyerowitz, E. M. (1996), 'Dimerization specificity of *Arabidopsis* MADS domain homeotic proteins APETALA1, APETALA3, PISTILLATA, and AGAMOUS', *Proceedings of the National Academy of Sciences of the United States of America* **93**(10), 4793–4798.

Sasaki, N., Kaido, M., Okuno, T. & Mise, K. (2005), 'Coat protein-independent cell-to-cell movement of bromoviruses expressing brome mosaic virus movement protein with an adaptation-related amino acid change in the central region', *Archives of Virology* **150**, 1231–1240.

Schellmann, S., Hülskamp, M. & Uhrig, J. (2007), 'Epidermal pattern formation in the root and shoot of *Arabidopsis*', *Biochemical Society Transactions* **35**, 146–148.

Schellmann, S., Schnittger, A., Kirik, V., Wada, T., Okada, K., Beermann, A., Thumfahrt, J., Juergens, G. & Hülskamp, M. (2002), '*TRIPTYCHON* and *CAPRICE* mediate lateral inhibition during trichome and root hair patterning in *Arabidopsis*', *The EMBO Journal* **21**(19), 5036–5046.

Schiefelbein, J. (2003), 'Cell-fate specification in the epidermis: a common patterning mechanism in the root and shoot', *Current opinion in plant biology* **6**, 74–78.

Schnittger, A., Folkers, U., Schwab, B., Jurgens, G. & Hülskamp, M. (1999), 'Generation of a spacing pattern: the role of *TRIPTYCHON* in trichome patterning in *Arabidopsis*', *The Plant Cell* **11**(6), 1105–1116.

Serna, L. (2005), 'Epidermal cell patterning and differentiation throughout the apical-basal axis of the seedling', *Journal of Experimental Botany* **56**(418), 1983–1989.

Sessions, A., Yanofsky, M. F. & Weigel, D. (2000), 'Cell-cell signaling and movement by the floral transcription factors *LEAFY* and *APETALA1*.', *Science* **289**(5480), 779–782.

Simon, M., Lee, M. M., Lin, Y., Gish, L. & Schiefelbein, J. (2007), 'Distinct and overlapping roles of single-repeat MYB genes in root epidermal patterning', *Developmental biology* **311**(2), 566–578.

Smith, R. S., Guyomarc'h, S., Mandel, T., Reinhardt, D., Kuhlemeier, C. & Prusinkiewicz, P. (2006), 'A plausible model of phyllotaxis', *Proceedings of the National Academy of Sciences of the United States of America* **103**(5), 1301–1306.

Sompornpailin, K., Makita, Y., Yamazaki, M. & Saito., K. (2002), 'A WD-repeat-containing putative regulatory protein in anthocyanin biosynthesis in *Perilla frutescens*.', *Plant Molecular Biology* **50**(3), 485–495.

Srinivas, B. P. (2004), 'Understanding the function of the *Arabidopsis GLABRA 2* gene in trichome patterning, morphogenesis and differentiation', *Ph.D Thesis* .

Stadler, R., Lauterbach, C. & Sauer, N. (2005), 'Cell-to-cell movement of green fluorescent protein reveals post-phloem transport in the outer integument and identifies symplastic domains in *Arabidopsis* seeds and embryos', *Plant physiology* **139**(2), 701–712.

Szymanski, D. B., Jilk, R. A., Pollock, S. M. & Marks, M. D. (1998), 'Control of *GL2* expression in *Arabidopsis* leaves and trichomes', *Development* **125**(7), 1161–1171.

Takada, S. & Jurgens, G. (2007), 'Transcriptional regulation of epidermal cell fate in the *Arabidopsis* embryo', *Development* **134**(6), 1141–1150.

Tassetto, M., Maizel, A., Osorio, J. & Joliot, A. (2005), 'Plant and animal homeodomains use convergent mechanisms for intercellular transfer', *EMBO reports* **6**(9), 885–890.

Thomas, C. L., Bayer, E. M., Ritzenthaler, C., Fernandez-Calvino, L. & Maule, A. J. (2008), 'Specific targeting of a plasmodesmal protein affecting Cell-to-Cell communication', *PLoS Biology* **6**(1), e7.

Tominaga, R., Iwata, M., Sano, R., Inoue, K., Okada, K. & Wada, T. (2008), '*Arabidopsis CAPRICE-LIKE* MYB 3 *(CPL3)* controls endoreduplication and flowering development in addition to trichome and root hair formation', *Development* **135**(7), 1335–1345.

Trutnyeva, K., Bachmaier, R. & Waigmann, E. (2005), 'Mimicking carboxyterminal phosphorylation differentially effects subcellular distribution and cell-to-cell movement of tobacco mosaic virus movement protein', *Virology* **332**, 563–577.

Tsutsui, H., Karasawa, S., Shimizu, H., Nukina, N. & Miyawaki, A. (2005), 'Semi-rational engineering of a coral fluorescent protein into an efficient highlighter', *EMBO reports* **6**(3), 233–238.

Turing, A. M. (1952), 'The chemical basis of morphogenesis', *Philosophical Transactions Of The Royal Society Of London. Series B, Biological Sciences* **B237**, 37–72.

Turner, A., Wells, B. & Roberts, K. (1994), 'Plasmodesmata of maize root tips: structure and composition', *Journal of Cell Science* **107**(12), 3351–3361.

Ueki, N., Oda, T., Kondo, M., Yano, K., Noguchi, T. & aki Muramatsu., M. (1998), 'Selection system for genes encoding nuclear-targeted proteins', *Nature Biotechnology* **16**, 1338–1342.

Wada, T. (1997), 'Epidermal cell differentiation in *Arabidopsis* determined by a myb homolog, *CPC*', *Science* **277**(5329), 1113–1116.

Wada, T., Kurata, T., Tominaga, R., Koshino-Kimura, Y., Tachibana, T., Goto, K., Marks, M. D., Shimura, Y. & Okada, K. (2002), 'Role of a positive regulator of root hair development, *CAPRICE,* in *Arabidopsis* root epidermal cell differentiation', *Development* **129**(23), 5409–5419.

Walker, A. R., Davison, P. A., Bolognesi-Winfield, A. C., James, C. M., Srinivasan, N., Blundell, T. L., Esch, J. J., Marks, M. D. & Gray, J. C. (1999), 'The *TRANSPARENT TESTA GLABRA1* locus, which regulates trichome differentiation and anthocyanin biosynthesis in Arabidopsis, encodes a WD40 repeat protein', *The Plant Cell* **11**(7), 1337–1349.

Wang, S., Hubbard, L., Chang, Y., Guo, J., Schiefelbein, J. & Chen, J. G. (2008), 'Comprehensive analysis of single-repeat R3 MYB proteins in epidermal cell patterning and their transcriptional regulation in *Arabidopsis*', *BMC Plant Biology* **8**, 81.

Wang, S., Kwak, S., Zeng, Q., Ellis, B. E., Chen, X., Schiefelbein, J. & Chen, J. (2007), '*TRICHOMELESS1* regulates trichome patterning by suppressing *GLABRA1* in *Arabidopsis*', *Development* **134**(21), 3873–3882.

Wester, K., Digiuni, S., Geier, F., Timmer, J., Fleck, C. & Hülskamp, M. (2009), 'Functional diversity of R3 single-repeat genes in trichome development', *Development* **136**(9), 1487–1496.

Western, T. L., Skinner, D. J. & Haughn, G. W. (2000), 'Differentiation of mucilage secretory cells of the *Arabidopsis* seed coat', *Plant physiology* **122**(2), 345–355.

White, T. W. & Paul, D. L. (1999), 'Genetic diseases and gene knockouts reveal diverse connexin functions', *Annual review of physiology* **61**(1), 283–310.

Willecke, K., Eiberger, J., Degen, J., Eckardt, D., Romualdi, A., Gueldenagel, M., Deutsch, U. & Soehl, G. (2002), 'Structural and functional diversity of connexin genes in the mouse and human genome', *Biological Chemistry* **383**(5), 725–737.

Wu, X., Dinneny, J. R., Crawford, K. M., Rhee, Y., Citovsky, V., Zambryski, P. C. & Weigel, D. (2003), 'Modes of intercellular transcription factor movement in the *Arabidopsis* apex', *Development* **130**(16), 3735–3745.

Wu, X., Weigel, D. & Wigge, P. A. (2002), 'Signaling in plants by intercellular RNA and protein movement', *Genes & Development* **16**(2), 151–158.

Yoshida, Y., Sano, R., Wada, T., Takabayashi, J. & Okada, K. (2009), 'Jasmonic acid control of *GLABRA3* links inducible defense and trichome patterning in *Arabidopsis*', *Development* **136**(6), 1039–1048.

Zambryski, P. (2004), 'Cell-to-cell transport of proteins and fluorescent tracers via plasmodesmata during plant development', *The Journal of Cell Biology* **164**(2), 165–168.

Zhang, F., Gonzalez, A., Zhao, M., Payne, C. T. & Lloyd, A. (2003), 'A network of redundant bHLH proteins functions in all TTG1-dependent pathways of *Arabidopsis*', *Development* **130**(20), 4859–4869.

Zhao, M., Morohashi, K., Hatlestad, G., Grotewold, E. & Lloyd, A. (2008), 'The TTG1-bHLH-MYB complex controls trichome cell fate and patterning through direct targeting of regulatory loci', *Development* **135**(11), 1991–1999.

Zimmermann, I. M., Heim, M. A., Weisshaar, B. & Uhrig, J. F. (2004), 'Comprehensive identification of *Arabidopsis thaliana* MYB transcription factors interacting with R/B-like BHLH proteins', *The Plant Journal* **40**(1), 22–34.

Erklärung

Hiermit versichere ich, dass ich die vorliegende Arbeit selbstständig verfasst und keine anderen als die angegebenen Quellen und Hilfsmittel benutzt habe, dass alle Stellen der Arbeit, die wörtlich oder sinngemäß aus anderen Quellen übernommen wurden, als solche kenntlich gemacht sind und dass die Arbeit in gleicher oder ähnlicher Form noch keiner Prüfungsbehörde vorgelegt wurde.

Köln, den 17. Oktober 2011 Rachappa Siddalingappa Balkunde